“AUREL VLAICU” UNIVERSITY OF ARAD
FACULTY OF FOOD ENGINEERING, TOURISM AND ENVIRONMENTAL PROTECTION
CHEMICAL AND TECHNOLOGICAL RESEARCH CENTER

# Scientific and Technical Bulletin

## Series CHEMISTRY, FOOD SCIENCE & ENGINEERING

**PRELIMINARY STUDIES ABOUT SOME FACTORS INFLUENCING THE PROPERTIES OF OLEO-GELS (Pages 34-42)**

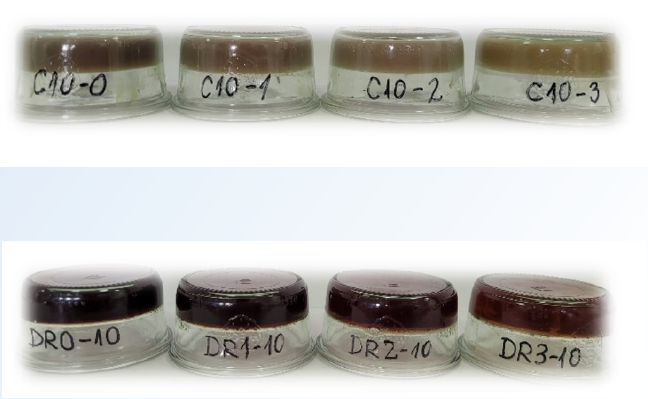

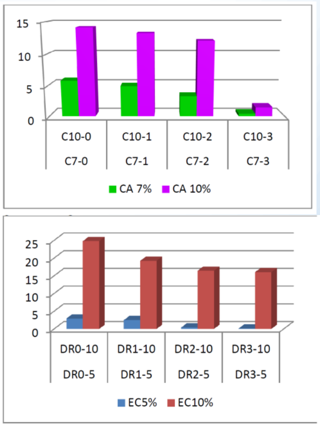

The visual appearance of pumpkin and rapeseed oil oleogels — Firmness of oleogels prepared from pumpkin seed oil and rapeseed oil

Year XX, Vol. 19, 2022
https://www.uav.ro/jour/index.php/stb-cfse/index

“AUREL VLAICU” UNIVERSITY OF ARAD

FACULTY OF FOOD ENGINEERING, TOURISM AND ENVIRONMENTAL PROTECTION

CHEMICAL AND TECHNOLOGICAL RESEARCH CENTER

# Scientific and Technical Bulletin

## Series CHEMISTRY, FOOD SCIENCE & ENGINEERING

Year XX, Vol. 19, 2022

ISSN 1582-1021

e-ISSN 2668-4764

EDITURA UNIVERSITĂȚII
AUREL VLAICU
A R A D

EDITURA UNIVERSITĂȚII
AUREL VLAICU
A R A D

# CONTENTS

**EDITORIAL BOARD**

**Dana M. COPOLOVICI, Editor-in-chief**

„Aurel Vlaicu” University of Arad, Romania

**EDITORS**
**Dorina CHAMBREE**, „Aurel Vlaicu” University of Arad, Romania
**Lucian COPOLOVICI**, „Aurel Vlaicu” University of Arad, Romania
**Calina Petruta CORNEA,** University of Agricultural Sciences and Veterinary Medicine Bucharest, Romania
**Nicolae DINCĂ**, „Aurel Vlaicu” University of Arad, Romania
**Simona GAVRILAŞ**, „Aurel Vlaicu” University of Arad, Romania
**Florentina MUNTEANU**, „Aurel Vlaicu” University of Arad, Romania
**Mariana-Atena POIANA**, Banat’s University of Agricultural Sciences and Veterinary Medicine “King Mihai I of Romania” from Timisoara, Romania
**Ionel POPESCU-MITROI**, „Aurel Vlaicu” University of Arad, Romania
**Diana RABA**, Banat’s University of Agricultural Sciences and Veterinary Medicine “King Mihai I of Romania” from Timisoara, Romania
**Dana RADU**, „Aurel Vlaicu” University of Arad, Romania
**Loredana SORAN**, National Institute for Research & Development of Isotopic and Molecular Technologies, Cluj-Napoca, Romania
**Elisabeta Ildiko SZERB**, Institute of Chemistry Timisoara of Romanian Academy
**Radu ŞUMALAN**, Banat’s University of Agricultural Sciences and Veterinary Medicine “King Mihai I of Romania” from Timisoara, Romania
**Renata ŞUMALAN**, Banat’s University of Agricultural Sciences and Veterinary Medicine “King Mihai I of Romania” from Timisoara, Romania
**Simona VICAŞ**, University of Oradea, Romania
**Irina VOLF**, „Gheorghe Asachi” Technical University of Iasi, Romania
**Alina D. ZAMFIR**, „Aurel Vlaicu” University of Arad, Romania
**Cristian MOISA**, „Aurel Vlaicu” University of Arad, Romania

COVER DESIGN
**Dana Copolovici,** "Aurel Vlaicu" University of Arad, Romania

ADDRESS
Faculty of Food Engineering, Tourism and Evironmental Protection,
„Aurel Vlaicu” University, Elena Dragoi St., Nr. 2, L31, Arad, Romania
Phone: 0040257369091
*E-mail:* dana.copolovici@uav.ro

**Scientific and Technical Bulletin, Series: Chemistry, Food Science and Engineering is covered/indexed/abstracted in:**

| | |
|---|---|
| DRJI Directory of Research Journals Indexing | **Directory of Research Journals Indexing** |
| ROAD DIRECTORY OF OPEN ACCESS SCHOLARLY RESOURCES | **Directory of Open Access Scholarly Resources** |
| OCLC WorldCat® | **World Cat** |
| Google scholar | **Google Scholar** |
| CABI | **CABI** |
| INDEX COPERNICUS INTERNATIONAL | **Index Copernicus International** |

*Scien. Tech. Bull-Chem. Food Sci. Eng., Vol. 19 (XX), 2022, 3-9*

# ARTICLE

# ESTIMATING METHANE EMISSIONS FROM DIFFERENT LAND-USE TYPES IN THE URBAN AREA

**Mustafa HMOUDAH**[1], **Cristian POP**[2], **Călin BACIU**[1*]

[1] *Faculty of Environmental Science and Engineering, University of Babeş-Bolyai, 30 Fantanele Street, RO-400294, Cluj-Napoca, Romania*
*Corresponding author email: mustafa.hmoudah@gmail.com*

***Abstract:*** *In the recent decades, greenhouse gas (GHG) emissions increased considerably; due to the remarkable growth in anthropogenic activities. These gasses have potential warming effects on the atmosphere as long as they accumulate in the atmosphere.*

*Methane ($CH_4$) as a GHG has very high radiative forces, with a short lifetime of approximately 10 years. Therefore, targeting $CH_4$ emissions would bring immediate climate benefits in the short-term. Land-use changing policies in the urban area decrease $CH_4$ sinks and affect the urban contribution in $CH_4$ budget. However, the uncertainty of $CH_4$ emissions in the urban area is very high, so that estimating $CH_4$ concentration is important to take appropriate mitigation measures.*

*In our study, we estimated street-level CH4 concentrations in the following four urban areas: the city center (CC), the central park (CP), a residential area (RA), and a commercial area (CA). An Enhanced Portable Fluxmeter device with a precise measurement of 0.1 parts per million (ppm) was used to perform these CH4 estimations between 10:00 and 12:00 am (EEST), from 20-30 March.*

*The results showed that the CC and CA have an elevated contribution in CH4 concentration with more than 2.3 ppm. The RA recorded the least as hypothesize. Surprisingly, the CP which was supposed to have the least contribution in CH4 concentration from the anthropogenic perspective, was estimated to have ascending records. These findings demonstrate the remarkable contribution of the urban area in influencing $CH_4$ concentration, and recommend further CH4 investigation in the urban area and to identify its potential sources.*

**Keywords**: greenhouse gas, methane concentration, urban area, land-use, pollution

## INTRODUCTION

In the recent decades and since 1850, emissions of greenhouse gas (GHG) such as: carbon dioxide ($CO_2$), methane ($CH_4$) and nitrous oxide ($N_2O$) increased considerably; due to the remarkable growth in anthropogenic activities(IPCC 2014). These gasses have significant warming effects on the atmosphere as long as they accumulate in the atmosphere. However, their lifetime in the atmosphere is different, their harmful climate effects vary as well (EPA 2022).

The effects of GHGs range from extreme phenomena of climate change, lack of potable water, loss of species, to increase in death rates (CDC 2022a; EPA 2022; Portier et al. 2010), in addition to mental health, respiratory difficulties and cardiovascular diseases (Luber et al. 2014; WHO 2022). These effects will mostly put the lives of old people, children and women under risk (CDC 2022b; Portier et al. 2010; WHO 2003). Therefore, acting fast in reducing GHG emissions would help in reversing this climate crisis (Klenske 2021).

Methane has extreme radiative forces, but at the same time its lifetime is quite short of approximately 10 years (IPCC 2013). For this reason, targeting $CH_4$ emissions would bring climate benefits in the short-term (Maazallahi et al. 2020).

Methane come from incomplete burning of organic matter (IPCC 2013), the transformation process of organic matter into fossil fuels (IPCC 2013; Kulongoski et al. 2018), from deep soil layers of high temperature and pressure (Kulongoski et al. 2018), wetlands, sea, rice paddies, combustion of biomass and fossil fuels (IPCC 2013), and it can also be produced in the soil rhizosphere from microbial activities (Kulongoski et al. 2018).

The potential sinks of $CH_4$ are its oxidation by soil methanotrophic in aerobic conditions (IPCC 2013; Kevin R. Tate 2015) and in the atmospheric layers of troposphere and stratosphere by OH radicals (IPCC 2013).

In Romania, energy and agriculture are primarily contributing to $CH_4$ emissions on the national level. Methane emission estimates between 1989 – 2000 showed that $CH_4$ emissions declined by more than 30%; due to the decrease in emissions from these two sectors (ANPM 2020).

In the urban area, $CH_4$ emissions come from industry, traffic, combustion of fossil fuels and wastewater treatment facilities (Barhoumi et al. 2019; Takano et Ueyama 2021). Also, leaks from natural gas networks in the urban area are other sources of environmental pollution, besides representing a loss of energy sources and a potential contributor in $CH_4$ fluxes in the urban atmosphere (von Fischer et al. 2017; Zazzeri et al. 2015).

Moreover, land-use policies in the urban area decrease $CH_4$ sinks and affect the urban contribution in $CH_4$ emissions (Kevin R. Tate 2015; K.R. Tate et al. 2007).

Von Fischer et al. (2017) stated that there is a high degree of uncertainty in $CH_4$ emissions in the urban area and therefore, it is important to quantify these emissions and to identify urban areas with high $CH_4$ concentrations, in order to take the appropriate mitigation measures.

In the current study, we aimed to investigate the influence of land-use policies on the concentration of atmospheric $CH_4$. To this extent, we conducted street-level $CH_4$ estimations in the following four urban areas: a highly congested area of the city center (CC), a green area with less human influence of the central park (CP) to represent as a background source for concentration, a residential area (RA) with low traffic density, and commercial area (CA) with high traffic density.

The selection of these four urban areas aimed to measure the difference of gas emission. The objectives of this study are to establish a better understanding of the correlation between land-use types and $CH_4$ concentration, to point out the importance for further investigation in the urban area in case of significant $CH_4$ concentrations and different variations, to reduce the degree of uncertainty regarding $CH_4$ emissions in the urban area and to give decision-makers indicators to potential $CH_4$ sources for applying appropriate mitigation measures.

**Figure 1.** The location of the study area in the city of Cluj-Napoca, Romania and the four land-use types, and the location of the measuring points in the commercial and the residential areas as illustrated in the legend.

## MATERIALS AND METHODS

The first step of this study was the preparation of a map for field work by identifying the locations of the main four sites, in order to estimate street-level $CH_4$ concentration in these different land-use sites. The four land-use locations are city center (CC), central park (CP), residential area (RA), and commercial area (CA) which differ in their land-use and human activities supposing different sources of $CH_4$ fluxes. The field map produced by utilizing online Google Map (Google, USA, 2022).

The measurements in these four sites were divided into two sections. The decision for doing such division aimed for targeting potential sources of $CH_4$. The first section included one single strategy in both RA and CA by placing the device of the Enhanced Portable Fluxmeter (Westsystems, Italy) at specific locations identified in Figure 1, by carrying the portable device on a human back and holding the inlet tube at approximately 1.5 m height; for estimating street-level concentrations caused by traffic flow or other potential sources. This portable device measures $CH_4$ and $CO_2$ simultaneously per second in parts per million (ppm) with a high measuring precision of 0.1 ppm. The second section was performed in CC and CP by walking around and within these two areas in order to cover any possible potential source of $CH_4$ within the identified areas in (Fig. 1).

The average $CH_4$ concentration in ppm was estimated at each second between 10:00 and 12:00 am (EEST), from 20-30 March 2021 for one time at each location, according to its specified method. The obtained data from each area was saved on-site and then extracted in the laboratory for further statistical and spatial analysis, by using Microsoft Excel and Word (Microsoft, USA, 2022).

## RESULTS AND DISCUSSIONS

In this study, we demonstrated the estimation of street-level $CH_4$ concentration in four urban areas as part of estimating the influence of urbanization on $CH_4$ budget. The current estimations were performed in four main land-use areas of city center (CC), central park (CP), residential area (RA), and commercial area (CA) (Figure 1). The atmospheric $CH_4$ concentrations in each area were plotted in ppm against the recording time (Figure 2).

In our study, we found out that $CH_4$ atmospheric concentration in CC has high records as observed in Figure 2. The mean value of all records in this area was 1.8 ppm. In addition, the maximum value was estimated at 2.8 ppm and the minimum value was 1.7 ppm, with 0.2 ppm standard deviation. Concentrations were changing in regard to traffic flow. At some point, concentrations hit 2.7 and 2.8 ppm as a truck vehicle passed by.

The $CH_4$ concentrations in the CP had 1.9 ppm for the mean value, and 2.2 ppm, 1.8 ppm and 0.1 for the max, min, and the standard deviation values, respectively. Concentrations of $CH_4$ seemed to be steady around 1.9 and 2.0 ppm. These numbers were aimed to be used as indicators to $CH_4$ background.

Moreover, the mean $CH_4$ concentration in RA was estimated at 1.6 ppm. Also, the minimum, the maximum, and the standard deviation values are 1.5 ppm, 1.7 ppm, and 0.1ppm, respectively. The values of $CH_4$ in this area fluctuated between 1.5 ppm and 1.6 ppm in a regular rhythm.

Also, the minimum and the maximum values of atmospheric $CH_4$ concentration estimated in CA were 1.7 ppm and 2.3 ppm, respectively. The mean value of these concentrations was 2.0 ppm with 0.1 ppm standard deviation. This area observes two steady stages of concentration, one between 1.9 and 2.0 ppm, and another between 2.0 and 2.1 ppm. High concentrations were recorded during the time when big vehicles were passing. These fluxes can be related to gas emissions released from vehicles and particularly from big trucks.

However, Table 1 summarizes all statistical findings in the four areas.

In CC and CA, records showed that land-use type can influence $CH_4$ concentration, but not in a considerable way as the maximum values in these two areas didn’t exceed 2.8 ppm confirming what was stated in (EC. JRC. 2021) that agriculture and energy sectors have a considerable influence.

The low emissions in RA can be referred to the absence of traffic, as proposed at the beginning of this study. However, winddirection fluctuated the emissions from time to time and these might be referred to some sources from household activities or from nearby sources.

These results confirm the suggestions of diversity in $CH_4$ concentrations according to the land-use type. It seems clear that concentrations of $CH_4$ in the urban area differ according to the type of use of this area. However, at some points of field work the device measured high concentrations of $CH_4$ which gives an indication towards the presence of a potential source.

In contrast, the results don't go along with what was hypothesized at the beginning for CP to have the lowest concentration of $CH_4$ compared with the other land-use types. Nevertheless, biogenic sources are mainly responsible for these high concentrations (Fernández-Baca et al. 2021).

Despite the results in the CP were not exactly as expected, fluctuation in concentrations in the CC and the CA recorded high concentrations as hypothesized.

This study didn't also succeed in identifying what is exactly behind these concentration differences. Therefore, further investigation is required for identifying the sources behind these $CH_4$ in the urban area.

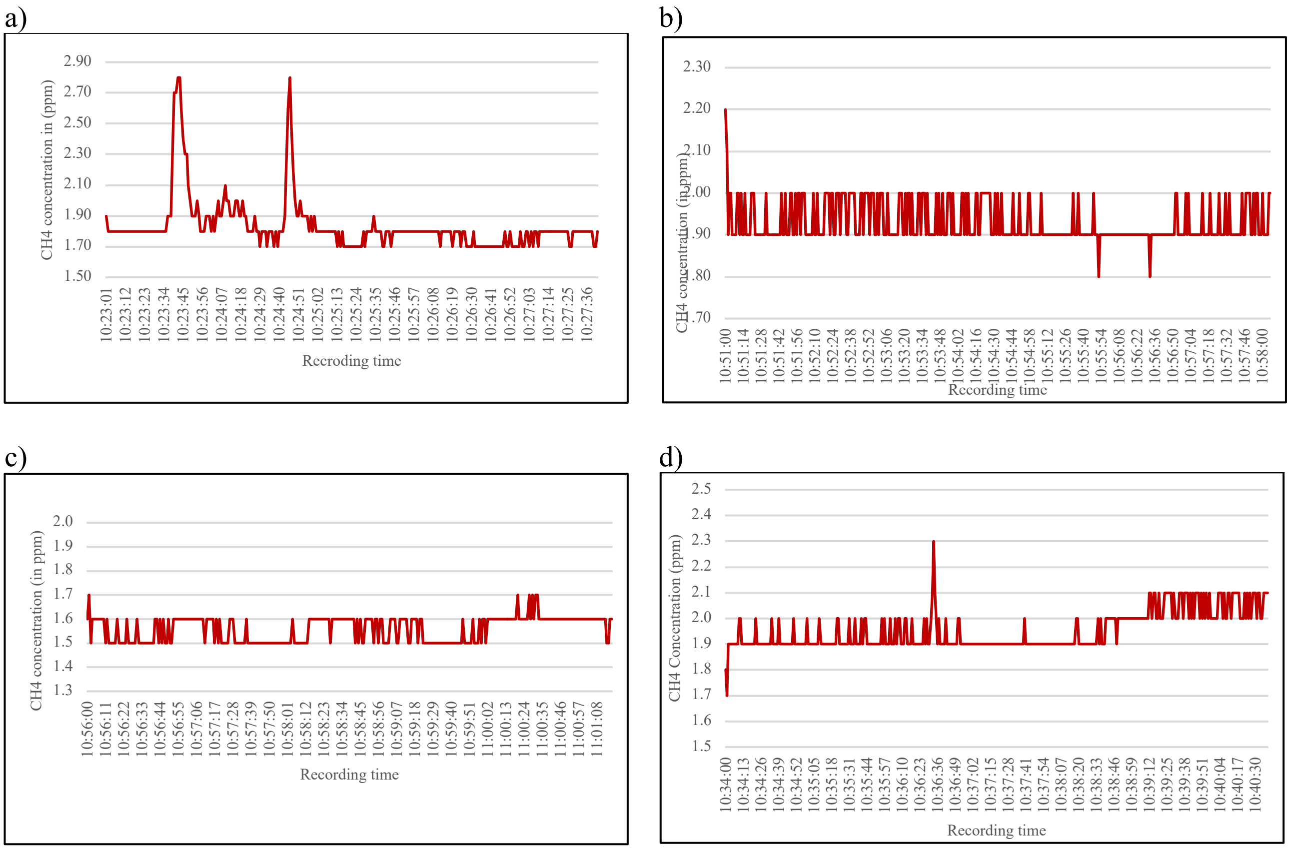

**Figure 2.** Atmospheric $CH_4$ concentrations (in ppm) per recording time estimated in the different land-use areas, a) city center CC, b) central park CP, c) residential area RA, and d) commercial area CA.

From anthropogenic perspective, the CP was considered away from human activities of traffic, industry or combustion of fossil fuels. However, from our estimation, as illustrated in Figure 2, average $CH_4$ concentrations are high in comparison with the commercial and the city center estimates. The average concentration of $CH_4$ was estimated at 1.9 ppm. In addition, the minimum and the maximum values of these concentrations were 1.8 and 2.2 ppm, respectively.

City center area is considered very busy with commercial activities and high traffic. This is supposed to influence $CH_4$ emissions and by default the quality of air. The average concentration of $CH_4$ in the city center is approximately high compared with the residential area average concentration, but still less with 0.1 ppm from the commercial area with high traffic. Nevertheless, this central area had high records of 2.3, 2.6, 2.7 and 2.8ppm.

**Table 1.** Statistics of $CH_4$ street-level concentration in (ppm) of the four land-use types including mean, maximum, and minimum values in addition to the standard deviation (SD)

| Land-use type | Mean | Max | Min | SD |
|---|---|---|---|---|
| CC | 1.8 | 2.8 | 1.7 | 0.2 |
| CP | 1.9 | 2.2 | 1.8 | 0.1 |
| RA | 1.6 | 1.7 | 1.5 | 0.1 |
| CA | 2.0 | 2.3 | 1.7 | 0.1 |

Results in our study of the four areas indicated that $CH_4$ concentrations increase in high traffic and the park area which signifies that $CH_4$ is emitted from natural and anthropogenic sources. Similarly, Takano & Ueyama (2021) estimated that $CH_4$ emissions from commercial areas are quite high; due to natural gas combustion and transportation in comparison with emissions from residential areas.

However, wind was also one of the main factors that affected the fluctuation of these emissions as stated by Lowry et al (2020), von Fischer et al (2017) and Weller et al (2019). The time and the used method are definitely important factors in estimating the actual $CH_4$ concentration and to determine their sources which was also mentioned by Lamb et al (2016).

Also, the application of other methods is much expensive in our case study and due to the lack of resources.

## CONCLUSIONS

Atmospheric $CH_4$ concentration estimation studies are important for indicating sources of $CH_4$ emissions on a city scale. This study estimated atmospheric $CH_4$ concentration in four different land-use areas, in order to highlight anthropogenic urban activities that are responsible for high $CH_4$ emissions. From the selected four types, the commercial area and the city center showed higher contribution in $CH_4$ emissions with more than 2.3 ppm.

However, the residential area recorded the least contribution in street-level $CH_4$ as supposed at the beginning of the study with a mean value of 1.6 ppm. Surprisingly, the central park, which was supposed to have the least contribution in $CH_4$ concentration, from an anthropogenic perspective, was estimated to have high records approximately close to the concentrations in CC and CA.

This study succeeded to indicate that land-use policies may affect $CH_4$ atmospheric concentration in the urban area and showed high concentrations in areas with increased anthropogenic activities in CC and CA. At the same time, this study couldn't precisely identify the actual sources behind those high concentration values which recommend further investigation in the urban area.

## REFERENCES

ANPM, National Environmental Protection Agency. 2020. « Romania's Greenhouse Gas Inventory 1989-2018 ». National Inventory report (NIR) 28.

Barhoumi, Badreddine, Mihail Simion Beldean-Galea, Abdulla M. Al-Rawabdeh, Carmen Roba, Ildiko Melinda Martonos, Ramona Bălc, Massoud Kahlaoui, et al. 2019. « Occurrence, Distribution and Ecological Risk of Trace Metals and Organic Pollutants in Surface Sediments from a Southeastern European River (Someşu Mic River, Romania) ». *Science of The Total Environment* 660 (avril): 660-76. https://doi.org/10.1016/j.scitotenv.2018.12.428.

CDC. 2022a. « Climate Effects on Earth ». Centers for Disease Control and Prevention. 2022. https://www.cdc.gov/climateandhealth/effects/default.htm.

———. 2022b. « Preparing for the Regional Health Impacts of Climate Chage in the United States ».

EC. JRC. 2021. *GHG Emissions of All World: 2021 Report.* LU: Publications Office. https://data.europa.eu/doi/10.2760/173513.

EPA. 2022. « Greenhouse Gases ». United States Environmental Protection Agency.

2022. https://www.epa.gov/report-environment/greenhouse-gases.

Fernández-Baca, Cristina P., Adam R. Rivers, Woojae Kim, Ryo Iwata, Anna M. McClung, Daniel P. Roberts, Vangimalla R. Reddy, et Jinyoung Y. Barnaby. 2021. « Changes in Rhizosphere Soil Microbial Communities across Plant Developmental Stages of High and Low Methane Emitting Rice Genotypes ». *Soil Biology and Biochemistry* 156 (mai): 108233. https://doi.org/10.1016/j.soilbio.2021.108233.

Fischer, Joseph C. von, Daniel Cooley, Sam Chamberlain, Adam Gaylord, Claire J. Griebenow, Steven P. Hamburg, Jessica Salo, Russ Schumacher, David Theobald, et Jay Ham. 2017. « Rapid, Vehicle-Based Identification of Location and Magnitude of Urban Natural Gas Pipeline Leaks ». *Environmental Science & Technology* 51 (7): 4091-99. https://doi.org/10.1021/acs.est.6b06095.

IPCC. 2013. « Carbon and Other Biogeochemical Cycles. In: Climate Change 2013: The Physical Science Basis. Contribution of Working Group I to the Fifth Assessment Report of the Intergovernmental Panel on Climate Change. Cambridge University Press, Cambridge, United Kingdom and New York, NY, USA. »

———. 2014. « Agriculture, Forestry and Other Land Use (AFOLU). In: Climate Change 2014: Mitigation of Climate Change. Contribution of Working Group III to the Fifth Assessment Report of the Intergovernmental Panel on Climate Change. Cambridge University Press, Cambridge, United Kingdom and New York, NY, USA. »

Klenske, Nick. 2021. « Nature and climate crises: two sides of the same coin ». European Comission. 2021. https://ec.europa.eu/research-and-innovation/en/horizon-magazine/nature-and-climate-crises-two-sides-same-coin.

Kulongoski, J. T., P. B. McMahon, M. Land, M. T. Wright, T. A. Johnson, et M. K. Landon. 2018. « Origin of Methane and Sources of High Concentrations in Los Angeles Groundwater ». *Journal of Geophysical Research: Biogeosciences* 123 (3): 818-31. https://doi.org/10.1002/2017JG004026.

Lamb, Brian K., Maria O. L. Cambaliza, Kenneth J. Davis, Steven L. Edburg, Thomas W. Ferrara, Cody Floerchinger, Alexie M. F. Heimburger, et al. 2016. « Direct and Indirect Measurements and Modeling of Methane Emissions in Indianapolis, Indiana ». *Environmental Science & Technology* 50 (16): 8910-17. https://doi.org/10.1021/acs.est.6b01198.

Lowry, David, Rebecca E. Fisher, James L. France, Max Coleman, Mathias Lanoisellé, Giulia Zazzeri, Euan G. Nisbet, et al. 2020. « Environmental Baseline Monitoring for Shale Gas Development in the UK: Identification and Geochemical Characterisation of Local Source Emissions of Methane to Atmosphere ». *Science of The Total Environment* 708 (mars): 134600. https://doi.org/10.1016/j.scitotenv.2019.134600.

Luber, G., K. Knowlton, J. Balbus, H. Frumkin, M. Hayden, J. Hess, M. McGeehin, et al. 2014. « Ch. 9: Human Health. Climate Change Impacts in the United States: The Third National Climate Assessment ». U.S. Global Change Research Program. https://doi.org/10.7930/J0PN93H5.

Maazallahi, Hossein, Julianne M. Fernandez, Malika Menoud, Daniel Zavala-Araiza, Zachary D. Weller, Stefan Schwietzke, Joseph C. von Fischer, Hugo Denier van der Gon, et Thomas Röckmann. 2020. « Methane Mapping, Emission Quantification, and Attribution in Two European Cities: Utrecht (NL) and Hamburg (DE) ». *Atmospheric Chemistry and Physics* 20 (23): 14717-40. https://doi.org/10.5194/acp-20-14717-2020.

Portier, Christopher J., Kimberly Thigpen Tart, Sarah R. Carter, Caroline H. Dilworth, Anne E. Grambsch, Julia Gohlke, Jeremy Hess, et al. 2010. « A Human Health Perspective On Climate Change: A Report Outlining the Research Needs on the Human Health Effects of Climate Change ».

Takano, Tsugumi, et Masahito Ueyama. 2021. « Spatial Variations in Daytime Methane and Carbon Dioxide Emissions in Two Urban Landscapes, Sakai, Japan ». *Urban Climate* 36 (mars): 100798. https://doi.org/10.1016/j.uclim.2021.100798.

Tate, Kevin R. 2015. « Soil Methane Oxidation and Land-Use Change – from Process to Mitigation ». *Soil Biology and Biochemistry* 80 (janvier): 260-72. https://doi.org/10.1016/j.soilbio.2014.10.010.

Tate, K.R., D.J. Ross, S. Saggar, C.B. Hedley, J. Dando, B.K. Singh, et S.M. Lambie. 2007. « Methane Uptake in Soils from Pinus Radiata Plantations, a Reverting Shrubland and Adjacent Pastures: Effects of Land-Use Change, and Soil Texture, Water and Mineral Nitrogen ». *Soil Biology and Biochemistry* 39 (7): 1437-49. https://doi.org/10.1016/j.soilbio.2007.01.005.

Weller, Zachary D., Duck Keun Yang, et Joseph C. von Fischer. 2019. « An Open Source Algorithm to Detect Natural Gas Leaks from Mobile Methane Survey Data ». Édité par Matthias Mauder. *PLOS ONE* 14 (2): e0212287. https://doi.org/10.1371/journal.pone.0212287.

WHO. 2003. « Climate change and human health - risk and responses summary ». 2003. https://www.who.int/globalchange/climate/summary/en/.

———. 2022. « Climate change and health ». 2022. https://www.who.int/news-room/fact-sheets/detail/climate-change-and-health.

Zazzeri, G., D. Lowry, R.E. Fisher, J.L. France, M. Lanoisellé, et E.G. Nisbet. 2015. « Plume Mapping and Isotopic Characterisation of Anthropogenic Methane Sources ». *Atmospheric Environment* 110 (juin): 151-62. https://doi.org/10.1016/j.atmosenv.2015.03.029.

ISSN 1582-1021
e-ISSN 2668-4764
Edited by “AUREL VLAICU” University
Arad, Romania

10.62591/Scien.Tech.Bull-Chem.FoodSci.Eng.2022.19.01

*Scien. Tech. Bull-Chem. Food Sci. Eng., Vol. 19 (XX), 2022, 10-14*

**Article**

# THE INVOLVEMENT AND ATTITUDE OF ROMANIAS IN PRO-ENVIRONMENTAL ACTIVITIES RELATED TO THE RISK OF MICROPLASTIC PARTICLES

**Valeria POP[1,2], Alexandru OZUNU[1,2,3]**

[1] Doctoral School "Environmental Science", Babes-Bolyai University, 1 M. Kogalniceanu Street,
400084 Cluj-Napoca, Romania
[2] Research Institute for Sustainability and Disaster Management Based on High Performance Computing, Faculty of Environmental Science and Engineering, Babeș-Bolyai University, 30 Fantanele Street, 400294 Cluj-Napoca, Romania; valeria.pop@ubbcluj.ro; alexandru.ozunu@ubbcluj.ro; orcid.org/0000-0001-9634-0787 (A.O.);
[3] Disaster Management Training and Education Centre for Africa (DiMTEC), University of the Free State, Nelson Mandela Street, Bloemfontein SA-9300, South Africa;
Corresponding author email: valeria.pop@ubbcluj.ro

**Abstract:** Microplastic particle (MPs) pollution is and will continue to be a real threat to the entire planet. There is still no clear and complete information about these effects of MPs. In the research area, the data held so far are enough to have reasons for concern about this global phenomenon that shows an upward trend in global plastic production. The persistence in all four environmental factors and the extreme diversity of MPs leads to high levels of uncertainty in hazard and exposure estimates for this type of risk.

Why do we produce plastic? Due to its durability, rigidity, and even abrasiveness. No technical and efficient way could eliminate nano and microplastic from the environment, and thus people's attitudes can play a significant role in reducing MPs emissions. Currently, few studies have examined how individuals perceive MPs. Our research is based on how Romanians perceive risks (MPs) and how such risk perception affects people's pro-environmental behavioral intention. The entire study is based on a survey (questionnaire) of 405 people, from all over Romania. The software used is SPSS and the questionnaire was sent online through different types of platforms. GDPR rules were taken into account when preparing the questionnaire so that respondents are not asked for their personal data. One of the questions in the questionnaire measures the following statements on a scale from 1 to 7: "Dedicating time, money and effort to my activities is more convenient for me than recycling plastic products"/ "Dedicating time, money and effort is more convenient for me than replacing plastic items with ecological products. On the scale used, 1 represents - Categorically No / 7 - Categorically Yes. We made the delimitation by groups of counties/regions so that we can see a result of the attitude of Romanians from Banat, Transylvania, Maramureș, Oltenia, Moldova, and Dobrogea, in relation to MPs.

The results of our study show that in Romania, the recycling process is on an upward curve. We still do not have this culture of being friendly to the environment, as developed as in the West.

**Keywords**: microplastic, recycling, risk, survey, purchase decision, environment

## 1. INTRODUCTION

Reducing the production and input of plastic into the environment must be prioritized first of all through a global multidisciplinary approach, because improperly managed waste becomes a major source of plastic pollution in the soil, water, air, and biodiversity that can be reduced by improving the life cycle of plastics, especially in production, consumption, and disposal (Prata et al., 2019).

The global production of plastic materials reached 322 million tons in 2016, with a high percentage reached in Europe of over 39.9%, being mostly used in packaging (Plastics Europe, 2018). Estimates show that between

4.8 and 12.7 million metric tons of mismanaged plastic waste entered the world's oceans in 2010, inevitably affecting the entire food chain (Jambeck et al., 2015). These plastics, when exposed to different environmental conditions, fragment through photo and thermo-oxidative degradation thus producing particles <5 mm, known as microplastic particles (MPs) (Andrady, 2011).

These microplastic particles are an emerging and at the same time critical problem for the environment, due to their high resistance to degradation and bioaccumulation. Unfortunately, at the moment, current technologies for removing, recycling, or degrading microplastic particles are insufficient for complete elimination. Thus, the development of effective MPs removal methods as well as new plastic recycling strategies is strong points to build an MPs-free environment (Chen et al., 2022).

It is predicted that the total mass of accumulated plastic debris in the ocean could increase to 250 million metric tons by 2025(Jambeck et al., 2015). The level of concern around MPS is so high that governments worldwide are legislating against plastic production (Mitrano & Wohlleben, 2020).

To save the entire planet from this major danger, could we humans take some action?

We should not leave everything in the hands of governments. Our plastic recycling actions, replacing plastic items with more environmentally friendly ecological products, could lead to a decrease in production in the first place and not in the end to the protection of the environment. In the long term, through the actions of the population, even the improvement of human health could follow an upward, improving trend.

Are people's attitudes and perceptions important in reducing the danger of MPs?

Microplastic particles have a high capacity to absorb a large number of pollutants due to their small volume and large surface area. Therefore, MPs can bring many pollutants into different types of environments, thus endangering the stability of the entire ecosystem. Also, MPs can be easily swallowed by different marine species and thus can accumulate in their bodies reaching through the food chain to ultimately affect human health in the long term (Boucher & Friot, 2017; Carbery et al., 2018). Until now, there is no effective technical or chemical way to remove MPs once they have entered the environment. Faced with this problem, it is necessary to understand that people's attitudes and perceptions are important in reducing this danger (Che et al., 2014).

Research on MPs began at the beginning of the 21st century, but the focus has been on MPs in recent years since it became a subject of extreme interest for the press, which has grown exponentially (Klingelhöfer et al., 2020).

People's attitude plays an extremely important role in this type of risk that we encounter in this topic. It is not a foreseeable risk, because nothing similar has happened before. It is an unpredictable risk with a possible estimate of the level of loss and at the same time, it can be a partially controllable risk at the moment. In the future, if measures are taken (producers, governments, etc.), this risk can be transferred to the area of controllable risks. Mps without awareness and a manifestation of the need for environmental protection will affect our lives in the long run. Pollution with MPs is a real global danger and represents a threat to any form of life on the planet, and we, through our decisions and civic spirit, can help reduce this type of risk that affects all four environmental factors (water, air, soil, and biodiversity). Currently, it is not known exactly what is the impact of microplastic ingestion on the human body, nor what the maximum amount tolerated by it, and then returning to the question in the questionnaire, "it is important to dedicate time, money and effort to these types of activities related to the environment?

## Experimental and/or Modelling

### Study area

The area chosen for the study includes the entire territory of Romania, with respondents from 31 counties of the country as well as the Capital.

**Fig. 1.** Survey study area https://www.teoalida.ro/lista-judete/

## 2. Method

Questionnaire

Our survey is based on a questionnaire that was written in Romanian and carried out on an online platform and the link created for the questionnaire was distributed on Facebook, Instagram, WhatsApp, mail, Messenger, etc. The survey was subject to GDPR, the respondents being anonymous, and not asking for their data.

## 3. Results and discussions

The main question around which the data for the article resulted was: Is devoting time, money, and effort to my activity a more convenient activity for me than recycling plastic products? On a scale from 1-7, the respondents answered: (1- Definitely No and 7- Definitely Yes). The results related to the Romanians' actions regarding Recycling were divided among the largest regions of the country: Transylvania, Oltenia, and Moldova. Of course, a large percentage of those surveyed are not yet ready to make a major change in this MPs risk area. Fortunately, a large percentage was obtained between the two poles (1- definitely No and 7 - definitely Yes). This thing is encouraging and helped by many messages from the mass media and of course, with the help of the European legislation transposed at the national level, the percentage related to recycling could be on an upward curve in the future.

Figure number 2 analyzes the recycling process obtained in percentages following the survey, in the northwestern region of the country. A little over 9% of the respondents committed, that for the next 3 months, they will change some habits and introduce the recycling process into their daily activities, as a lifestyle. Percentage of over 20%, expressed their desire not to make a change in this area (1- definitely No), but over 10% of the respondents answered that they are still thinking, following this questionnaire. A percentage of almost 60% of the respondents from Transylvania answered that they are not sure, their daily life is attacked by many other problems, but they do not say no to the recycling process in the future, which is an encouraging thing.

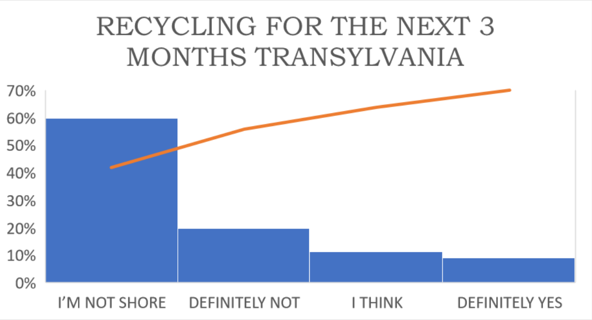

**Fig. 2.** Recycling for the next 3 months Transylvania

Following the survey for the south-eastern region of the country, figure 3, the percentages are identical both in accepting recycling actions (5%), and answering with an undecided (5%) to this process related to plastic. There may be some problems related to time, related to the ignorance of this type of risk, but no such questions were found in this questionnaire, only answers on a scale from 1-7 between yes and no. More than 40% of the respondents from Oltenia expressed their desire to think about and then make a decision related to the plastic recycling process. Here the percentage is much higher compared to the respondents from Transylvania. Below 50%, they are undecided, they are not sure and they do not know this environmental problem extremely well.

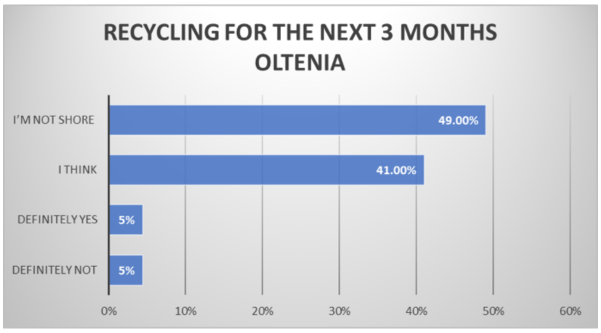

**Fig. 3.** Recycling for the next 3 months Oltenia

As can be seen in figure 4, 7% of those surveyed from the northeastern part of Romania proposed to introduce recycling actions in their households into their lifestyle for the next 3 months. Few under the percentage of 30% answered definitely no. This thing is not encouraging and actions of this type will be absent from their lives, even if more recently many supermarket chains encourage this recycling process, offering discounts and vouchers in exchange for plastic recycling.

Almost 20% are still thinking and over 40% are not sure.

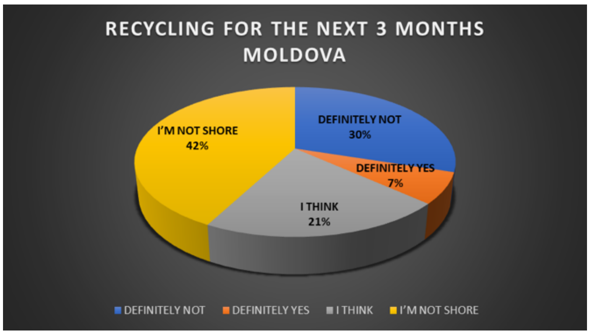

**Fig. 4.** Recycling for the next 3 months Moldova

## 4. Conclusions

In Romania, the recycling process is on an upward curve. We still do not have this culture of being friendly to the environment, as developed as in the West. Only a small percentage of over 9% of Romanians in Transylvania have committed that they will recycle in the next 3 months (Fig.2).

For the N-E part of the country, the percentage related to recycling is 6.7% (Fig.3). For the S-E part of the country, the percentages are similar, but very low at the same time, reaching a value of 5%, for those who answered 1- Definitely Yes. Those who answered 2 – categorically No, have an equally low percentage, which is encouraging, in increasing the percentage of plastic recycling (Fig 4).

There is a need for such actions either from governments, as I stated above, or from the media in the field of plastic recycling, but last but not least, a pro-environmental attitude, from each individual, could encourage the percentage of future plastic recycling.

In conclusion, people's attitudes could play an important role in reducing PM pollution, and concrete actions at the level of each individual could reduce the percentage of this type of risk, which acts along the food chain, affecting the environment and human health because the invasion of plastic waste has not been just a movie scenario for a long time, but a real threat to the entire planet. The anti-plastic directive, which aims to reduce the impact of single-use plastic products, had visible effects on Romanian society. New legislation for the entire European territory, new actions of non-governmental organizations, the mass media, and of course the attitude of the individual, all together can increase the percentage on the recycling curve and, last but not least, can lead to a decrease in plastic production.

As a result, MPs risk could be understood as an early exposure and contamination problem that could cause much greater damage and costs in the future if precautions are neglected (European Environment Agency, 2013).

## Limitations

The results of our study regarding the attitude and interest of Romanians related to the risk of microplastic particles are interesting, but our study may have some limitations. The first limitation would be the one related to Covid 19. The population was subjected to the survey following a blockade during the pandemic period. Secondly, a survey done on the Internet may have some limitations because people cannot be contacted face to face. Thirdly, a safety assessment of the risk of microplastics depends on certain factors, such as events in political and social life as well as certain personal experiences. The risk of MPs is a risk, which also results from our study, which is less known, is a snapshot of ongoing development and that is precisely why the study should be repeated.

## REFERENCES

Andrady, A. L. (2011). Microplastics in the marine environment. Marine Pollution Bulletin, 62(8), 1596–1605. https://doi.org/10.1016/j.marpolbul.2011.05.030

Boucher, J., & Friot, D. (2017). Primary microplastics in the oceans: A global evaluation of sources. IUCN International Union for Conservation of Nature. https://doi.org/10.2305/IUCN.CH.2017.01.en

Carbery, M., O'Connor, W., & Palanisami, T. (2018). Trophic transfer of microplastics and mixed contaminants in the marine food web and implications for human health. Environment International, 115, 400–409. https://doi.org/10.1016/j.envint.2018.03.007

Che, Y., Li, W., Shang, Z., Liu, C., & Yang, K. (2014). Residential Preferences for River Network Improvement: An Exploration of Choice Experiments in Zhujiajiao, Shanghai, China. Environmental Management, 54(3), 517–530. https://doi.org/10.1007/s00267-014-0323-x

Chen, J., Wu, J., Sherrell, P. C., Chen, J., Wang, H., Zhang, W., & Yang, J. (2022). How to Build a Microplastics-Free Environment: Strategies for Microplastics Degradation and Plastics Recycling. Advanced Science, 9(6), 2103764. https://doi.org/10.1002/advs.202103764

European Environment Agency. (2013). Late lessons from early warnings: Science, precaution, innovationSummaryEEA Report No 1/2013ISSN 1725-9177. https://www.eea.europa.eu/publications/late-lessons-2

Jambeck, J. R., Geyer, R., Wilcox, C., Siegler, T. R., Perryman, M., Andrady, A., Narayan, R., & Law, K. L. (2015). Plastic waste inputs from land into the ocean. Science, 347(6223), 768–771. https://doi.org/10.1126/science.1260352

Klingelhöfer, D., Braun, M., Quarcoo, D., Brüggmann, D., & Groneberg, D. A. (2020). Research landscape of a global environmental challenge: Microplastics. Water Research, 170, 115358. https://doi.org/10.1016/j.watres.2019.115358

Mitrano, D. M., & Wohlleben, W. (2020). Microplastic regulation should be more precise to incentivize both innovation and environmental safety. Nature Communications, 11(1), 5324. https://doi.org/10.1038/s41467-020-19069-1

Plastics Europe. (2018). Industry's reaction to the EC's Packaging and Packaging Waste Regulation (PPWR) proposal. https://plasticseurope.org/

Prata, J. C., Silva, A. L. P., da Costa, J. P., Mouneyrac, C., Walker, T. R., Duarte, A. C., & Rocha-Santos, T. (2019). Solutions and Integrated Strategies for the Control and Mitigation of Plastic and Microplastic Pollution. International Journal of Environmental Research and Public Health, 16(13), 2411. https://doi.org/10.3390/ijerph16132411

ISSN 1582-1021
e-ISSN 2668-4764
Edited by "AUREL VLAICU" University
Arad, Romania

10.62591/Scien.Tech.Bull-Chem.FoodSci.Eng.2022.19.02

*Scien. Tech. Bull-Chem. Food Sci. Eng., Vol. 19 (XX), 2022, 15-33*

**Article**

# WEATHERING AND DETERIORATION OF CARBONATE STONES FROM HISTORICAL MONUMENTS: A REVIEW

**Lorena Aliana Cioban[1], Mihaela DOCHIA[2], Claudia MUREŞAN[3], Dorina Rodica CHAMBRE[3*]**

*[1]Interdisciplinary School of Doctoral Studies, "Aurel Vlaicu" University, Romania, 2 Elena Drăgoi, Arad 310330, Romania*
*[2]Research Development Innovation in Natural and Technical Sciences Institute, "Aurel Vlaicu" University, Romania, 2 Elena Drăgoi, Arad 310330, Romania*
*[3]Faculty of Food Engineering, Tourism and Environmental Protection, "Aurel Vlaicu" University, Romania, 2 Elena Drăgoi, Arad 310330, Romania*
*Corresponding author email: dorinachambree@yahoo.com*

**Abstract:** *The degradation of historical monuments due to atmospheric and anthropogenic factors is a frequently encountered phenomenon on all continents, being intensively investigated to understand the type and degree of damage and to choose an appropriate restoration method. Based on extensive bibliographic documentation, this study presents a comprehensive review of the physical, chemical, and biological weathering processes induced by extrinsic factors (atmospheric, biological, and anthropic) that lead to the deterioration of limestone and marble, the most common construction materials found in historic buildings of humanity's architectural heritage.*

**Keywords**: heritage building, historical monuments, limestone, marble, weathering, deterioration, extrinsic factors

## 1. INTRODUCTION

Historical monuments constitute the architectural heritage of each country and include thousands of history years. They are present in a wide range of architectural styles and have an important economic, touristic, and cultural role for humanity (Kanani and Zandi, 2011). Practically, historical heritage represents the identity and pride of each country and contributes to maintaining the culture and tradition of the respective country. Unfortunately, world heritage buildings and monuments were not built to withstand the aggressive action of today's air pollutants and, since many of them are located in or near industrial cities, they have developed considerable damage over time (Fistos et al., 2022). Therefore, the accurate diagnosis of the building's materials' deterioration together whit choosing the appropriate methods for reconditioning process of the historical monuments are important nowadays aspects. Atmospheric weathering of building materials (i.e. stone) is defined by Vergès-Belmin et al. as "the result of natural atmospheric phenomena on the surface" while deterioration is "any chemical or physical change in intrinsic properties that lead to a loss of value or use" (Vergès-Belmin and Siedel, 2005). Atmospheric weathering and deterioration processes led to building materials degradation and the decay of the monuments. Over time, historic building materials such as natural stones, bricks, mortars, and concrete, etc. have been weathered as a result of daily and seasonal changes in temperature and humidity, wind, snow, and rain, transported soluble salts of water, air pollutants, bacteria, plants, and plant roots, etc. (Cardell et al., 2008; Fistos et al., 2022; Oguchi and Yu, 2021; Saltık, 2018; Sena da Fonseca et al., 2020). Natural factors have acted on heritage buildings since their construction. Even Herodotus mentioned in his History that the stone materials of the pyramids from Egypt were already damaged when he saw them in the 5th century BC

(Oguchi and Yu, 2021). Starting with the industrial revolution, the world's built heritage developed significant deteriorations induced by the increasing concentration of some pollutants in the atmosphere (i.e. $SO_2$, $NO_2$, material particles, PM, etc.) (Mascaro et al., 2022; Olaru et al., 2010; Reyes-Trujeque et al., 2016; Saltık, 2018; Vidal et al., 2019).

To create a sustainable urban and non-urban environment with an appropriate managerial development plan, it is important to study the degradation degree of heritage monuments determined by atmospheric pollutants and climate changes. This is valid both for the correct planning of their restoration and conservation process, and for the monitoring of the pollution sources themselves (Bogdan et al., 2022; Fistos et al., 2022). Atmospheric pollution is a main challenge for urban and sub-urban areas both in terms of development policies and traffic efficiency strategies connected with aspects related to the protection of cultural heritage. The change in climatic factors (e.g. precipitation, wind circulation, large temperature variations, etc.), caused by the increase in the level of pollution, generates a series of negative effects that determine the accelerated decay of historical monuments that are part of the UNESCO cultural heritage (Bogdan et al., 2022; Sesana et al., 2021; Vyshkvarkova and Sukhonos, 2023).

Rainwater, combined with gaseous air pollutants (i.e. $SO_2$, $NO_2$), leads to the formation of acid precipitations, and the formed sulphurous, sulphuric, and nitric acids can react with the calcite ($CaCO_3$) from limestone, marble, concrete, mortar, etc. causing the surfaces' destruction in the exposed areas of the monuments. Additionally, acid precipitations can dissolve limestone by direct contact. (Basu et al., 2020; Battista and de Lieto Vollaro, 2017; Vidal et al., 2019). Dry and wet acidic deposits together with water, moulds, and lichens are the main degradation factors causing irreversible structural damage and aesthetic problems to the buildings and statues (Comite et al., 2020b; Hall and Hall, 1996; Mascaro et al., 2022).

A recent study by Spezzano P. in 2020 provided an estimate of the air pollution effects on the cultural sites included in the UNESCO World Heritage throughout Europe. In this study, the potential risk for UNESCO heritage monuments in the EU was evaluated based on exceeding the tolerable degradation thresholds recommended for each type of construction material (Spezzano, 2021). The results highlighted that, despite the improvements in the air quality at the European level noticed in the last decades, air pollution is still significant and continues to play an important role in the processes of cultural heritage degradation, especially in densely populated urban and sub-urban areas with intense traffic and polluting industrial activities (Spezzano, 2021; Török et al., 2011).

According to Kanani and Zandi, the factors that lead to the deterioration of historical monuments can be classified as follows: natural factors with instantaneous function (i.e. earthquakes, lightning, natural fires, floods, etc.); natural factors with gradual function; physical factors (wind, sunlight, changes in humidity, temperature changes, etc.); chemical and electrochemical factors (atmospheric pollutants and acid rain that lead to dry and wet acid deposition); plant destructive factors (plants and micro-plants); biological and microbiological factors; complex factors; social factors due to profit or negligence and defective management (Kanani and Zandi, 2011). These extrinsic factors act synergistically with intrinsic factors of the building materials (i.e. mineralogy, chemical composition, porosity, permeability, strength, fractures, etc.) causing decay of the historic heritage by various weathering and deterioration processes such as salts crystallization and dissolution, freeze-thaw, Krast effect, efflorescence and sub-florescence, black crust depositions, etc., (Kryza et al., 2009; Livingston, 2016; Pappalardo et al., 2022; Vidal et al., 2019) as can be seen in **Figure 1.**

The weathering and deterioration processes of building materials can occur on the entire surface of monuments and buildings or only in certain more exposed and reactive areas (Aucouturier and Darque-Ceretti, 2007; Badouna et al., 2020; Bogdan et al., 2022; Cardell et al., 2008; Kanani and Zandi, 2011; Kryza et al., 2009; Livingston, 2016; Olaru et al., 2010; Vidal et al., 2019).

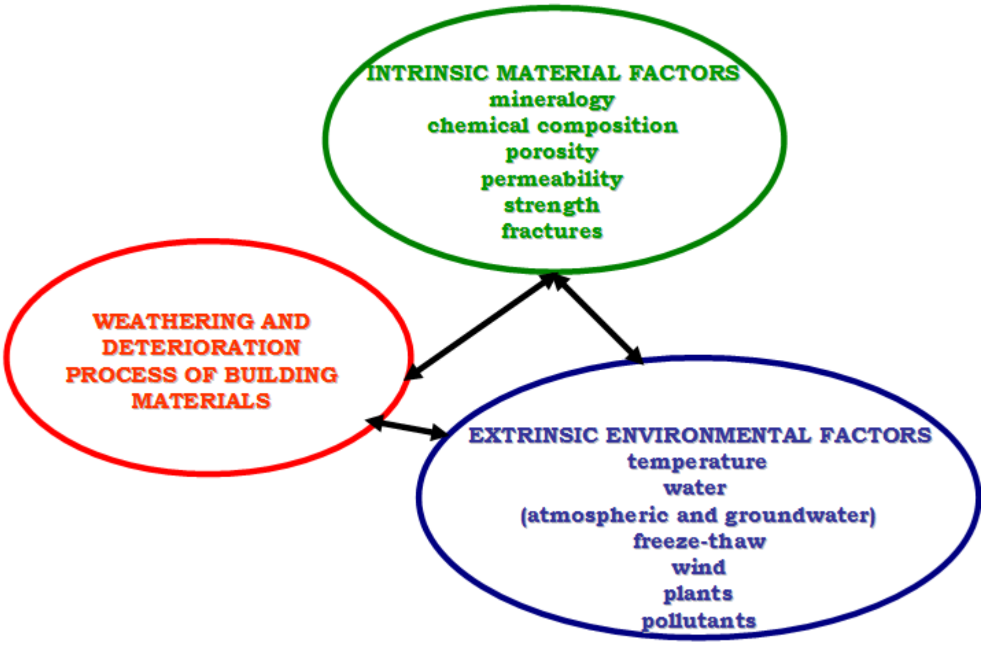

**Figure 1**. Synergistically interaction of extrinsic and intrinsic factors leads to weathering/ degradation processes of heritage materials

The paper aims to present a comprehensive review of the most important weathering and deterioration (degradation) processes induced by extrinsic factors (atmospheric, biological, and anthropic) and their effect on the carbonic stones materials (limestone and marble) from historical monuments. For this purpose, 74 articles published in indexed specialized journals were selected, of which ~40% are recent studies published in the 2019-2023 period.

## 2. NATURAL STONES AS BUILDINGS MATERIALS FOR THE HERITAGE STRUCTURES

One of the oldest natural materials used for buildings, monuments, and statues is stone. In general, the stone has a porous structure and the chemical composition consists of different minerals such as carbonates, silicates, and alumino-silicates (Bogdan et al., 2022).

Natural stones that have been used over time as building materials can be classified as follows:

- inclusive rocks (granite, gabbro, anorthosite, etc.);
- extrusive rocks (basalt, andesite, etc.);
- sedimentary rocks (sandstone, limestone, dolomite, diatomite, etc.);
- metamorphic rocks (marble, travertine, etc.).

Despite the unique properties of stones, environmental pollutants can damage them (Vidal et al., 2019). The stone's surface may undergo structural changes as a result of the interaction with various physical, chemical, and biological factors. According to Aucouturier and Darque-Ceretti the stone's deterioration surface is "a superficial thin layer with a different composition from the stone's bulk and unique characteristics due to the disturbances that have taken place such as roughness, colouration, black crust, etc." (Aucouturier and Darque-Ceretti, 2007)

The attack of atmospheric pollutants, the dissolution and crystallization of salts in water, and the neutralization of rain acidity are the main physicochemical processes that cause the deterioration of the stone surface. An important role is also played by biological factors such as cyanobacteria, mosses, lichens, algae, etc. which cause bio-deterioration processes (Schiavon, 2002).

Frequently found in nature, limestone is a rock with a soft structure, being composed of calcite and aragonite ($CaCO_3$) or sometimes, of dolomite (double carbonate of calcium and magnesium, $[CaMg(CO_3)_2]$). Limestone was formed either by biological processes (i.e. accumulation of coral and shell fossils, etc.) or by non-biological processes such as precipitation of minerals from water containing dissolved calcium (Corvo et al., 2010; Schiavon et al., 2004; Wahab et al., 2019). Limestone often contains fossils, as can be seen in **Figure 2,** which provide interesting information on ancient environments and the evolution of life.

Major geological events caused some natural limestone deposits to undergo a series of metamorphic changes that led to calcite re-crystallization in the form of marble (Amer Khalil, 2020).

Travertine, a carbonate non-foliated stone, is a form of terrestrial limestone that occurs around mineral or thermal springs by rapid precipitation of $CaCO_3$ dissolved in water. Usually, travertine has a fibrous or concentric appearance, but there are also varieties of white, brown, cream, and even rust, depending on the metal oxides present (i.e.$Fe_2O_3$). It is the most frequently encountered variant of limestone in caves where it can form stalactites, stalagmites, and other speleothems. Since ancient times, limestone and marble have been widely used in architectural applications for buildings, walls, ornamental-decorative details, and statues (Amer Khalil, 2020). Many of the monuments included in the UNESCO world heritage were built from limestone and marble, some of the most famous ones being shown in **Figure 3**.

Due to their structure and chemical composition, calcareous stones are vulnerable to weathering and deterioration processes, many studies reported the results related to the effect of natural factors and acidic atmospheric pollutants on these materials (Basu et al., 2020; Comite et al., 2020b; Fistos et al., 2022; Ivaskova et al., 2015; Kanani and Zandi, 2011; Mascaro et al., 2022; Vidal et al., 2019; Vyshkvarkova and Sukhonos, 2023; Wahab et al., 2019).

## 3. DETERIORATION OF CARBONATE STONES

In the following paragraphs, we will briefly present the most important natural and anthropogenic factors involved in the degradation of carbonate stone materials, emphasizing the weathering and deterioration processes generated by these factors. The deterioration types of the carbonate stones are schematically presented in **Figure 4**.

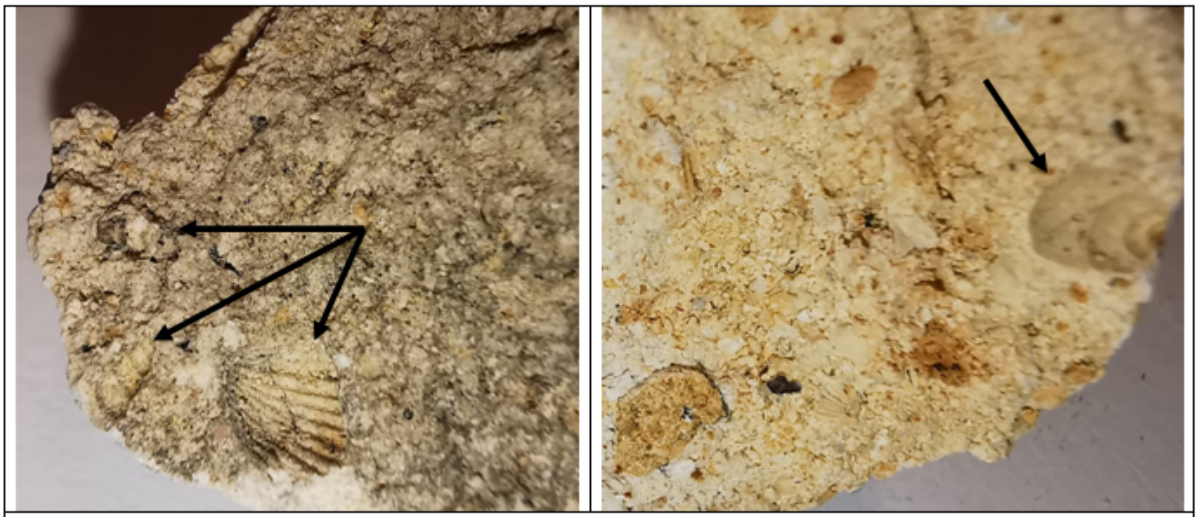

**Limestone with seashell and snail fossils**
Samples taken from Limestone street wall, Eternitatea Cemetery, Arad, Romania
photo by D.R.C.

**Figure 2.** Natural limestone formed by biological processes

Taj Mahal, India (marble)

Marble Arch in London, England

Davide di Michelangelo statue, Firenze, Italy (marble)

The Pantheon in Athens, Greece (limestone)

The Great Pyramid of Giza, Egypt (limestone)

The limestone temple, Sarmisegetusa Regia Dacian fortress, Hunedoara, Romania

**Figure 3.** World heritage monuments and statues from carbonate stones

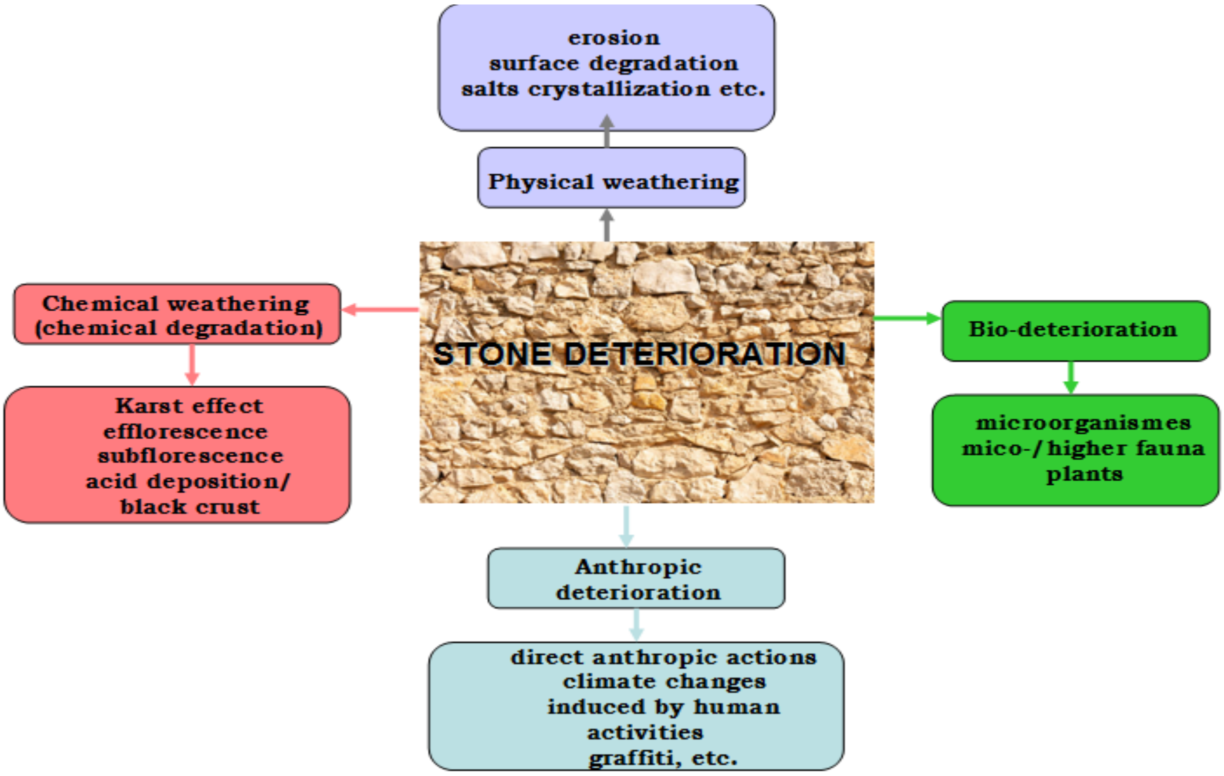

**Figure 4.** Deterioration types of the carbonate stones

### 3.1. Physical weathering

Physical weathering is a natural process for most types of stone materials, but it is predominant in the case of carbonate stones. This damage type is caused by some natural factors such as winds, temperature variations, humidity, etc. (Reyes-Trujeque et al., 2016; Saltık, 2018). In the presence of abrasive particles, the winds lead over time to the erosion of the carbonate materials' surfaces. Water from the atmosphere (precipitation, atmospheric humidity) or underground (phreatic water) plays an important role in the physical weathering of limestone and marble.

The presence of water can lead to the degradation of the stone's surface through expansion/contraction phenomena or freeze/thaw cycles, generating cracks, exfoliation, spalling, delamination, or descaling of the contour (Fistos et al., 2022; Pappalardo et al., 2022; Vidal et al., 2019). In **Figure 5**, some heritage structures degraded by physical weathering processes are exemplified.

Another predominant mechanism that causes physical weathering is the salts' crystallization induced by humidity and temperature variations. A decrease in the relative humidity inside the stones causes an increase in the concentration of some salts (in a dissolved state) in the material's pores. These salts, which come from the chemical structure of stone, masonry, and finishing mortars, the capillary migration of ions from the soil, agricultural works, de-icing solutions, metabolites of micro-organisms, etc. can finally crystallize inside the pores.

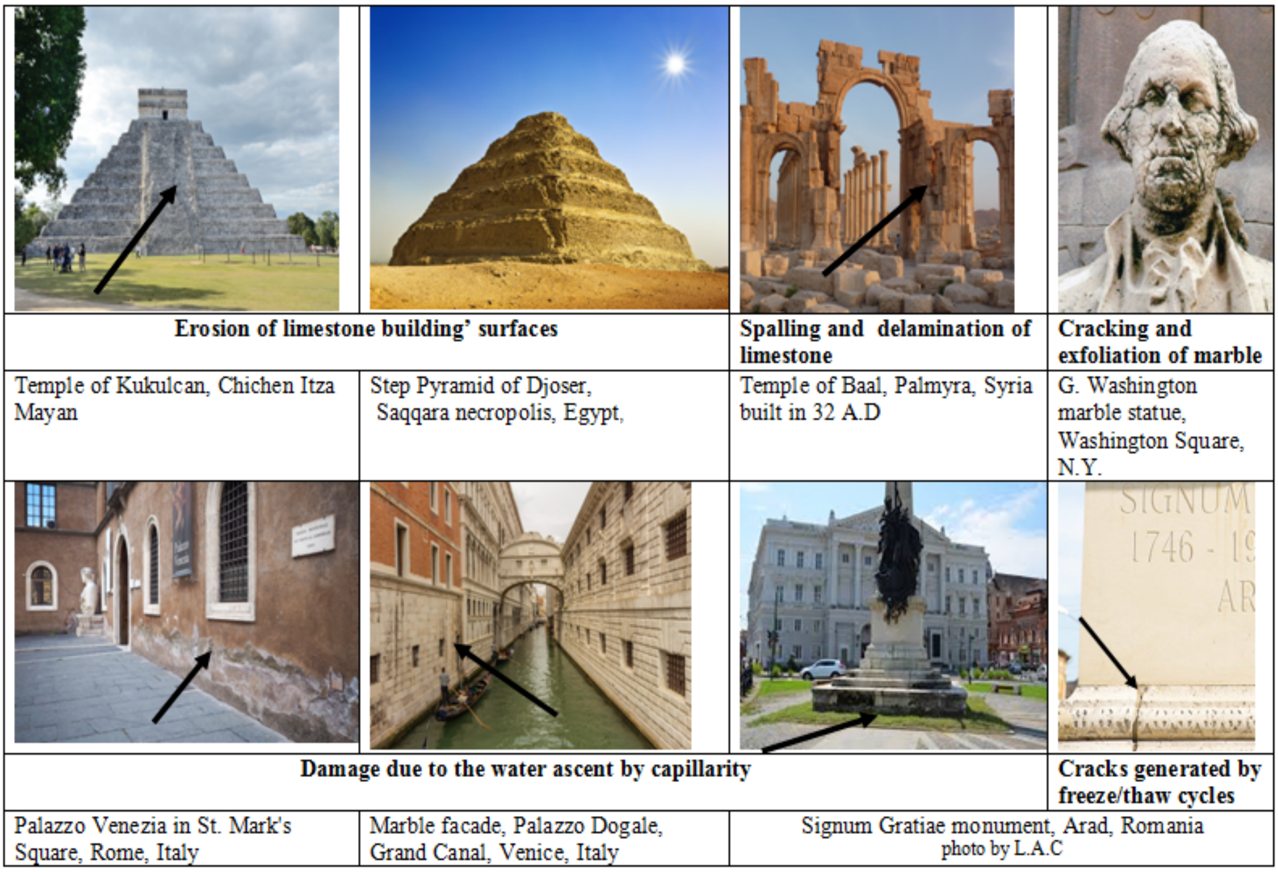

**Figure 5.** Heritages' deterioration due to physical weathering processes

As the relative humidity increases, the crystals are rehydrated/ dissolved, and thus repeated crystallization/rehydration cycles can create significant mechanical stress on the stones, thereby causing physical weathering (also called "salts weathering") (Cardell et al., 2008; Comite et al., 2020b; Fistos et al., 2022; Oguchi and Yu, 2021; Vidal et al., 2019).

According to Pappalardo et al., the pressures generated by salts' crystallization in the pores of carbonate rocks (resulting from the percolation of supersaturated solutions through the rock) are a major cause of the alveolar structures formation called "honeycombs". (Pappalardo et al., 2022). Many studies have shown that weathered carbonate stones from historical constructions widely present visible cavities (alveoli) variable in shape and size (Frank-Kamenetskaya et al., 2009; Gulotta et al., 2013; Oguchi and Yu, 2021; Reyes-Trujeque et al., 2016; Saltık, 2018). This phenomenon is amplified by the abrasive effect of the incoherent rocks, which are taken over by the turbulent air currents, thus contributing to the increase in the size of the cavities where salt crystallization takes place (Cardell et al., 2008; Oguchi and Yu, 2021; Weththimuni et al., 2022), as can be seen in **Figure 6.**

Computer modeling of experimental results together with a pragmatic case analysis has contributed to the improvement of the practical methods used to limit the building's materials damage due to the “salt weathering” phenomenon (Weththimuni et al., 2022).

The damage caused by the development of some plants or plant roots (**Figure 7.**) in the existing cracks of the constructions can also be considered physical weathering (Mascaro et al., 2022).

Earthquakes, landslides, or massive floods play an important role in the physical damage to buildings and monuments.

| **"Honeycombs weathering"** | **Visible cavities (alveoli)** | **Salt crystals grown in the pores of the calcareous material** |
|---|---|---|
| Signum Gratiae monument, Arad, Romania<br>photo by L.A.C | Limestone street wall, Eternitatea Cemetery, Arad, Romania<br>photo by L.A.C | Limestone street wall, Holy Trinity Cathedral, Arad, Romania<br>photo by L.A.C |

**Figure 6**. The “salts weathering” of the limestone material

| The Leshan Giant Buddha, China | The Franciscan Church inside the Arad Fortress, Arad, Romania<br>photo by L.A.C | Şoimoş Fortress, Arad, Romania<br>photo by L.A.C |
|---|---|---|

**Figure 7.** Plants growing between stones of historic buildings

### 3.2. Chemical weathering

The chemical weathering, also called "chemical degradation", of stone materials represents the change in stone composition caused by several chemical processes and leads to the surface's deterioration.

According to Pappalardo et al., chemical weathering of the stone is a spontaneous and irreversible degradation process that leads the affected material to a more stable state under given temperature and pressure conditions (Pappalardo et al., 2022).

#### *3.2.1. Karst effect*

The Karst effect is one of the most frequent weathering processes that particularly affects limestone and refers to the natural dissolution of calcareous stones in the presence of clean water (pH ~ 5.6) (Cardell et al., 2008; Fistos et al., 2022; Vidal et al., 2019). The fact that calcite is naturally soluble in pure water leads to a natural dissolution of stone by rain. In the presence of atmospheric $CO_2$ and humidity, the carbonation reaction takes place on the carbonate stone surface.

The Karst effect represents the chemical transformation of calcium carbonate ($CaCO_3$) into calcium bicarbonate ($Ca(HCO_3)_2$) in the presence of dissolved carbon dioxide ($CO_2$) in rainwater ($H_2O$) according to eq.1.

$$CO_{2(g)}+H_2O_{(l)}+CaCO_{3(s)} \Leftrightarrow Ca\left(HCO_3\right)_{2(aq)} \quad (1)$$

insoluble soluble

Fistos and col. showed that, the Karst effect is amplified by the increase in $CO_2$ concentration due to anthropogenic pollution and can cause an increase in the stone pH through the carbonic acid formation and subsequent processes which are necessary to restore the chemical equilibrium (Fistos et al., 2022). The aggressive $CO_2$ action is more intense in urban areas than in rural, where, it is known that the $CO_2$ concentration is higher and the precipitations' pH is lower (acid rain).

According to Fassina, the action of acid precipitation on limestone and marble surfaces can cause the re-crystallization of water-soluble calcium bicarbonate (Fassina, 1988). Carbon dioxide dissolved in water tends to evaporate when the solution temperature increases and, consequently, the following reaction (eq.2) takes place:

$$Ca\left(HCO_3\right)_2 \rightarrow CaCO_3 + CO_2 + H_2O \quad (2)$$

The calcium carbonate formed has larger crystals and a more porous structure than the original calcite (from the carbonate rock), which is microcrystalline and non-porous. The increase of stone's surface porosity due to the re-crystallization process of calcium bicarbonate is a harmful phenomenon because it allows acid precipitations containing sulfuric acid and soluble salts (e.g. sulfates and chlorides) to penetrate deeper into the stone and accelerate its degradation.

#### *3.2.2. Efflorescence and Subflorescence*

Efflorescence is caused by salts crystallization (e.g. sulfates, nitrates, chlorides, and carbonates of sodium, potassium, and calcium, etc.) and their deposition on the stone' surface (Pappalardo et al., 2022), as can be seen in **Figure 8**. Efflorescence (also called "white crust" or "white deposit") is considered a chemical weathering process, and its presence has been observed in the last decades on the surfaces of many heritage monuments (Benavente et al., 2021; La Russa et al., 2015; Oguchi and Yu, 2021; Pappalardo et al., 2022; Přikryl et al., 2007). Salts can act both as a physical force and saline solutions which increases the dissolution rates of minerals into rocks (Benavente et al., 2021). Since this process involves the presence of water, the appearance of white deposits suggests the existence of water infiltration phenomena through the rock and the related consequences, previously presented. It has been observed that the efflorescence caused by salts can lead to haloclastic ruptures of the materials, being a serious problem for construction (Benavente et al., 2021; Pappalardo et al., 2022; Vergès-Belmin and Siedel, 2005). In the case of natural carbonate stones, the overpressure generated by the salt crystals causes them to exfoliate through a progressive detachment of the shallower portions.

According to Pappalardo et al., the results of crystallization and precipitation of salts below the building material surface causing spalling and/or flaking are recognized as sub-florescence (Pappalardo et al., 2022). If efflorescence is relatively easy to remove, sub-florescence is difficult to remove because it forms below the rock surface (Mineo et al., 2022; Pappalardo et al., 2020). Studies have shown that porous calcite formed by the re-crystallization process of calcium bicarbonate plays an important role in efflorescence and sub-florescence formation (Oguchi and Yu, 2021; Pappalardo et al., 2022; Pappalardo et al., 2020).

### *3.2.3. Black crust*

The black crust, also called “black patina”, is an indicator of the chemical weathering/degradation of heritage monuments due to atmospheric pollution and defines “accumulation areas of the resulting compounds from the chemical alteration of carbonate rocks and of the atmospheric particle depositions” (Rodrigues, 2015; Sabbioni et al., 2001). The black crust is a superficial layer with a porous structure composed mainly of gypsum crystals ($CaSO_4.2H_2O$) in which atmospheric dust, materials particle, organic compounds, metals, etc. can be entrapped or some microorganisms can develop.

The primary atmospheric pollutants causing black crust formation on the carbonate stone surface are sulphur dioxide ($SO_2$), nitrogen dioxide ($NO_2$), and particulate matter (PM). Interaction mechanisms between acid atmospheric gases and building carbonate materials occur via dry and wet depositions (Bogdan et al., 2022; Kryza et al., 2009; Olaru et al., 2010). The dry and wet acid depositions can react with the $CaCO_3$ to generate $CaSO_4.2H_2O$, as is shown in the following equations (eq.3., eq.4., eq.5.):

(i) wet deposition reactions:

$$SO_2 \xrightarrow{+H_2O\ from\ atmpsphere} SO_2 \cdot H_2O \xrightarrow{catalytic\ oxidation} H_2SO_4(droplets) \xrightarrow{+CaCO_3/-(H_2O+CO_2)} CaSO_4 \quad (3)$$

$$SO_2 \xrightarrow{+1/2\,O_2\ c\ catalytic\ \ oxidation} SO_3(aerosol) \xrightarrow{+H_2O} H_2SO_4(droplets) \xrightarrow{+CaCO_3/-(H_2O+CO_2)} CaSO_4 \quad (4)$$

(ii) dry deposition reactions:

$$CaCO_3 + SO_2 \xrightarrow{H_2O/-CO_2} \begin{Bmatrix} CaSO_3 \cdot 1/2H_2O \\ CaSO_3 \cdot 2H_2O \end{Bmatrix} \xrightarrow{+1/2O_2\ and\ H_2O(atmosphere)} CaSO_4 \cdot 2H_2O \quad (5)$$

Because gypsum is more water soluble than calcite (2.4 g/L at 25°C), the majority of it can precipitate on the carbonate stone surfaces that are not washed directly by rain leading to the black crust formation (Comite et al., 2020b; Pozo-Antonio et al., 2022; Searle and Mitchell, 2006).

In areas subjected to rainwater washing, a fraction of gypsum is removed from the limestone surface by dissolving. This phenomenon leads to the loss of calcareous material and damage to the details of the monuments/statues. Additionally, new calcite layers are exposed to the acidic actions, and additional gypsum is formed (Comite et al., 2020b; Pozo-Antonio et al., 2022).

The development of the superficial gypsum layer on the limestone surface is a relatively rapid process and can be catalyzed by a series of metals and metal oxides (McAlister et al., 2008).

During the formation of the gypsum layer, some aerosol particles, carbon particles from the air, or particles originating from anthropogenic activities (e.g. fuel burning, transport, construction, industrial activities, agriculture, etc.) can be trapped in the crystal matrix of gypsum and calcite and the formed layer may darken over time resulting the black crust (Searle and Mitchell, 2006; Urosevic et al., 2012) Black crust is considered to be one of the most dangerous deterioration forms of building materials caused by anthropogenic air pollution (Battista and de Lieto Vollaro, 2017; Comite et al., 2020a). Based on the stratographic studies carried out by Ivaskova et. al. and Schiavon et al. it was discovered that the black crusts grow both inwards and outwards to the original surface of the stone (Ivaskova et al., 2015; Schiavon, 2002; Schiavon et al., 2004).

Nitrogen dioxides ($NO_2$) are also important atmospheric pollutants with acidifying effects on limestone and marble. Along with $H_2SO_4$, nitric acid plays an important role in wet and dry acid depositions. Although $HNO_3$ can react with calcium carbonate in limestone leading to calcium nitrate [$Ca(NO_3)_2$] formation, still, its role in the deterioration process of carbonate stone is not very clear (Reyes-Trujeque et al., 2010).

Even if marble is more compact than limestone, it is affected by dry and wet acid depositions and forms superficial layers of black crusts but at a lower rate (Christodoulakis et al., 2017; Ruffolo et al., 2015). Bugini et al., studying the kinetics of the black crust formation process on the surface of two Carrara marble monuments, showed that the amount of gypsum formed per surface unit was 5-13 mg/cm$^2$, and the formation rate of gypsum in the black crust was about 0.2 mg/cm$^2$ per year (Bugini et al., 2000).

Studies on the chemical composition of black crusts have shown that, in addition to gypsum crystals, they may contain traces of iron oxides, heavy metals, elements of the stone substrate such as quartz and calcite, organic compounds, elementary carbon, alkaline chlorides, dust, etc. In some cases, even traces of calcium oxalate resulting from the partial oxidation of organic carbon were found. (La Russa et al., 2018; La Russa et al., 2017; McAlister et al., 2008; Pozo-Antonio et al., 2022; Vidal et al., 2019).

The formation of black crusts is a complex process that is sometimes correlated with the growth of bacteria, algae, lichens, and fungi (Li et al., 2018; Ortega-Morales et al., 2019; Pinheiro et al., 2018; Schiavon, 2002). **Figure 8** shows some limestone and marble monuments affected by chemical weathering processes.

### *3.2.4. Analytical techniques for characterizing the limestone chemical weathering*

Various investigative techniques have been employed to characterize the stone materials from historic buildings or monuments as well as the composition of the black crust. Thus, techniques such as optical microscopy (OM), polarized light optical microscopy (PLOM), and fluorescence optical microscopy (FLOM) were used in petrographic and topographic analysis both to determine the textural characteristics of carbonate stone and to evaluate the morphology and the growth rate of black crusts (Cardell et al., 2008; Comite et al., 2020b; Gulotta et al., 2013; La Russa et al., 2017; Pozo-Antonio et al., 2017).

X-ray powder diffraction (XRPD) and X-ray fluorescence (XRF) techniques were used to investigate the carbonate stone and black crusts' mineralogical composition (Comite et al., 2020a; Comite et al., 2020b; Graue et al., 2013; Wahab et al., 2019).

Electron microscopy technique (SEM) was specifically used to acquire images of carbonate stones and black crusts at high magnification (Comite et al., 2020a; Comite et al., 2020b; Graue et al., 2013; Pozo-Antonio et al., 2022; Wahab et al., 2019; Zhao et al., 2019), and coupled with energy dispersive X-ray spectrometry (EDX) was a useful technique for obtaining information about the micro-morphology and chemical composition, in terms of major elements, of the building materials and black crusts (La Russa et al., 2018; La Russa et al., 2017; Livingston, 2016; Vyshkvarkova and Sukhonos, 2023; Zoghlami et al., 2019).

Laser ablation–inductively coupled plasma–mass spectrometry (LA-ICP-MS) was useful for geochemical composition analysis in terms of elements traces of the black crusts (Comite et al., 2020b; Pozo-Antonio et al., 2022; Ruffolo et al., 2015).

Atomic force microscopy (AFM) provided real three-dimensional topographies that showed the surface properties of the carbonate stones (Pozo-Antonio et al., 2022; Zhao et al., 2019).

Fourier transform infrared spectroscopy coupled with attenuated total reflectance (FTIR-ATR) was performed to identify the mineralogical phases of the carbonate building materials and also identify the presence of black crusts and entrapped organic and silicate compounds (La Russa et al., 2018; La Russa et al., 2017; McAlister et al., 2008; Ruffolo et al., 2015).

Thermogravimetric analysis (TGA/DTG) coupled with differential thermal analysis (DTA) was used to determine the content of moisture and calcium carbonate in calcareous materials, as well as to determine the content of elemental carbon (EC), inorganic carbon (AC) and organic (OC) from black crusts (Comite et al., 2020b).

Ion chromatography (IC) has been employed for quantification of the main ions from black crusts (Zhao et al., 2019).

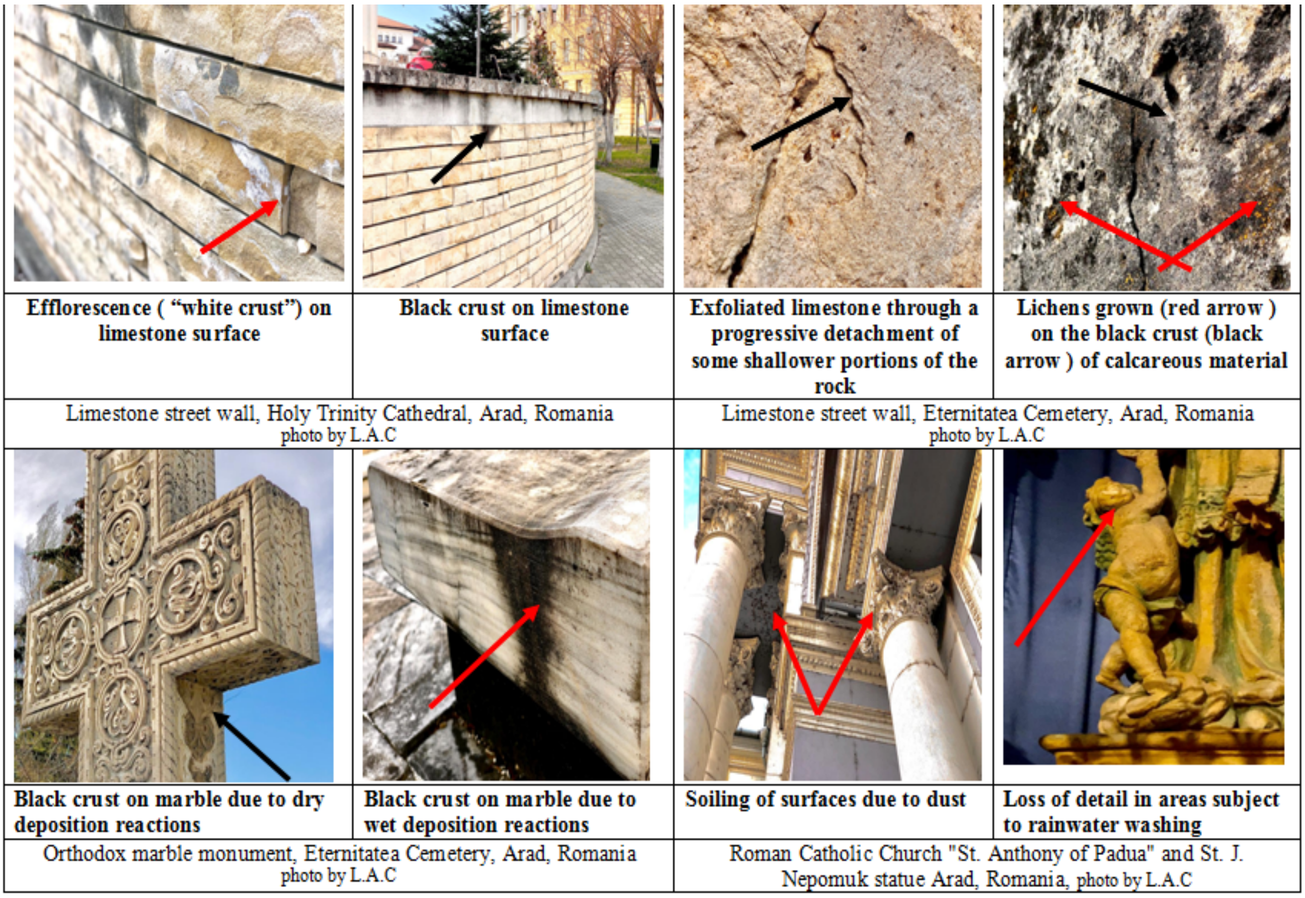

**Efflorescence ( "white crust") on limestone surface**

**Black crust on limestone surface**

**Exfoliated limestone through a progressive detachment of some shallower portions of the rock**

**Lichens grown (red arrow ) on the black crust (black arrow ) of calcareous material**

Limestone street wall, Holy Trinity Cathedral, Arad, Romania
photo by L.A.C

Limestone street wall, Eternitatea Cemetery, Arad, Romania
photo by L.A.C

**Black crust on marble due to dry deposition reactions**

**Black crust on marble due to wet deposition reactions**

**Soiling of surfaces due to dust**

**Loss of detail in areas subject to rainwater washing**

Orthodox marble monument, Eternitatea Cemetery, Arad, Romania
photo by L.A.C

Roman Catholic Church "St. Anthony of Padua" and St. J. Nepomuk statue Arad, Romania, photo by L.A.C

**Figure 8.** Chemical weathering (chemical degradation) of limestone and marble building materials

### *3.2.5. Soiling*

Along with the black crust, the soiling phenomenon leads to the darkening of the heritage buildings' surfaces (**Figure 8**.- the case of the street facade at the entrance to the Roman Catholic Church "St. Anthony of

Padua", Arad, Romania). Although it is related to the formation of dark depositions, soiling is not a chemical degradation process because it represents an accumulation of dust particles on the non-reactive surfaces of buildings and statues. Unlike the black crusts consisting of gypsum and calcite crystals, the solid particles accumulated in the soiling layer can be easily removed by a washing treatment. The soiling phenomenon of the facades depends on several factors, such as meteorological factors, wind-rain interaction, porosity and roughness of the surfaces, the facade's setup, the inclination of the walls and windows, the existence of architectural edges, etc. (Urosevic et al., 2012; Vidal et al., 2019; Weththimuni et al., 2022). All these factors act synergistically leading to localized accumulations of dust and dirt particles. According to Grosii and Brimblecombe, the soiling process of the buildings and monuments is only an aesthetic problem, largely dependent on the degree of public acceptance (Grossi and Brimblecombe, 2004).

### 3.3. Bio-deterioration

The historical buildings' stones, due to the contained minerals, are ideal substrates for the growth and proliferation of various microorganisms such as cyanobacteria, algae, fungi, or some macroscopic organisms such as lichen mosses, plants (Li et al., 2018; Liu et al., 2022).

The microorganisms formed on the stones' surface so-called "biofilms" represent the microorganisms' growth communities. According to Mascaro et al., biofilms are complex mono- or multilayered systems of one or more species of microorganisms that can grow attached to any solid substrate and can excrete protective materials, usually proteins and sugar polymers, to produce extracellular exopolysaccharides matrix (EPS) in which phototrophic and heterotrophic organisms are incorporated. (Mascaro et al., 2022). From bacterial metabolism, a series of secondary acidic compounds (i.e. oxalic acid) can result that cause chemical degradation of stone materials. In addition, EPS accelerates the physical deterioration processes of materials, as the biofilm swells and shrinks in the stones pore network, which can cause micro-fractures (Skipper et al., 2016; Warscheid and Braams, 2000). The composition of the biofilm microbiota depends on various factors, such as environmental ecology, microbial biodiversity, climatic conditions, physico-chemical properties of the stone substrate, nutrient availability, etc (Ortega-Morales et al., 2019). The aspect and color of biofilm depend on microorganisms' growth level, microbiological formations thickness, surrounding environment characteristics, and type of biocenosis (Mascaro et al., 2022; Pinheiro et al., 2018).

The algal partner, also called photobiont, through the process of photosynthesis and $CO_2$ fixation produces polysaccharides that constitute food for the fungal partner (Liu et al., 2022). This helps the fungus survive in nutrient-poor conditions. On the other hand, algae take advantage of the fungus presence that protects them from the action of UV radiation and ensures the necessary humidity for their development. According to Warscheid and Braams, fungi form a dense crust around an inner layer, the latter being composed of loose hyphae associated with algal cells (Warscheid and Braams, 2000).

A pair of symbiotic organisms consisting of an alga (or cyanobacteria) in close spatial and physiological association with a fungus forms lichens with different thallus (e.g. foliose lichens form a coral-like thallus; fruticose lichens form a leaf-like thallus; squamulose lichen forms a flat thallus with small lobes at the top, etc.). The symbiotic relationship between fungus-algae/cyanobacteria favors the lichen's development on stones that are poor in nutrients and arid places (Matteucci et al., 2019). In the case of stones and rocks, crustose lichens are predominating and can strongly adhere to surfaces (Cozzolino et al., 2022; Santo et al., 2021).

The bio-deterioration or bio-degradation phenomena due to some organisms or microorganisms can occur on all types of stone substrates and in all climatic zones (Paiva et al., 2022; Zhang et al., 2023).

For instance, in environments with natural light and high humidity, the phototrophic subaerial biofilm consisting of epilithic organisms is growing (Mascaro et al., 2022; Skipper et al., 2016) while in arid and semi-arid areas, the biodeteriogens that develop on stones' surfaces are black rock fungi, also known as rock-inhabiting fungi or micro-colonial fungi (Gadd, 2017; Isola et al., 2022).

According to Isola et al., the black rock fungi are a polyphyletic poikilotolerant morpho-ecological group excellently adapted to extreme temperature changes, drought, starvation, osmotic stress, and high ultraviolet solar radiation (Isola et al., 2022). Anyway, fungi are considered the most important colonizers of stones, being omnipresent on the surfaces of monuments and buildings in all climatic zones. Fungi are heterotrophic organisms with a more versatile metabolism than other biodeteriogenic agents, which allows them to colonize a wide range of substrates (e.g. wood, metal, stone, etc.) (Gadd, 2017; Liu et al., 2022; Paiva et al., 2022).

Bio-deterioration is defined as "any unwanted modification of a material caused by the vital activities of organisms or microorganisms" and is a secondary phenomenon that frequently occurs on buildings' stone surfaces (Mascaro et al., 2022; Ortega-Morales et al., 2019). The bio-deterioration is influenced by the stone's bio-receptivity, which represents the availability of a material to be invaded by a living species. Each heritage monument is characterized by its bio-receptivity that depends on several factors such as the construction structure, petro-physical and chemical properties of the building materials, materials' pH and moisture quantity, chemical or physical degradation degree of the surfaces, preservation state, weathering conditions or surrounding atmosphere pollution, etc. (Fistos et al., 2022; Liu et al., 2022).

The interaction between the building material and the biodeteriogen is a complex one. Caneva and Ceschin proposed the "ecology of bio-deterioration" concept that highlights the close relationship between the colonization organisms of the stone materials and all the environmental factors that regulate their growth (Caneva and Ceschin, 2009). Calcareous substrates such as limestone and marble have a high intrinsic bio-receptivity being vulnerable materials to bio-deterioration. (Paiva et al., 2022; Pinheiro et al., 2018; Trovão et al., 2020).

Recent studies have shown that black fungi can penetrate and develop in deep areas within limestone and marble materials (Isola et al., 2022; Liu et al., 2022; Paiva et al., 2022; Vyshkvarkova and Sukhonos, 2023; Warscheid and Braams, 2000; Zhang et al., 2023).

In the case of historical monuments made of calcareous materials, the bio-deterioration produced both aesthetic damage and irreversible degradations due to the changes in the chemical composition of carbonate stones. For example, epilithic organisms such as cyanobacteria and green algae caused the marble's colour change, affecting the aesthetics of the monuments (Isola et al., 2022; Mascaro et al., 2022; Skipper et al., 2016). The accumulation of photosynthetic biomass over time facilitates the penetration of the microbial biofilm into the cracks and pores of the limestone and marble, thus intensifying the activity of the endolithic organisms that decomposed the stone material through various physico-chemical processes (Sterflinger and Piñar, 2013; Warscheid and Braams, 2000). Over time, fungi have led to the bio-deterioration of carbonate rocks in historical monuments through several physico-chemical mechanisms, often with synergistic action. These mechanisms resulted in the appearance of bio-pitting, the dislocation of minerals, the dissolution and re-precipitation of carbonic salts, etc. (Gautam et al., 2022; Paiva et al., 2022; Skipper et al., 2016; Warscheid and Braams, 2000).

Studies have shown that both epilithic and endolithic lichens are present in historic calcareous materials. In the case of epilithic lichens, their thallus is mostly on the materials' surface and only single hyphae (filaments) have penetrated the substrate. In the case of endolithic lichens, most of the thallus is inside the cracks and fissures of the substrate and only the fruiting bodies are visible on the surface (Mascaro et al., 2022; Matteucci et al., 2019; Pinheiro et al., 2018; Santo et al., 2021; Schiavon, 2002; Urosevic et al., 2012).

In addition, under favorable growth conditions, also vascular plants were able to colonize the calcareous materials contributing to their damage (Mascaro et al., 2022; Schiavon, 2002), as shown in **Figure 9**.

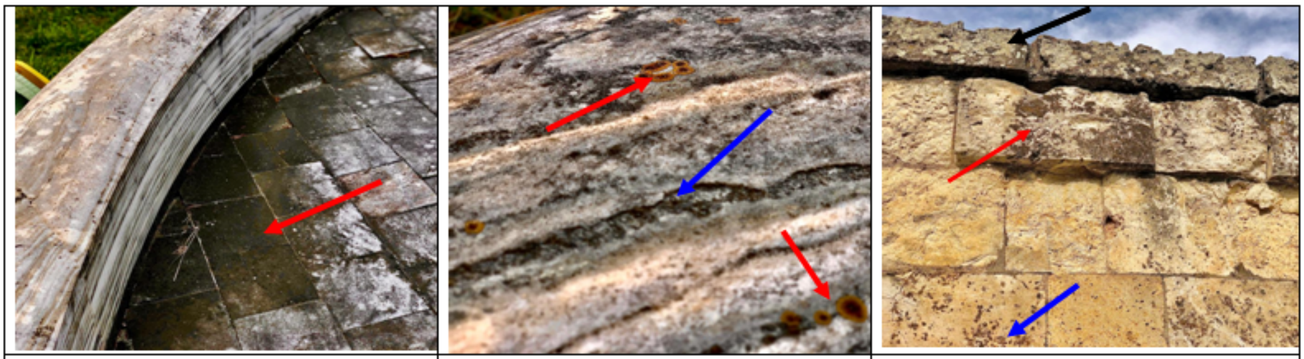

**Algae developed on the marble surface**

**Lichens developed on the marble surface** (red arrows: epilithic lichens; blue arrow: the marble' cracking and delamination due to bio-deterioration)

**Lichens developed on the limestone surface** (red arrow: epilithic ; black arrow: endolithic; blue arrow: bio-pitting)

Orthodox marble monument, Eternitatea Cemetery, Arad, Romania
photo by L.A.C

Limestone street wall, Holy Trinity Cathedral, Arad, Romania
photo by L.A.C

**Figure 9**. Bio-deteriorations of limestone and marble building materials

Studies have shown that both epilithic and endolithic lichens are present in historic calcareous materials. In the case of epilithic lichens, their thallus is mostly on the materials' surface and only single hyphae (filaments) have penetrated the substrate. In the case of endolithic lichens, most of the thallus is inside the cracks and fissures of the substrate and only the fruiting bodies are visible on the surface (Mascaro et al., 2022; Matteucci et al., 2019; Pinheiro et al., 2018; Santo et al., 2021; Schiavon, 2002; Urosevic et al., 2012).

### 3.4. Atrophic deterioration

Along with physical, chemical, and biological factors, some human actions can contribute to the degradation of heritage monuments. Thus, inefficient drain and sewerage systems or inadequate urban systematization or landscaping works can lead to an increase in humidity through capillarity inside the building materials (Fistos et al., 2022).

The gaseous emissions resulting from combustion processes at the domestic, industrial, or transport levels amplify climate changes and increase the aggressiveness of dry and wet acid deposits with the previously shown consequences on historical buildings (Sesana et al., 2021; Vyshkvarkova and Sukhonos, 2023).

Agricultural activities or those involving the enrichment with nitrates or chlorides of the soil in direct contact with the heritage monuments represent a real danger for them.

Conservation works and inappropriate restoration treatments play an important role in the deterioration of cultural heritage (Doehne and Price, 2011; Gulotta et al., 2013; Rodrigues, 2015).

Another frequently encountered damage factor in today's society is represented by graffiti, which can be considered an act of vandalism (Merrill, 2011). Present around us, graffiti affects historic monuments and it is particularly difficult to counteract because the materials associated with graffiti include a series of agents (i.e. paints, polyurethanes, varnishes, enamels, chalk, adhesives, etc.) that can induce several physico-chemical degradation processes with a damaging effect on the historical monuments. Additionally, graffiti removal works may involve the use of abrasive materials leading to further degradation (Fistos et al., 2022).

## CONCLUSIONS

The protection and preservation of historical monuments, as part of the world's architectural heritage, plays an important role in the development of modern communities.

The intrinsic properties and structure of the stone materials that were used for the historical monuments were affected by the atmospheric environment since the construction moment. Several studies reviewed in this paper have shown that with the development of industrial activities and transport, buildings, and monuments of the world heritage have shown a series of significant damages induced by a significant increase in the concentrations of some atmospheric pollutants.

Following the aspects and examples presented in this paper, daily or seasonal temperature variations, the underground water and atmospheric humidity, the freeze-thaw cycles, the winds, snows, and rains, the repeated processes of dissolution/re-crystallization of water-soluble salts inside pores or on surfaces, the biological/micro-biological agents (cyanobacteria, algae, fungi, lichen mosses, etc.), the particulate matter and polluting gases with an acidifying action (i.e. $CO_2$, $SO_2$, $NO_2$, PM, etc., resulting from anthropogenic activities) are the most important extrinsic factors that have induced, over time, a series of physical, chemical or biological weathering and deterioration processes or aesthetic problems of the carbonate stones (limestone and marble) from heritage buildings.

Surface erosion, fissures, exfoliation, splitting, delamination or contour scaling, formation of alveolar structures (honeycombs), increase in cavity and pore size, and development of plants or plant roots in cracks are the physical weathering processes, while, the Karst effect, the efflorescence ("white crust")/sub-florescence appearance, and the black crust formation are the main chemical weathering processes leading to the deterioration of carbonate building stones.

The existence of biofilm and lichens and black rock fungi colonies on the calcareous stones surfaces is an indicator of bio-deterioration, which together with some anthropogenic actions (improper works, wrong reconditioning, graffiti, etc.) determines the physical, chemical, or aesthetic degradation of historical buildings.

## REFERENCES

Amer Khalil, N., 2020. The possibility of using limestone rocks in sculpture as an alternative to marble: An empirical study. PalArch's Journal of Archaeology of Egypt / Egyptology 17, 15061-15069.

Aucouturier, M., Darque-Ceretti, E., 2007. The surface of cultural heritage artefacts: Physicochemical investigations for their knowledge and their conservation. Chemical Society reviews 36, 1605-1621.

Badouna, I., Koutsovitis, P., Karkalis, C., Laskaridis, K., Koukouzas, N., Tyrologou, P., Patronis, M., Papatrechas, C., Petrounias, P., 2020. Petrological and geochemical properties of greek carbonate stones associated with their physico-mechanical and aesthetic characteristics. Minerals 10, 507.

Basu, S., Orr, S.A., Aktas, Y.D., 2020. A geological perspective on climate change and building stone deterioration in London: Implications for urban stone-built heritage research and management. Atmosphere 11, 788.

Battista, G., de Lieto Vollaro, R., 2017. Correlation between air pollution and weather data in urban areas: Assessment of the city of Rome (Italy) as spatially and temporally independent regarding pollutants. Atmospheric Environment 165, 240-247.

Benavente, D., de Jongh, M., Cañaveras, J.C., 2021. Weathering Processes and Mechanisms Caused by Capillary Waters and Pigeon Droppings on Porous Limestones. Minerals 11, 18.

Bogdan, A., Chambre, D., Copolovici, D.M., Bungau, T., Bungau, C.C., Copolovici, L., 2022. Heritage building preservation in the process of sustainable urban development: The case of Brasov medieval city, Romania. Sustainability 14, 6959.

Bugini, R., Tabasso, M., Realini, M., 2000. Rate of formation of black crusts on marble. A case study. Journal of Cultural Heritage - J CULT HERIT 1, 111-116.

Caneva, G., Ceschin, S., 2009. Ecology of biodeterioration. Plant Biology for Cultural Heritage. Biodeterioration and Conservation, 35-58.

Cardell, C., Benavente, D., Rodríguez-Gordillo, J., 2008. Weathering of limestone building material by mixed sulfate solutions. Characterization of stone microstructure, reaction products and decay forms. Materials Characterization 59, 1371-1385.

Christodoulakis, J., Tzanis, C.G., Varotsos, C.A., Ferm, M., Tidblad, J., 2017. Impacts of air pollution and climate on materials in Athens, Greece. Atmospheric Chemistry and Physics 17, 439-448.

Comite, V., Pozo-Antonio, J.S., Cardell, C., Rivas, T., Randazzo, L., Russa, M.F.L., Fermo, P., 2020a. Environmental impact assessment on the Monza cathedral (Italy): a multi-analytical approach.

Comite, V., Ricca, M., Ruffolo, S.A., Graziano, S.F., Rovella, N., Rispoli, C., Gallo, C., Randazzo, L., Barca, D., Cappelletti, P., La Russa, M.F., 2020b. Multidisciplinary approach for evaluating the geochemical degradation of building stone related to pollution sources in the historical center of Naples (Italy). Applied Sciences 10, 4241.

Corvo, F., Reyes-Trujeque, J., Valdés, C., Villaseñor, F., Cuesta, O., Aguilar, D., Quintana, P., 2010. Influence of Air Pollution and Humidity on Limestone Materials Degradation in Historical Buildings Located in Cities Under Tropical Coastal Climates. Water Air and Soil Pollution 205, 359-375.

Cozzolino, A., Adamo, P., Bonanomi, G., Motti, R., 2022. The Role of Lichens, Mosses, and Vascular Plants in the Biodeterioration of Historic Buildings: A Review. Plants 11, 3429.

Doehne, E., Price, C., 2011. Stone Conservation: An Overview of Current Research.

Fassina, V., 1988. Environmental pollution in relation to stone decay. Durability of building materials 5, 317-358.

Fistos, T., Fierascu, I., Doni, M., Chican, I.E., Fierascu, R.C., 2022. A short overview of recent developments in the application of polymeric materials for the conservation of stone cultural heritage elements. Materials 15, 6294.

Frank-Kamenetskaya, O., Vlasov, D., Zelenskaya, M., Knauf, I., Timasheva, M., 2009. Decaying of the marble and limestone monuments in the urban environment. Case studies from Saint Petersburg, Russia. Studia Universitatis Babes-Bolyai, Geologia 54.

Gadd, G., 2017. Fungi, Rocks, and Minerals. Elements 13, 171-176.

Gautam, A., Verma, R., Avasthi, S., Sushma, Bohra, Y., Devadatha, B., M, N., Suwannarach, N., 2022. Current Insight into Traditional and Modern Methods in Fungal Diversity Estimates. Journal of Fungi 8, 226.

Graue, B., Siegesmund, S., Oyhantcabal, P., Naumann, R., Licha, T., Simon, K., 2013. The effect of air pollution on stone decay: The decay of the Drachenfels trachyte in industrial, urban, and rural environments-a case study of the Cologne, Altenberg and Xanten cathedrals. Environmental Earth Sciences 69.

Grossi, C., Brimblecombe, P., 2004. Aesthetics of Simulated Soiling Patterns on Architecture. Environmental science & technology 38, 3971-3976.

Gulotta, D., Bertoldi, M., Bortolotto, S., Fermo, P., Piazzalunga, A., Toniolo, L., 2013. The Angera stone: A challenging conservation issue in the polluted environment of Milan (Italy). Environ Earth Sci 69, 1085-1094.

Hall, K., Hall, A., 1996. Weathering by wetting and drying: Some experimental results. Earth Surface Processes and Landforms 21, 365-376.

Isola, D., Bartoli, F., Meloni, P., Caneva, G., Zucconi, L., 2022. Black Fungi and Stone Heritage Conservation: Ecological and Metabolic Assays for Evaluating Colonization Potential and Responses to Traditional Biocides. Applied Sciences 12, 2038.

Ivaskova, M., Kotes, P., Brodnan, M., 2015. Air pollution as an important factor in construction materials deterioration in Slovak Republic. Procedia Engineering 108, 131-138.

Kanani, S., Zandi, H., 2011. A Study of the Damages to Historical Monuments due to Climatic Factors and Air Pollution and Offering Solutions. World Academy of Science, Engineering and Technology, International Journal of Social, Behavioral, Educational, Economic, Business and Industrial Engineering 5, 1018-1021.

Kryza, R., Prell, M., Czechowski, F., Domaradzka, M., 2009. Acidic weathering of carbonate building stones: experimental assessment. Studia Universitatis Babes-Bolyai, Geologia 54, 33-36.

La Russa, M.F., Belfiore, C.M., Fichera, G.V., Maniscalco, R., Calabrò, C., Ruffolo, S.A., Pezzino, A., 2015. The behaviour to weathering of the Hyblean limestone in the Baroque architecture of the Val di Noto (SE Sicily): An experimental study on the “calcare a lumachella” stone. Construction and Building Materials 77, 7-19.

La Russa, M.F., Comite, V., Aly, N., Barca, D., Fermo, P., Rovella, N., Antonelli, F., Tesser, E., Aquino, M., Ruffolo, S.A., 2018. Black crusts on Venetian built heritage, investigation on the impact of pollution sources on their composition. The European Physical Journal Plus 133, 370.

La Russa, M.F., Fermo, P., Comite, V., Belfiore, C.M., Barca, D., Cerioni, A., De Santis, M., Barbagallo, L.F., Ricca, M., Ruffolo, S.A., 2017. The Oceanus statue of the Fontana di Trevi (Rome): The analysis of black crust as a tool to investigate the urban air pollution and its impact on the stone degradation. Science of The Total Environment 593-594, 297-309.

Li, Q., Zhang, B., Yang, X., Ge, Q., 2018. Deterioration-Associated Microbiome of Stone Monuments: Structure, Variation, and Assembly. Appl Environ Microbiol 84, e02680-02617.

Liu, X., Qian, Y., Wu, F., Wang, Y., Wang, W., Gu, J.-D., 2022. Biofilms on stone monuments: biodeterioration or bioprotection? Trends in Microbiology 30, 816-819.

Livingston, R.A., 2016. Acid rain attack on outdoor sculpture in perspective. Atmospheric Environment 146, 332-345.

Mascaro, M.E., Pellegrino, G., Palermo, A.M., 2022. Analysis of Biodeteriogens on Architectural Heritage. An Approach of Applied Botany on a Gothic Building in Southern Italy. Sustainability 14, 34.

Matteucci, E., Scarcella, A.V., Croveri, P., Marengo, A., Borghi, A., Benelli, C., Hamdan, O., Favero-Longo, S.E., 2019. Lichens and other lithobionts on the carbonate rock surfaces of the heritage site of the tomb of Lazarus (Palestinian territories): diversity, biodeterioration, and control issues in a semi-arid environment. Annals of Microbiology 69, 1033-1046.

McAlister, J.J., Smith, B.J., Török, A., 2008. Transition metals and water-soluble ions in deposits on a building and their potential catalysis of stone decay. Atmospheric Environment 42, 7657-7668.

Merrill, S., 2011. Graffiti at Heritage Places: Vandalism as Cultural Significance or Conservation Sacrilege? Time and Mind: The Journal of Archaeology, Consciousness and Culture 4, 59-75.

Mineo, S., Caliò, D., Pappalardo, G., 2022. UAV-Based Photogrammetry and Infrared Thermography Applied to Rock Mass Survey for Geomechanical Purposes. Remote Sensing 14, 473.

Oguchi, C.T., Yu, S., 2021. A review of theoretical salt weathering studies for stone heritage. Progress in Earth and Planetary Science 8, 32.

Olaru, M., Aflori, M., Simionescu, B., Doroftei, F., Stratulat, L., 2010. Effect of SO2 Dry Deposition on Porous Dolomitic Limestones. Materials 3, 216-231.

Ortega-Morales, O., Montero-Munoz, J.L., Neto, J.A.B., Beech, I.B., Sunner, J., Gaylarde, C., 2019. Deterioration and microbial colonization of cultural heritage stone buildings in polluted and unpolluted tropical and subtropical climates: A meta-analysis. International Biodeterioration & Biodegradation 143.

Paiva, D.S., Fernandes, L., Trovão, J., Mesquita, N., Tiago, I., Portugal, A., 2022. Uncovering the Fungal Diversity Colonizing Limestone Walls of a Forgotten Monument in the Central Region of Portugal by High-Throughput Sequencing and Culture-Based Methods. Applied Sciences 12, 10650.

Pappalardo, G., Mineo, S., Caliò, D., Bognandi, A., 2022. Evaluation of Natural Stone Weathering in Heritage Building by Infrared Thermography. Heritage 5, 2594-2614.

Pappalardo, G., Mineo, S., Imposa, S., Grassi, S., Leotta, A., La Rosa, F., Salerno, D., 2020. A quick combined approach for the characterization of a cliff during a post-rockfall emergency. Landslides 17, 1063-1081.

Pinheiro, A., Mesquita, N., Trovão, J., Soares, F., Tiago, I., Coelho, C., Paiva de Carvalho, H., Gil, F., Catarino, L., Pinar, G., Portugal, A., 2018. Limestone biodeterioration: A review on the Portuguese cultural heritage scenario. Journal of Cultural Heritage 36.

Pozo-Antonio, J.S., Cardell, C., Comite, V., Fermo, P., 2022. Characterization of black crusts developed on historic stones with diverse mineralogy under different air quality environments. Environmental Science and Pollution Research 29, 29438-29454.

Pozo-Antonio, J.S., Pereira, M.F.C., Rocha, C.S.A., 2017. Microscopic characterisation of black crusts on different substrates. Science of The Total Environment 584-585, 291-306.

Přikryl, R., Melounová, L., Varilova, Z., Weishauptová, Z., 2007. Spatial relationships of salt distribution and related physical changes of underlying rocks on naturally weathered sandstone exposures (Bohemian Switzerland National Park, Czech Republic). Environmental Geology 52, 409-420.

Reyes-Trujeque, J., Perez, T., Castañeda, A., Corvo, F., 2010. Role of NOx in material corrosion and degradation. Revista CENIC. Ciencias Químicas 41, 1-10.

Reyes-Trujeque, J., Rivera, J., Owen, P., Bartolo, P., Pérez López, T., Casanova-González, E., Corvo, F., 2016. Weathering effects of an historic building in San Francisco de Campeche, Mexico. Intervención Revista Internacional de Conservación Restauración y Museología 7, 22-31.

Rodrigues, J., 2015. Defining, mapping and assessing deterioration patterns in stone conservation projects. Journal of Cultural Heritage 16, 267-275.

Ruffolo, S.A., Comite, V., La Russa, M.F., Belfiore, C.M., Barca, D., Bonazza, A., Crisci, G.M., Pezzino, A., Sabbioni, C., 2015. An analysis of the black crusts from the Seville Cathedral: A challenge to deepen the understanding of the relationships among microstructure, microchemical features and pollution sources. Science of The Total Environment 502, 157-166.

Sabbioni, C., Piccolo, D., Bonazza, A., Favoni, O., Zappia, G., 2001. Soluble and non water soluble sulphates in damage layers on hydraulic mortars. WIT Transactions on the Built Environment 55, 561-569.

Saltık, E., 2018. Atmospheric weathering of historic monuments and their related conservation issues. MATEC Web of Conferences 149, 01009.

Santo, A.P., Cuzman, O.A., Petrocchi, D., Pinna, D., Salvatici, T., Perito, B., 2021. Black on White: Microbial Growth Darkens the External Marble of Florence Cathedral. Applied Sciences 11, 6163.

Schiavon, N., 2002. Biodeterioration of calcareous and granitic building stones in urban environments. Geological Society, London, Special Publications 205, 195-205.

Schiavon, N., Chiavari, G., Fabbri, D., 2004. Soiling of limestone in an urban environment characterized by heavy vehicular exhaust emissions. Environmental Geology 46, 448-455.

Searle, D., Mitchell, D., 2006. The effect of coal and diesel particulates on the weathering loss of Portland Limestone in an urban environment. The Science of the total environment 370, 207-223.

Sena da Fonseca, B., Ferreira Pinto, A.P., Vaz Silva, D., 2020. Compositional and textural characterization of historical bedding mortars from rubble stone masonries: Contribution for the design of compatible repair mortars. Construction and Building Materials 247, 118627.

Sesana, E., Gagnon, A., Ciantelli, C., Cassar, J., Hughes, J., 2021. Climate change impacts on cultural heritage: A literature review. WIREs Climate Change 12.

Skipper, P., Schulze, H., Williams, D., Dixon, R., 2016. Biodeterioration of limestone built heritage: A multidisciplinary challenge.

Spezzano, P., 2021. Mapping the susceptibility of UNESCO World Cultural Heritage sites in Europe to ambient (outdoor) air pollution. Science of The Total Environment 754, 142345.

Sterflinger, K., Piñar, G., 2013. Microbial deterioration of cultural heritage and works of art--tilting at windmills? Applied microbiology and biotechnology 97, 9637-9646.

Török, Á., Licha, T., Simon, K., Siegesmund, S., 2011. Urban and rural limestone weathering; the contribution of dust to black crust formation. Environmental Earth Sciences 63, 675-693.

Trovão, J., Tiago, I., Catarino, L., Gil, F., Portugal, A., 2020. In vitro analyses of fungi and dolomitic limestone interactions: Bioreceptivity and biodeterioration assessment. International Biodeterioration & Biodegradation 155, 105107.

Urosevic, M., Yebra-Rodriguez, A., Sebastián, E., Cardell, C., 2012. Black soiling of an architectural limestone during two-year term exposure to urban air in the city of Granada (S Spain). The Science of the total environment 414, 564-575.

Vergès-Belmin, V., Siedel, H., 2005. Desalination of Masonries and Monumental Sculptures by Poulticing: A Review / Entsalzen von Mauerwerk und Steinfiguren mit Hilfe von Kompressen: Ein Überblick. Restoration of Buildings and Monuments 11.

Vidal, F., Vicente, R., Mendes Silva, J., 2019. Review of environmental and air pollution impacts on built heritage: 10 questions on corrosion and soiling effects for urban intervention. Journal of Cultural Heritage 37, 273-295.

Vyshkvarkova, E., Sukhonos, O., 2023. Climate Change Impact on the Cultural Heritage Sites in the European Part of Russia over the Past 60 Years. Climate 11, 50.

Wahab, G.M.A., Gouda, M., Ibrahim, G., 2019. Study of physical and mechanical properties for some of Eastern Desert dimension marble and granite utilized in building decoration. Ain Shams Engineering Journal 10, 907-915.

Warscheid, T., Braams, J., 2000. Biodeterioration of stone: a review. International Biodeterioration & Biodegradation 46, 343-368.

Weththimuni, M.L., Chobba, M.B., Sacchi, D., Messaoud, M., Licchelli, M., 2022. Durable Polymer Coatings: A Comparative Study of PDMS-Based Nanocomposites as Protective Coatings for Stone Materials. Chemistry 4, 60-76.

Zhang, Y., Su, M., Wu, F., Gu, J.-D., Li, J., He, D., Guo, Q., Cui, H., Zhang, Q., Feng, H., 2023. Diversity and Composition of Culturable Microorganisms and Their Biodeterioration Potentials in the Sandstone of Beishiku Temple, China. Microorganisms 11, 429.

Zhao, C., Zhang, Y., Hou, M., Li, A., 2019. Recent progress in instrumental techniques for architectural heritage materials. Heritage Science 7.

Zoghlami, K., López-Arce, P., Zornoza-Indart, A., 2019. Case Study Differential Stone Decay of the Spanish Tower Façade in Bizerte, Tunisia.

ISSN 1582-1021
e-ISSN 2668-4764
Edited by "AUREL VLAICU" University
Arad, Romania

10.62591/Scien.Tech.Bull-Chem.FoodSci.Eng.2022.19.03

*Scien. Tech. Bull-Chem. Food Sci. Eng., Vol. 19 (XX), 2022, 34-42*

**Article**

# PRELIMINARY STUDIES ABOUT SOME FACTORS INFLUENCING THE PROPERTIES OF OLEOGELS

**Claudiu-Ștefan URSACHI[1], Simona PERȚA-CRIȘAN[1], Iolanda TOLAN[1], Bianca-Denisa CHEREJI[1], Florentina-Daniela MUNTEANU[1*]**

*[1]Faculty of Food Engineering, Tourism and Environmental Protection, "Aurel Vlaicu" University, Romania, 2 Elena Dragoi, Arad 310330, Romania*

***Abstract:*** *Nowadays, the use of oleogels offers several advantages in food products. They can mimic the functionality of solid fats, providing structure, stability, and mouthfeel to various food formulations. By replacing solid fats or hydrogenated oils with oleogels, manufacturers can reduce or eliminate trans fats and therefore produce healthier food products. The present study focuses on the formulation of oleogels based on pumpkin seeds and rapeseed oils and the use of beeswax or ethylcellulose as oleogelators. The preliminary results indicate that the pumpkin seeds oil contributes to the formation of oleogels with higher consistency. Furthermore, the mechanical properties of oleogels can be manipulated, by adjusting some parameters, such as the type of oil and the kind and concentration of the oleogelator.*

**Keywords**: oleogels, pumpkin seed oil, rapeseed oil, texture

## INTRODUCTION

Oleogels, also known as structured oils, are semi-solid materials that are formed by solidifying vegetable oils with oleogelators, leading to the formation of three-dimensional micro-structured systems where the structuring molecules network immobilises the fraction of liquid oil (Alongi et al., 2022; Li et al., 2022). Oleogelation is a relatively new food technology, considered innovative due to its potential for creating semi-solid gels from liquid oils with no chemical modifications, thus improving the functional properties of food products while these promising ingredients are incorporated (Jeong et al., 2021).

Oleogelators are important substances for modifying the viscosity of the oil phase, with a variable efficiency in oleogelation processes depending on their chemical structure, used concentration, and formulation conditions, thus being selected by the intended food-application specific requirements. There is a large number of compounds used as oleogelators for obtaining food-grade oleogels that can be divided into two major categories depending on their molecular weight: (i) low-molecular-weight gelators, i.e. lipid components such as fatty acids, esters of fatty acids (especially waxes), glycerolipids (especially monoglycerides), glycerophospholipids (especially lecithins), sterol lipids (especially phytosterols and phytosterol esters), sphingolipids (especially ceramides), and fatty alcohols; (ii) high-molecular-weight or polymeric gelators, i.e. non-lipid components such as proteins (e.g. soy protein, whey protein, zein, casein, gelatin), and polysaccharides (e.g. agar, xanthan gum, pectins, chitin and chitosan, ethylcellulose) (Perta-Crisan et al., 2023). The low-molecular-weight oleogelators form three-dimensional crystal networks or self-assembled fibrillary networks (Wang et al., 2022), while the high-molecular-weight ones develop a three-dimensional network that is stabilized by hydrogen bonds, electrostatic, and hydrophobic interactions between molecules and that traps the liquid oil (Sivakanthan et al., 2022).

Depending on the oleogelator solubility, two categories of methods are used to formulate the oleogels: direct dispersion into the oil heated to the upper temperature of its melting point, which is specific to hydrophobic oleogelators, is simple and therefore is the most frequently used (Martins et al., 2020), and indirect pathways such as foam method, biphasic emulsion method or solvent exchange, which are specific to hydrophilic compounds that cannot be dispersed directly into the oil and consist of the initial structural network formation in a water-continuous system and the subsequent removal of the aqueous phase (Floter et al., 2021; Singh et al., 2017). None of these methods produces chemical or structural changes in the oils, thus preserving their nutritional value (Silva et al., 2021b).

Currently, oleogels are extensively studied for their technological and nutritional advantages in foods development, such as replacing or reducing saturated, trans- or hydrogenated fats, which lead to healthier products with unaffected texture, mouthfeel or stability, in extending food shelf-life, in bioactive compounds delivering, in obtaining low-calorie and functional food products, or in preventing oil leaks in various foodstuffs (Davidovich-Pinhas, 2016; Lupi et al., 2013; Manzoor et al., 2022; Temkov and Muresan, 2021). Applications of oleogels in foods can also be categorized by the intended purpose, as follows: in meat and dairy products as animal fat replacers; in baked products, chocolate and chocolate spreads, or filling creams as shortening replacers; in breakfast spreads; in different foods as edible coatings, delivery systems of bioactive compounds, or as frying medium (Perta-Crisan et al., 2023).

Following the encouraging results reported in the scientific literature and considering the current state of knowledge in the field, the present paper shows the results of preliminary studies on the influence of several factors on some properties of different oleogels. As a relatively new element, pumpkin seed oil was used in their formulation, either alone or combined in various proportions with rapeseed oil. To the best of our knowledge, quite a few studies can be found so far on the formulation and characterization of pumpkin seed oil-based oleogels. In this sense, direct dispersion oleogelation methods have been applied, and several factors influencing the consistency and visual appearance of the obtained oleogels have been evaluated: type and proportion of oils, nature and concentration of the oleogelator. Preliminary conclusions have been formulated, but further studies are imperatively needed to draw more detailed conclusions that are related to the final intended purpose of incorporating formulated oleogels as animal fat substitutes in certain food products.

### 1.1. Oleogelator characterisation

### a. Beeswax (BW)

Food-grade beeswax is obtained by purifying the honeycomb of bees from the genus *Apis mellifera L.* (Tinto et al., 2017). Depending on the purification method of the raw wax, it is obtained yellow beeswax (CAS Registry Number: 8006-40-4), a yellow-brown solid, and white beeswax (CAS Registry Number: 8012-89-3), a yellowish-white solid, obtained by bleaching yellow beeswax (Gupta and Anjali, 2023). Beeswax has no nutritional value because it is not digested in the human body. The physical properties of beeswax vary depending on its geographical origin and its age and are presented in Table 1.

**Table 1.** The physicochemical characteristics of beeswax (Tinto et al., 2017)

| Physical properties | Description |
|---|---|
| Smell | honey-like odour |
| Taste | insipid |
| Melting range | 61 - 66°C |
| Density at 20°C | 0.960 – 0.970 g/cm$^3$ |
| Solubility | insoluble in water; sparingly soluble in alcohol; soluble in organic solvents (chloroform, ether); after warming, soluble in fatty oils |

Chemically, beeswax is a mixture of fatty acid esters (also called wax esters), free fatty acids, free fatty alcohols, hydrocarbons, and other minor compounds (Table 2). Due to its composition, beeswax is a gelling agent for various oils, including fish oil, rapeseed oil, olive oil, canola oil, linseed oil sunflower oil (Frolova et al., 2022; Gao et al., 2021; Silva et al., 2021a; Yi et al., 2017; Zhang et al., 2021).

**Table 2.** Chemical composition of beeswax (Tinto et al., 2017)

| Component | Amount (%) | Description |
|---|---|---|
| Wax esters | 58 - 71 | fatty alcohols esterified by fatty acids or hydroxy acids:<br>- monoesters and diesters<br>- hydroxymonoesters and hydroxydiesters<br>eg: saturated alkyl esters of palmitic acid ($C_{38}$-$C_{52}$)<br>- unsaturated alkyl esters of oleic acid ($C_{46}$ $C_{54}$) |

| | | |
|---|---|---|
| Hydrocarbons | 12 - 26 | long chains with odd carbon numbers<br>- n-alkanes ($C_{27}$- $C_{33}$)<br>- n-alkenes ($C_{21}$- $C_{41}$) |
| Free fatty acids | 8 - 18 | unbranched saturated acids with even carbon numbers ($C_{16}$ -$C_{34}$), eg: Palmitic acid (16:0) |
| Free fatty alcohols | 1 - 6 | unbranched alcohols with even carbon numbers ($C_{24}$-$C_{34}$) |

### b. Ethylcellulose (EC)

Ethylcellulose (CAS Registry Number: 9004-57-3), is a semi-synthetic polymer built from cellulose by partial substitution of hydrogen from the hydroxyl groups with ethyl groups (Puscas et al., 2021). By this etherification, various degrees of substitution (DS) are obtained. Ethylcellulose is characterized by the viscosity value because there is a correlation between the DS, water solubility and viscosity of the polymer (Davidovich-Pinhas et al., 2014). The physicochemical characteristics of ethylcellulose are presented in Table 3.

**Table 3**. The physicochemical characteristics of ethylcellulose (EFSA, 2004; Kim et al., 2014)

| Characteristics | Descriptions |
|---|---|
| Appearance | free-flowing powder |
| Color | white to off-white |
| Smell | odourless |
| Taste | tasteless |
| Density at 20ºC | 1.09 - 1.17 g/cm$^3$ |
| Solubility | - insoluble in water (hydrophobic character); after warming soluble in fatty oils |
| Structure | - polymer; semicrystalline |

Ethylcellulose is an accepted food additive in the EU, known as E462, and it is used as an emulsifier, stabilizer and thickener or carrier agent for other additives (Kim et al., 2014). Ethylcellulose is non-digestible in the human body, thus it has no nutritional value. Ethylcellulose is representative of polymeric gelling agents of vegetable oils by direct dispersion. The semi-crystalline structure and the hydrophobic character are the arguments for the functioning of ethyl cellulose as an oleogelator (Garcia-Ortega et al., 2021; Giacintucci et al., 2018; Gómez-Estaca et al., 2019a).

## 1.2. Oil characterization

### a. Pumpkin seed oil

Pumpkin seeds oil is achieved by pressing or extraction and further processing like decanting and filtering. The physicochemical characteristics of pumpkin seed oil are shown in Table 4.

**Table 4.** Physicochemical characteristics of pumpkin seed and rapeseed oil (Encinar et al., 2018; Tsaknis et al., 1997)

| Parameter | Rapeseed oil | Pumpkin seed oil |
|---|---|---|
| Color | yellow to greenish-yellow | dichromatic - dark brown with a green tint |
| Smell | pleasant, without foreign, bitter or rancid smell | a mild nutty odour |
| Taste | pleasant, without foreign, bitter or rancid taste. | pleasant, without foreign, bitter or rancid taste |
| Density at 20°C | 0.909 - 0.925 g/cm$^3$ | 0.918 - 0.927 g/cm$^3$ |
| Viscosity at 2°C, mPa.s | – | 70 – 72 |
| Refractive index at 40°C | 1.466 - 1.47 | 1.465 - 1.474 |
| Saponification index | 189 - 195 mg KOH/g | 185 -203 mg KOH/g |
| Iodine index | 120 - 143 g I/100 g | 103 - 134 g I/100 g |
| Unsaponifiable matter | max 1.5% | 0.79 - 1.22% |
| Peroxide index | max 10 meq/kg | 9.04 - 9.20 meq/kg |
| Free acidity as oleic acid | max 0.1% | max 0.4% |

The chemical composition of the pumpkin seed oil may vary depending on the variety, geographical area, etc. The predominant compounds of pumpkin seed oil are triacylglycerols, while diacylglycerols, monoacylglycerols and free fatty acids are practically absent. In the composition of triacylglycerols of pumpkin seed oil, unsaturated fatty acids are found in the greatest proportion, primarily represented by linoleic acid, followed by oleic acid, while saturated fatty acids are represented by palmitic acid and stearic acid, Table 5.

**Table 5.** Fatty acids composition of pumpkin seed oil (Bardaa et al., 2016; Tsaknis et al., 1997)

| Type of fatty acid | Amount (%) | Major representants |
|---|---|---|
| Saturated (SFA) | 20 | palmitic acid (C16:0); stearic acid (C18:0) |
| Unsaturated (UFA) | 80 | |
| Polyunsaturated (PUFA) | 42 - 43 | linoleic acid (C18:2) |
| Monounsaturated (MUFA) | 37 - 38 | oleic acid (C18:1) |

In recent years, pumpkin seed oil has attracted a lot of attention due to its high nutritional value. It has been shown that the intake of pumpkin seed oil can have beneficial effects on health, such as preventing prostate enlargement, improving diabetes, and protecting against high blood pressure and carcinogenic diseases. These positive health effects could be attributed not only to the high content of polyunsaturated fatty acids, especially oleic and linoleic acids but also due to the presence of substances such as pigments, phytosterols, vitamins, minerals and phenolic compounds with functional properties.

**b. Rapeseed oil**

Rapeseed oil is obtained from rapeseed (*Brassica napus var. napus*). It can be prepared through various processes such as pressing (cold or hot) extraction (enzymatic or with hexane), followed necessarily by refining. The processes used for preparation influence the characteristics and composition of the obtained oil (Wu et al., 2019). At room temperature, refined rapeseed oil appears as a clear, suspension-free and sediment-free liquid. The physicochemical characteristics of rapeseed oil are presented in Table 4.

The chemical composition of the rapeseed oil may vary depending on the processes used for preparation, the variety of rapeseed, geographical area, etc. Table 7, contains the fatty acids composition of rapeseed oil. Refined rapeseed oil was found to have higher antioxidant activity but significantly lower levels of phenolic acids (0,008 mg/kg oil) than cold-pressed rapeseed oil (0.46 mg/kg oil). In contrast, tocopherol levels are similar in cold-pressed and refined rapeseed oils (Cristea et al., 2018; Wu et al., 2019).

**Table 6.** Fatty acids composition of rapeseed oil (Encinar et al., 2018; Wu et al., 2019)

| Type of fatty acid | Amount (%) | Major representants |
|---|---|---|
| Saturated (SFA) | 6 -7 | palmitic acid (C16:0); stearic acid (C18:0) |
| Unsaturated (UFA) | | |
| Polyunsaturated (PUFA) | 27 - 28 | linoleic acid (C18:2); α-linolenic acid (C18:3) |
| Monounsaturated (MUFA) | 63 - 65 | oleic acid (C18:1) |
| Trans fatty acids | 2 | |

## MATERIALS AND METHODS

### 2.1. Materials

Ethylcellulose with 64 cP viscosity and beeswax refined were purchased from Sigma-Aldrich.

Pumpkin seed oil and rapeseed oil were purchased from Arad, Romania's local market, and used for the preparation of the oleogels.

### 2.2. Oleogel preparation

### a. Ethylcellulose oleogels preparation

Ethylcellulose oleogels were obtained using the method described by Gravelle et al (Gravelle, 2017). Mixtures of different proportions of pumpkin seed oil and rapeseed oil (mass ratio of 1:0, 3:1, 1:1 and 1:3) were used to prepare oleogels with 5 and 10% ethylcellulose, Table 8.

**Table 7**. Ethylcellulose oleogel samples

| Sample | Pumpkin seed oil [%] | Rapeseed oil [%] | Ethylcellulose [%] |
|---|---|---|---|
| DR0-5 | 100 | 0 | 5 |
| DR1-5 | 75 | 25 | 5 |
| DR2-5 | 50 | 50 | 5 |
| DR3-5 | 25 | 75 | 5 |
| DR0-10 | 100 | 0 | 10 |
| DR1-10 | 75 | 25 | 10 |
| DR2-10 | 50 | 50 | 10 |
| DR3-10 | 25 | 75 | 10 |

The oils were previously heated at 100°C and the oleogelator was added by stirring at 200 rpm, using a magnetic stirrer. The mixture was heated, not exceeding 140°C, with continuous stirring until ethylcellulose was completely dissolved in the oil and a clear solution was obtained. After that, the mixture was cooled at room temperature to form the gels and finally stored at 4°C.

### b. Beeswax oleogels preparation

Beeswax oleogels were obtained according to the procedure described by Gómez-Estaca et al. (Gómez-Estaca et al., 2019b). Mixtures of different proportions of pumpkin seed oil and rapeseed oil (mass ratio of 1:0, 3:1, 1:1 and 1:3) were used to prepare oleogels with 7 and 10% BW, Table 9. The oils were heated at 62°C, and beeswax was added under continuous stirring (200 rpm) until complete dissolution. After that, the samples were cooled down to ambient temperature until gelification and stored in a refrigerator at 4°C.

**Table 8**. Beeswax oleogels samples

| Sample | Pumpkin seed oil [%] | Rapeseed oil [%] | Beeswax [%] |
|---|---|---|---|
| C7-0 | 100 | 0 | 7 |
| C7-1 | 75 | 25 | 7 |
| C7-2 | 50 | 50 | 7 |
| C7-3 | 25 | 75 | 7 |
| C10-0 | 100 | 0 | 10 |
| C10-1 | 75 | 25 | 10 |
| C10-2 | 50 | 50 | 10 |
| C10-3 | 25 | 75 | 10 |

### 2.3. Texture measurement - penetration test

The oleogel texture is an important parameter attribute related to their structure, overall performance and future application. Firmness of the oleogel samples was measured by penetration test using a PCE-PTR 200 texturometer (PCE Instruments UK Ltd. Hampshire, UK). Before the analysis of oleogel, the samples were tempered to about 20°C. Each sample was penetrated by an 8 mm diameter stainless plunger to a depth of 5 mm. Three independent measurements were performed for each sample, and the maximum force (N) was recorded.

### 2.4. Visual appearance

After the oleogels preparation, they were disposed of in 80 ml containers and maintained at room temperature until gelification. After this period, the containers were turned upside down to observe the stability, including phase separation and liquid oil exudation on the surface. After that, the visual appearance examination started with analyzing the oleogels: texture, color, opacity, shine, and homogeneity.

## RESULTS AND DISCUSSIONS

### 3.1. Texture measurement

### a. Ethylcellulose oleogels

The firmness is one of the most important physical properties of structured fats as they will be used as substitutes for solid fats in different food products. The firmness of the EC oleogel samples is shown in Figure 1. It can be seen that the texture was significantly higher with the increase in the EC concentration. As the concentration of EC increased from 5 to 10%, the firmness of oleogels increased exponentially for all samples from 0.11N to 24.79N.

On the other hand, the nature of the oil also influences the firmness of oleogels. The highest firmness was found for the pumpkin seed oil oleogels, 2.93 N for DR0-5 and 24.78 for DR0-5. The mixture of pumpkin seed oil with rapeseed oil leads to a linear decrease in the texture of the oleogels, proportional to the amount of substituted pumpkin seed oil. For the 5% EC samples, a 75% replacement of pumpkin seed oil with rapeseed oil resulted in a significant reduction of oleogel firmness by 96.2% while in the case of the 10% EC samples, the replacing of pumpkin seed oil induced a 35.4% decreasing of texture.

### b. Beeswax oleogels

In both cases of BW oleogels, the firmness is significantly affected by wax concentration. As the concentration of BW increased from 7 to 10%, the firmness of oleogel samples increased from 0.42 N to 14.16 N. On the other hand, figure 2 shows that the oleogel prepared only from pumpkin seed oil with 10% EC has the highest firmness and the replacement with rapeseed oil decreased the oleogel firmness proportionally with the ratio amount.

The higher firmness for the oleogel prepared only by pumpkin seed oil, in the case of EC and BW, may be attributed to the fatty acid composition of the oils since rich unsaturated fatty acids oils produce stronger gels (Wang et al., 2023; Zetzl et al., 2014).

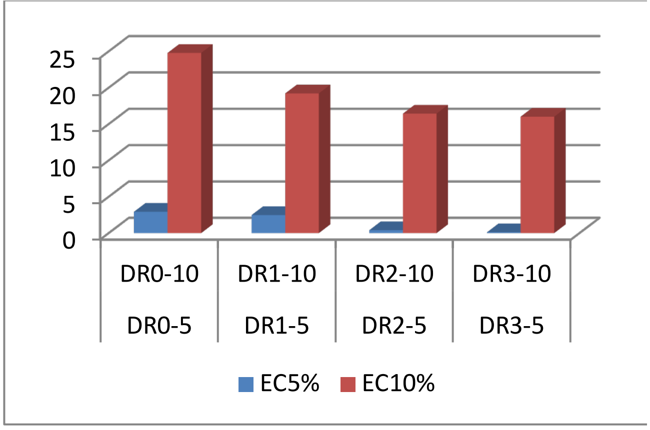

**Figure 1**. Firmness of oleogels prepared from pumpkin seed oil and rapeseed oil with 5 and 10% EC

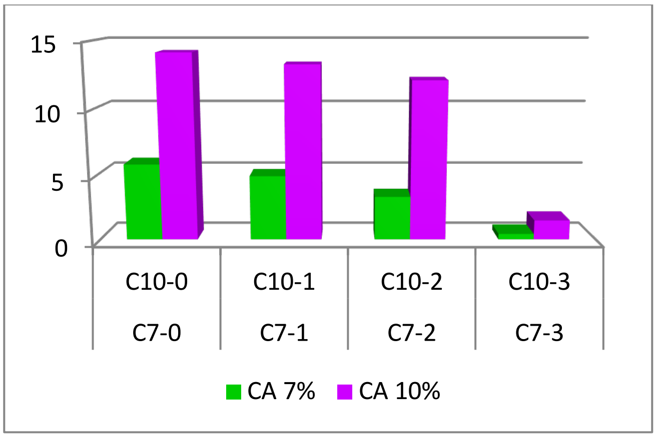

**Figure 2**. Firmness of oleogels prepared from pumpkin seed oil and rapeseed oil with 7 and 10% BW

### 3.2. Visual appearance

The visual appearance of the oleogelation phenomenon was monitored for the oleogels obtained with pumpkin and rapeseed oil with ethylcellulose and beeswax at 10% w/w concentration.

**Tabel 9.** Visual aparence of pumpkin and rapseed oil oleogels with 10% BW and 10% EC

| **Characteristics** | **Pumpkin and rapeseed oil oleogels with 10% BW** | **Pumpkin and rapeseed oil oleogels with 10% EC** |
|---|---|---|
| Texture | the oleogel have typically a smooth and creamy texture due to the presence of beeswax. The texture may be slightly firm, but still spreadable. | the oleogels made with ethylcellulose have a smooth and homogeneous texture. The gel formed by ethylcellulose helps to distribute the oil uniformly, creating a consistent and cohesive appearance |
| Color | the color of the oleogel depends on the natural color of the pumpkin and rapeseed oil. Pumpkin oil typically has a rich, golden, or dark green color, while rapeseed oil is often yellow. The combination of these oils results in a blend of colors ranging from golden yellow to deeper green. | the pumpkin oil and rapeseed oil possess their characteristic colors, and the addition of ethylcellulose in the oleogel formulation does not significantly alter the natural color of these oils. Therefore, the oleogels retain the original color of the oils used. |
| Opacity | the oleogels made with beeswax at a 10% concentration have a translucent appearance. The presence of beeswax can create a certain level of opacity, but it should still allow some light to pass through. | the ethylcellulose based oleogels tend to be transparent or translucent, allowing light to pass through, and in the concentration used the translucent presents homogeneity. |
| Shine | the beeswax can provide a natural shine to the oleogels surface, giving it a glossy or satin-like finish. This can enhance the visual appeal of the product. | the ethylcellulose oleogels exhibit a certain level of glossiness on the surface. The presence of the gelling agent contributes to the reflective properties of the gel, resulting in a shiny appearance. |
| Homogeneity | the oleogel has a uniform appearance, without any visible separation or clumps. Proper formulation and thorough mixing of the ingredients is essential to achieve a consistent texture throughout the product. | although oleogels are technically semi-solids, they can resemble solid fats in their visual appearance. The addition of ethylcellulose allows the oil to take on a solid-like form, giving the oleogel a more rigid and structured appearance. |

### a. Pumpkin and rapeseed oil oleogels with 10% BW

The visual appearance of oleogels made from a mixture of pumpkin and rapeseed oil with 10% BW (Figure 3) can vary depending on several factors such as the formulation, preparation, and storage conditions. Table 10 shows the main visual characteristics of the samples.

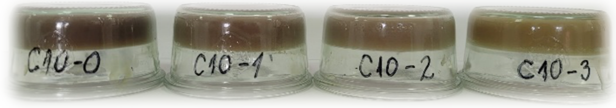

**Figure 3**. The visual appearance of pumpkin and rapeseed oil oleogels with 10% BW

### b. Pumpkin and rapeseed oil oleogels with 10% EC

The method of visual appearance for oleogels made with pumpkin and rapeseed oil using 10% EC (Figure 4) involves observing the physical characteristics of the resulting gel. Table 10 shows the main visual characteristics of the samples.

**Figure 4.** The visual appearance of pumpkin and rapeseed oil oleogels with 10% EC

## CONCLUSIONS

The present results are in good agreement with the ones previously published by other authors proving that EC and BW are efficient oleogelators for obtaining oleogels. Moreover, the mechanical properties of EC and BW oleogels can be manipulated, by adjusting some parameters, such as the type of oil and oleogelator concentration. An important aspect that should be considered when oleogels are used in food products is that for developing the right texture, it is essential to optimize the properties of the formulated oleogel to meet the desired expectations for consumers' satisfaction.

Our preliminary results indicate that pumpkin seed oil, due to its higher content of polyunsaturated fatty acids (≈ 61%) compared to rapeseed oil (≈28%), forms oleogels with a higher consistency, which might be considered an advantage for future applications.

For choosing the optimal oleogelator, additional studies are needed as the results indicate that each of the oleogelators used in the present study has advantages and disadvantages. Moreover, oleogels obtained with BW are processed at lower temperatures, which can positively influence the oxidative stability of the oleogel, while oleogels obtained with EC present a higher consistency and a more pleasant appearance.

## ACKNOWLEDGEMENTS

This work was supported by a grant of the Ministry of Research, Innovation and Digitization, CCCDI-UEFISCDI, project number PN-III-P2-2.1-PED-2021-3240, within PNCDI III.

## REFERENCES

Alongi, M., Lucci, P., Clodoveo, M.L., Schena, F.P., Calligaris, S., 2022. Oleogelation of extra virgin olive oil by different oleogelators affects the physical properties and the stability of bioactive compounds. Food Chem 368, 130779.

Bardaa, S., Ben Halima, N., Aloui, F., Ben Mansour, R., Jabeur, H., Bouaziz, M., Sahnoun, Z., 2016. Oil from pumpkin (Cucurbita pepo L.) seeds: evaluation of its functional properties on wound healing in rats. Lipids Health Dis 15, 73.

Cristea, G.C., Cazamir, D., Dima, D., Georgescu, C., Deleanu, L., 2018. Influence of TiO2 as nano additive in rapeseed oil. IOP Conference Series: Materials Science and Engineering 444.

Davidovich-Pinhas, M., 2016. Oleogels: a promising tool for delivery of hydrophobic bioactive molecules. Therapeutic delivery 7, 1-3.

Davidovich-Pinhas, M., Barbut, S., Marangoni, A.G., 2014. Physical structure and thermal behavior of ethylcellulose. Cellulose 21, 3243-3255.

EFSA, 2004. Opinion of the Scientific Panel on Food Additives, Flavourings, Processing Aids and Materials in Contact with Food (AFC) on a request from the Commission related to Ethyl Cellulose as a food additive. EFSA Journal 2.

Encinar, J., Pardal, A., Sánchez, N., Nogales, S., 2018. Biodiesel by Transesterification of Rapeseed Oil Using Ultrasound: A Kinetic Study of Base-Catalysed Reactions. Energies 11.

Floter, E., Wettlaufer, T., Conty, V., Scharfe, M., 2021. Oleogels-Their Applicability and Methods of Characterization. Molecules 26, 19.

Frolova, Y., Sarkisyan, V., Sobolev, R., Makarenko, M., Semin, M., Kochetkova, A., 2022. The Influence of Edible Oils' Composition on the Properties of Beeswax-Based Oleogels. Gels 8, 17.

Gao, Y., Li, M., Zhang, L., Wang, Z., Yu, Q., Han, L., 2021. Preparation of rapeseed oil oleogels based on beeswax and its application in beef heart patties to replace animal fat. Lwt 149.

Garcia-Ortega, M.L., Toro-Vazquez, J.F., Ghosh, S., 2021. Development and characterization of structured water-in-oil emulsions with ethyl cellulose oleogels. Food Res. Int. 150, 15.

Giacintucci, V., Di Mattia, C.D., Sacchetti, G., Flamminii, F., Gravelle, A.J., Baylis, B., Dutcher, J.R., Marangoni, A.G., Pittia, P., 2018. Ethylcellulose oleogels with extra virgin olive oil: the role of oil minor components on microstructure and mechanical strength. Food Hydrocolloids 84, 508-514.

Gómez-Estaca, J., Herrero, A.M., Herranz, B., Álvarez, M.D., Jiménez-Colmenero, F., Cofrades, S., 2019a. Characterization of ethyl cellulose and beeswax oleogels and their suitability as fat replacers in healthier lipid pâtés development. Food Hydrocolloids 87, 960-969.

Gómez-Estaca, J., Pintado, T., Jiménez-Colmenero, F., Cofrades, S., 2019b. Assessment of a healthy oil combination structured in ethyl cellulose and beeswax oleogels as animal fat replacers in low-fat, PUFA-enriched pork burgers. Food and Bioprocess Technology 12, 1068-1081.

Gupta, G., Anjali, K., 2023. Environmentally Friendly Beeswax: Properties, Composition, Adulteration, and its Therapeutic Benefits. IOP Conference Series: Earth and Environmental Science 1110.

Jeong, S., Lee, S., Oh, I., 2021. Development of Antioxidant-Fortified Oleogel and Its Application as a Solid Fat Replacer to Muffin. Foods 10.

Kim, J.Y., Yi, B., Kim, M.-J., Lee, J., 2014. Oxidative stability of solid fats containing ethylcellulose determined based on the headspace oxygen content. Food Science and Biotechnology 23, 1779-1784.

Li, Y., Zou, Y., Que, F., Zhang, H., 2022. Recent advances in fabrication of edible polymer oleogels for food applications. Current Opinion in Food Science 43, 114-119.

Lupi, F.R., Gabriele, D., Baldino, N., Mijovic, P., Parisi, O.I., Puoci, F., 2013. Olive oil/policosanol organogels for nutraceutical and drug delivery purposes. Food Funct. 4, 1512-1520.

Manzoor, S., Masoodi, F.A., Naqash, F., Rashid, R., 2022. Oleogels: Promising alternatives to solid fats for food applications. Food Hydrocolloids for Health 2.

Martins, A.J., Vicente, A.A., Pastrana, L.M., Cerqueira, M.A., 2020. Oleogels for development of health-promoting food products. Food Science and Human Wellness 9, 31-39.

Perta-Crisan, S., Ursachi, C.S., Chereji, B.D., Tolan, I., Munteanu, F.D., 2023. Food-Grade Oleogels: Trends in Analysis, Characterization, and Applicability. Gels 9.

Puscas, A., Muresan, V., Muste, S., 2021. Application of Analytical Methods for the Comprehensive Analysis of Oleogels-A Review. Polymers (Basel) 13.

Silva, P.M., Martins, A.J., Fasolin, L.H., Vicente, A.A., 2021a. Modulation and Characterization of Wax-Based Olive Oil Organogels in View of Their Application in the Food Industry. Gels 7.

Silva, T.J., Barrera-Arellano, D., Ribeiro, A.P.B., 2021b. Oleogel-based emulsions: Concepts, structuring agents, and applications in food. J Food Sci 86, 2785-2801.

Singh, A., Auzanneau, F.I., Rogers, M.A., 2017. Advances in edible oleogel technologies - A decade in review. Food Res Int 97, 307-317.

Sivakanthan, S., Fawzia, S., Madhujith, T., Karim, A., 2022. Synergistic effects of oleogelators in tailoring the properties of oleogels: A review. Compr. Rev. Food. Sci. Food Saf. 21, 3507-3539.

Temkov, M., Muresan, V., 2021. Tailoring the Structure of Lipids, Oleogels and Fat Replacers by Different Approaches for Solving the Trans-Fat Issue-A Review. Foods 10.

Tinto, W.F., Elufioye, T.O., Roach, J., 2017. Waxes, Pharmacognosy, pp 443-455.

Tsaknis, J., Lalas, S., Lazos, E.S., 1997. Characterization of crude and purified pumpkin seed oil. Grasas y Aceites 48, 267-272.

Wang, Q., Espert, M., Larrea, V., Quiles, A., Salvador, A., Sanz, T., 2023. Comparison of different indirect approaches to design edible oleogels based on cellulose ethers. Food Hydrocolloids 134.

Wang, Z., Chandrapala, J., Truong, T., Farahnaky, A., 2022. Oleogels prepared with low molecular weight gelators: Texture, rheology and sensory properties, a review. Crit Rev Food Sci Nutr, 1-45.

Wu, Y., Zhou, R., Wang, Z., Wang, B., Yang, Y., Ju, X., He, R., 2019. The effect of refining process on the physicochemical properties and micronutrients of rapeseed oils. PLoS One 14, e0212879.

Yi, B., Kim, M.J., Lee, S.Y., Lee, J., 2017. Physicochemical properties and oxidative stability of oleogels made of carnauba wax with canola oil or beeswax with grapeseed oil. Food Sci Biotechnol 26, 79-87.

Zetzl, A.K., Gravelle, A.J., Kurylowicz, M., Dutcher, J., Barbut, S., Marangoni, A.G., 2014. Microstructure of ethylcellulose oleogels and its relationship to mechanical properties. Food Structure 2, 27-40.

Zhang, R.F., Zhang, T., Hu, M.Y., Xue, Y., Xue, C.H., 2021. Effects of oleogels prepared with fish oil and beeswax on the gelation behaviors of protein recovered from Alaska Pollock. LWT-Food Sci. Technol. 137, 9.

ISSN 1582-1021
e-ISSN 2668-4764
Edited by “AUREL VLAICU” University
Arad, Romania

10.62591/Scien.Tech.Bull-Chem.FoodSci.Eng.2022.19.04

Scien. Tech. Bull-Chem. Food Sci. Eng., Vol. 19 (XX), 2022, 43-52

ARTICLE

# URBAN AQUEOUS SYSTEM AS A HOTSPOT FOR WATER-ATMOSPHERE EXCHANGE OF $CH_4$

**Mustafa HMOUDAH**[1], **Cristian POP**[2], **Călin BACIU**[1*]

[1] *Faculty of Environmental Science and Engineering, University of Babeş-Bolyai, 30*
*Fantanele Street, RO-400294, Cluj-Napoca, Romania*
*Corresponding author email: mustafa.hmoudah@gmail.com*

***Abstract:*** *Methane ($CH_4$), a potent greenhouse gas, has negative radiative impacts on the atmosphere, reaching up to 20 times compared with $CO_2$. However, mitigating $CH_4$ emissions from its sources, either natural or anthropogenic, will reduce global warming consequences in the short run, given that $CH_4$ has a short lifetime which takes approximately a decade.*

*The urban aqueous system is part of the natural sources of $CH_4$ in the urban area, which could be influenced by microorganisms or increased human activities and the discharging of sewage water into the system.*

*Recent studies have stated that high organic matter in river sediments is the primary source for increased production of $CH_4$ in the river bed. However, the contribution of the urban aqueous system in $CH_4$ annual fluxes is still uncertain, so a research gap needs to be filled to understand further $CH_4$ emissions from this system.*

*This study aims to detect $CH_4$ content in the urban aqueous system and identify locations with high concentrations to establish further investigation and determine the factors behind these concentrations.*

*In our study, the aqueous system is classified into three main categories: rivers, lakes, and ponds. Water samples were collected from each of these sub-systems for estimating $CH_4$ concentration. Samples from Somes River were gathered from three segments: upstream, urban segment within the urban area, and downstream river. Moreover, samples were also taken from lakes and ponds, considering spatial even distribution between sampling points.*

*Our samples were analyzed via head-space extraction method using Tunable Diode Laser Absorption Spectroscopy (TDLAS), which precisely detects emissions up to 0.1 ppmv.*

*The results showed that water samples are oversaturated with $CH_4$ concentration. In other words, the aqueous system in the selected urban area represents an active hotspot for $CH_4$ exchange from water into the atmosphere.*

*However, $CH_4$ fluxes should be quantified to understand better the contribution of the urban aqueous system to the $CH_4$ budget and to take appropriate abatement measures for reducing these emissions.*

**Keywords**: greenhouse gas, methane ($CH_4$), urban area, headspace method, aqueous system, gas concentration.

## INTRODUCTION

Methane ($CH_4$) is a potent greenhouse gas (GHG) with radiative forces of more than 86 times $CO_2$ in terms of global warming potential (GWP) over 20 years (Kang et al. 2016). Eliminating methane emissions from the atmosphere will be significantly noticed in the short term which will also accelerate the process of reversing the climate's negative effects due to the short lifetime of approximately 10 years (Fernandez et al. 2022; Kang et al. 2016; Lamb et al. 2016; UNEP 2021).

Methane emissions have gradually increased since the industrial era due to growing anthropogenic activities of agriculture, fossil fuel combustion, and waste disposal.

The methane budget is attributed to high uncertainty; therefore, precisely quantifying its sources and sinks will be the first toward its abatement (Saunois et al., 2020). Wetlands, permafrost, oceans, lakes, rivers, termites, and wild animals are examples of natural sources. While rice paddies, ruminants, waste management activities, fossil fuel, and biomass burning are among the anthropogenic ones responsible for more than half of $CH_4$ total emissions (IPCC 2013).

However, the oxidation of $CH_4$ in the stratosphere and the troposphere is considered an essential sink of $CH_4$ (Cuna et al. 2008; Isaksen et al. 2014). Moreover, methanotrophic bacteria is another $CH_4$ sink that oxidizes about 45 – 85 % of soil $CH_4$, depending on soil humidity and texture (Tate 2015). Although sediments in anoxic environments are potential sources for methane production, the upper water columns with high dissolved oxygen represent an oxidation layer for these emissions (Magen et al. 2014).

Gas exchange between air and water is a biochemical cycle controlled by environmental factors. These factors can be determined through air-water exchange characterization. Some of these factors are: rain, wind speed, bubble entrainment, stability of the boundary layer, and surface films (Wanninkhof et al., 2009). Wind speed affects gas transfer and fluxes from water by causing surface turbulence and bubble hatch push out the gas, but it's not the only factor influencing water-air gas transfer (Wanninkhof 1992).

The wide range of $CH_4$ sources and sinks increases the confusion in effectively estimating its actual annual budget (Saunois et al., 2020; Ito et Inatomi 2012). In other words, it isn't very easy to determine all the environmental and biological implicated factors in the $CH_4$ budget. Using one approach in this estimation doesn't guarantee the inclusion of all $CH_4$ sources and sinks. As a sequence, missing the understanding of the actual budget of $CH_4$ results in inefficiently applying appropriate measures for reducing its emissions (Ito et Inatomi 2012).

Urbanization and land use policies have shifted lands from being a $CH_4$ sink into representing a potential source (De Bernardi et al. 2022; Harris et al. 2018). In contrast, land use management policies like afforestation can reverse these effects and promote $CH_4$ soil consumption (Benanti et al. 2014). In the urban area, traffic and high energy demand are main sources of anthropogenic $CH_4$ in addition to the leak from natural gas distribution networks (Isaksen et al. 2014).

Recent studies of methane emissions in Urban Areas characterized sources of natural gas leaks (Chamberlain, Ingraffea, et Sparks 2016; McKain et al. 2015; Phillips et al. 2013) and to sewer systems (Beelen et Parker 2022; Guisasola et al. 2008; Kyung et al. 2017).

Water systems contribute to $CH_4$ annual budget of approximately 103 $TgCH_4$ (Bastviken et al. 2011), but the actual contribution of the aqueous system in the urban area needs to be more studied in the literature. Many studies were interested in understanding $CH_4$ concentration in water resources for health evaluation and inflammable potential estimation of $CH_4$ from these resources (Magen et al. 2014)

Water bodies like rivers and streams are considered important sources of $CH_4$ emissions in the urban area, mainly due to land use changes after the industrial era leading to water pollution from wastewater. The contribution of polluted urban rivers to $CH_4$ annual fluxes is uncertain (Wang et al. 2020).

However, recent studies estimated methane emissions from urban rivers (Hu et al. 2018; Yang et al. 2015; Zhao et al. 2022) and have determined that high concentrations of dissolved $CH_4$ are influenced by urban pollution and by the discharging of wastewater into rivers in addition to the land-use changing policies. Nevertheless, other studies have not covered the entire aqueous system in the urban area, particularly in Romania.

While the urban aqueous system is poorly covered by the literature and almost neglected, it is important to determine the actual position of the urban aqueous system from CH4 emissions as either a potential contributor or an essential sink.

This study is a preliminary exploration to determine $CH_4$ concentration in urban aqueous systems. It also represents a reference for further investigation to quantify the actual contribution of these systems in the $CH_4$ budget to apply specific abatement strategies.

## MATERIALS AND METHODS

The sampling locations were selected based on spatial distribution by considering the variety of the surrounding activities.

About 49 water samples were collected, in the period between December 2022 and January 2023, from 49 different locations; in addition to the recording of their geographic coordinates and site description to establish a clear image of the actual locations and for relatively analyzing them spatially, **Figure 1**.

A liter of water was collected from each sampling point, shown in **Figure 1,** using a one-liter sampling bottle. The bottles were entirely filled with water slowly down the side to avoid bubbles production or entrapping air inside the sample, and to keep the dissolved gas in the samples not affected until the analysis process.

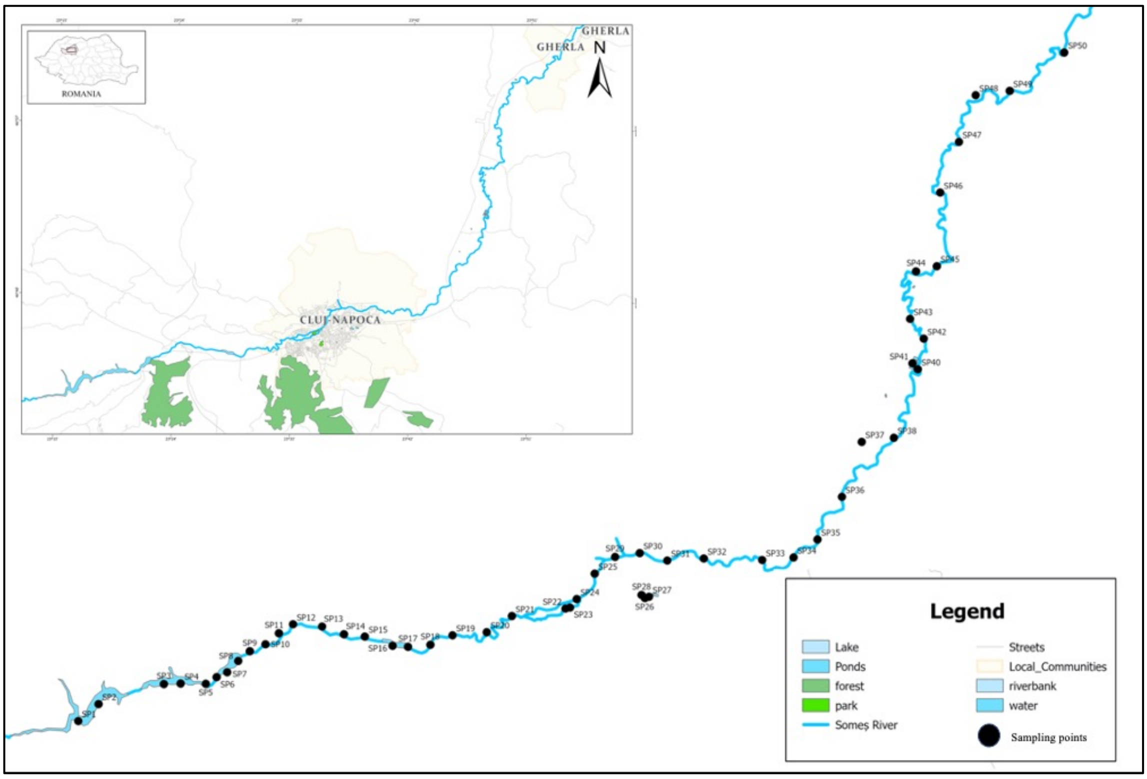

**Figure 1.** Water sampling locations were distributed evenly over the urban aqueous system from which one liter of water was collected from each site.

The samples' temperature was raised to room temperature of approximately 18˚C. A subsample of 700 mL water was transferred from the sampling bottles into a 1000 mL sample vial, while a volume of 300 mL was filled up with the ambient atmospheric air to function as a headspace.

However, ambient air inside the lab was circulating in order to keep on the actual atmospheric background and to avoid any influence from precedent $CH_4$ measurements to affect the measuring of the next ones, and also to effectively recalibrate the Tunable Diode Laser Absorption Spectroscopy (TDLAS) to be prepared for the following $CH_4$ estimation.

Samples were analyzed on the same day of collection to reduce the chance of any potential influence from biological activities or any chemical reaction inside the samples and to skip the step of adding preservatives to the samples.

Each sample is described in a table indicating the sample number, coordinate, spatial description, and its order in the process $CH_4$ measurement. Sampling bottles were arranged according to their field description to effectively conduct laboratory analysis.

After filling up the sample vial with 700 mL of water sample X and letting the 300 mL of the headspace be filled up with atmospheric air, the vial septum sample was shaken for 2-3 minutes in order to equilibrate the gas concentration between the headspace and the water, **Figure 2**.

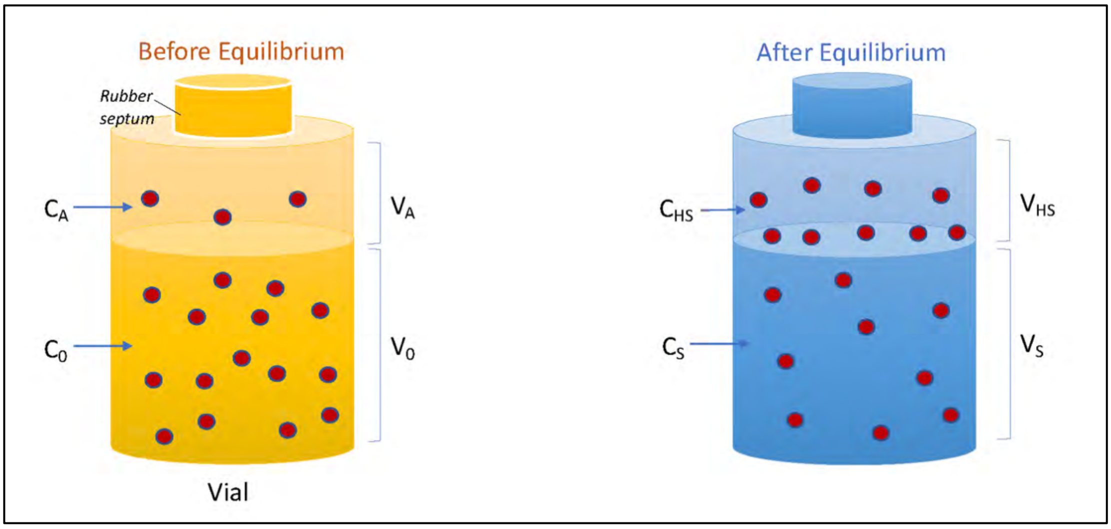

**Figure 2.** Headspace conceptual method before and after equilibrium, where $C_A$ is the concentration of $CH_4$ before the equilibrium, $C_0$ is the initial concentration, and $V_A$ and $V_0$ are the initial volumes of the headspace and the sample, respectively. After the equilibrium, $C_{HS}$ is the headspace concentration, $C_S$ is the sample concentration, $V_{HS}$ is the headspace volume, and $V_S$ is the sample volume.

After the equilibrium, two needles connected to the TDLAS were inserted simultaneously inside the vial through its rubber septum cap. At the same time, the TDLAS was just calibrated to the background of the ambient atmosphere, **Figure 3**.

The measurements lasted 1 minute for each sample, and the readings of $CH_4$ concentration in the headspace were recorded up to 0.1 ppmv $s^{-1}$. The delay time was estimated to be between 3-4 seconds.

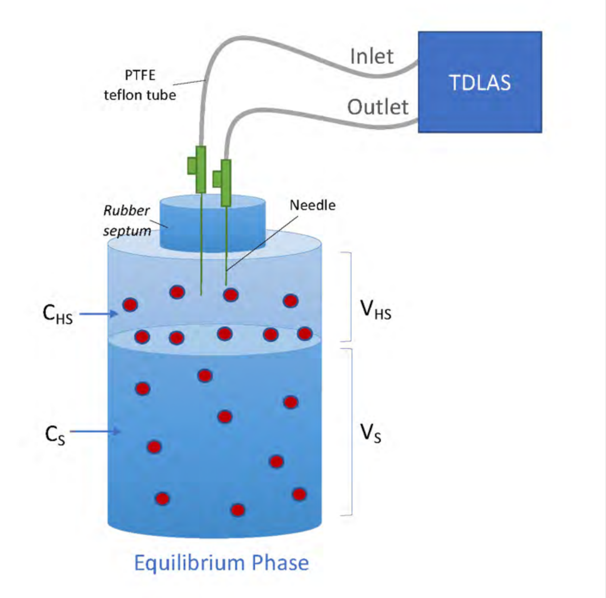

**Figure 3.** Methane headspace concentration measurement technique after the equilibrium by simultaneously inserting inlet and outlet needles connected with TDLAS. Given that the vial headspace is 300mL, it's recommended to take caution for keeping the hands away

### Calculation

In our headspace theory, no gas chromatography was used; the headspace $CH_4$ concentration was determined via TDLAS, as described in **Figure 3**. In the headspace method and at a specific temperature, an equilibrium is reached between the volatile in the sample and the headspace.

The volume of the sample would almost remain the same after the transfer of the analyte into the headspace. Therefore, the sample volume will be considered the same, $\mathbf{V_0}$ equals $\mathbf{V_s}$, and $\mathbf{V_{HS}}$ remains unchanged by default.

The ratio phase (**ß**) is the ratio of the headspace volume $\mathbf{V_{HS}}$ to the sample volume $\mathbf{V_S}$ (Kolb et Ettre 2006), **Equation 1**.

$$\mathbf{ß = V_{HS}/V_S} \qquad \textbf{(1)}$$

Also, the concentration in the original sample $\mathbf{C_0}$ equals the initial amount of the analyte $\mathbf{Q_0}$ ($CH_4$ in our case) divided by the sample initial volume $\mathbf{V_0}$ in the vial (Kolb et Ettre 2006), **Equation 2**.

$$\mathbf{C_0 = Q_0/V_0} \qquad \textbf{(2)}$$

The sum of the amount of $CH_4$ in the headspace and the sample after the equilibrium equals its initial amount in the sample before the equilibrium.

The concentration equilibrium is influenced by the thermodynamic force that can be expressed by the coefficient (K), which is the ratio between concentration in the sample $\mathbf{C_S}$ and the concentration in the headspace $\mathbf{C_{HS}}$ (Kolb et Ettre 2006; Snow et Bullock 2010), subtracting the amount in the initial headspace (which equals the ambient amount in the atmosphere), because the TDLAS reading doesn't represent the added amount of $CH_4$ from the initial sample, **Equation 3**.

$$\mathbf{K = C_S/C_{HS}} \qquad \textbf{(3)}$$

After considering all the relations mentioned above, the amount of $CH_4$ in the initial sample, **Equation (2)** becomes:

$$\mathbf{Q_0 = C_0.V_{0\ Before}}$$
$$\mathbf{Q_0 = (C_S.V_S + C_{H.S}.V_{HS})_{After} - C_A.V_{HS\ Before}} \qquad \textbf{(4)}$$

By substituting **Equation 3** in **Equation 4**:

$$\mathbf{Q_0 = K.C_{HS}.V_S + C_{HS}.V_{HS} - C_A.V_{HS}} \qquad \textbf{(5)}$$

For determining $CH_4$ concentration in the initial sample, **Equation 5** is rearranged in terms of $\mathbf{C_0}$ by combining **Equations 2** and **5** in **Equation 6.**

$$\mathbf{C_0 = K.C_{HS} + \frac{V_{HS}}{V_S}\,(C_{HS} - C_A)} \qquad \textbf{(6)}$$

The solubility coefficient K will be considered as the Bunsen coefficient 0.035 $L_g/L_s$ at atmospheric pressure 1 atm and at room temperature 18°C with 0 - 10 salinity (Donval et Guyader 2017). Bunsen coefficient is expressed by temperature and salinity. It is a volume of gas dissolved in water at specific temperature and salinity values (Wiesenburg et Guinasso 1979).

According to Weiss (1970), the atmospheric equilibrium of the gas depends on its solubility in a relationship that integrates the temperature and the salinity.

## RESULTS AND DISCUSSIONS

After analyzing all the collected 49 samples and obtaining the water concentration of $CH_4$ in the original sample by headspace method applying **Equation (6)**, the results can be illustrated in **Figure 4.**

**A.**

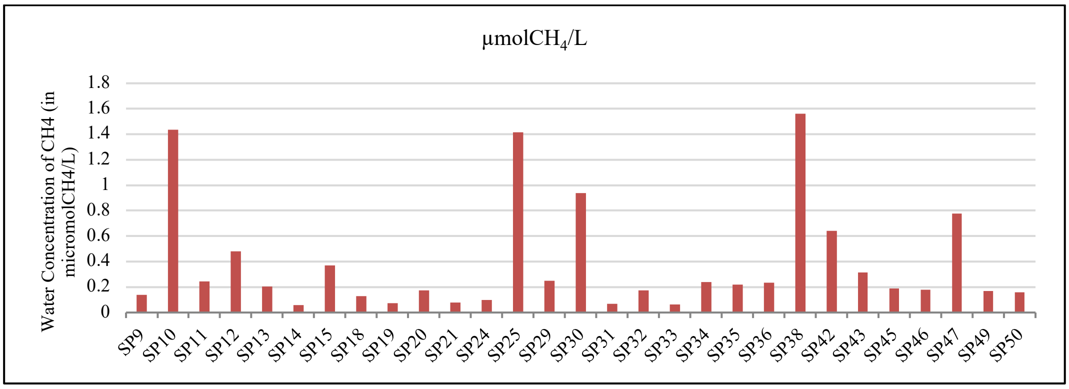

**B.**

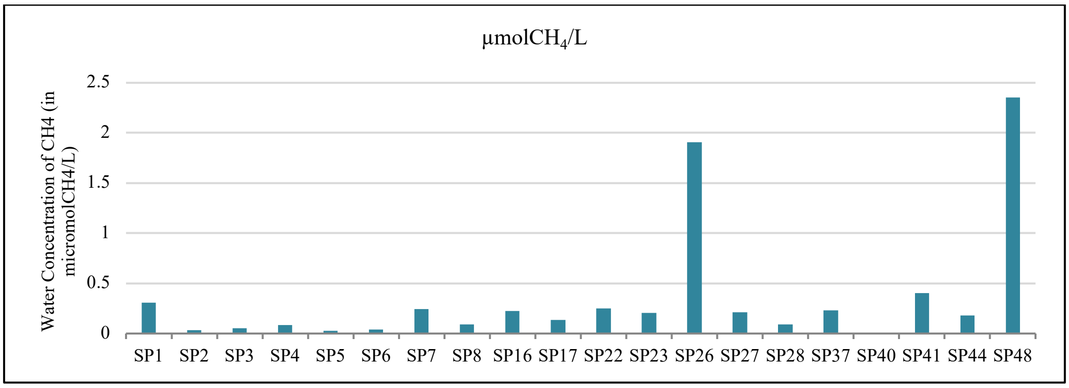

**Figure 4.** Methane concentration in water samples (in µmol/L) for samples collected from **A**. Someș River; **B.** Lakes and ponds.

It's important to mention that the reason for the separation of the results for river samples and lakes and ponds is related to the differences between these systems and to observe the influence of any changes over river segments before and after the urban area to estimate the impact of the urban activities down-stream. Moreover, the total number of samples is 49, which is less than the real number in the initially prepared plan for fieldwork. This change is due to the inaccessibility of some sampling locations.

The concentration of $CH_4$ in the samples varied between a minimum value of 0.03 µmol/L to a maximum value of 2.35 µmol/L, with a mean value of 0.38 µmol/L, **Table 1**.

**Table 1.** Statistics of $CH_4$ street-level concentration in (ppm) of the four land-use types, including mean, maximum, and minimum values in addition to the standard deviation (SD)

| Min | Max | Mean | SD |
|---|---|---|---|
| 0.03 | 2.35 | 0.38 | 0.51 |

Approximately 90% of the samples have values over 1 µmol/L, and 10% have values between 1 – 2.35 µmol/L. However, given that the estimated background level is 2.0 ppm, the saturation value of $CH_4$ concentration in the water sample is calculated as 0.01 µmol/L.

By comparing all $CH_4$ water concentration values with this saturation level, the result is that water samples from all sampling locations are oversaturated with methane, as it's evident by also that the minimum value is higher than the saturation estimate.

It's clear that sampling locations within and after the urban area have high dissolved $CH_4$, similar to sampling locations in lakes and ponds.

The results obtained by (Wang et al. 2020) stated that the dissolved $CH_4$ varied between 0.4 – 27 µmol/L with an average of 5.4 µmol/L which seems to be significantly similar to our results of high $CH_4$ concentrations.

In other words, our survey of dissolved methane in the urban aqueous system shows an oversaturated system of dissolved $CH_4$.

Therefore, this system is a potential source of $CH_4$ in the urban area.

The study of Hu et al., (2018) stated that $CH_4$ concentrations in water were positively correlated to temperature but negatively to dissolved oxygen DO. It also estimated high $CH_4$ concentrations at polluted water sampling locations.

Large quantities of organic matter in river sediments are the main sources of high river $CH_4$ concentrations. Nevertheless, we still can't specify the natural source behind these high concentrations in our results if they either come from microbial activities of the methanogenesis in the sediments or being influenced by urban pollution, or even from discharging of wastewater into this system.

Here, we can confirm that our urban aqueous system is a hotspot for $CH_4$ exchange from water into the urban atmosphere. Therefore, the degree of this contribution and the actual fluxes should be investigated in future studies, beside the reason behind them.

## CONCLUSIONS

Methane is one of our main approaches toward gaining short-term climate benefits. With its diverse sources and sinks, determining its actual budget has become a challenging mission.

Urban Areas are responsible for more than 50% of $CH_4$ emissions following its growing anthropogenic activities (IPCC 2013).

Previous studies have not explored the aqueous system in the urban area for determining its contribution to $CH_4$ annual budget. And the degree of uncertainty is relatively high which puts more challenges and stresses the need for effectively understanding the system's behavior.

In this study, $CH_4$ concentration in each water sample was determined by applying the headspace method combined with the TDLAS estimation.

The results of this study revealed a high concentration of $CH_4$ in the urban aqueous system and even a case of oversaturation in all water samples concluding that this system is an active hotspot for $CH_4$ exchange from water to the urban atmosphere.

This study represents a reference for future urban $CH_4$-relevant studies. Nevertheless, it is a preliminary study that points out the significance of the aqueous system in atmospheric methane, which in turn influences the total methane coming from urban sources. Still, it failed to associate environmental factors and seasons with these concentrations.

This observation of oversaturation points can result from water pollution due to urbanization and industrialization, or simply from active microorganisms in the sediments.

However, the sources behind these concentrations as well as the actual contribution of the aqueous system to the $CH_4$ budget, should be determined in future studies.

Also, methane fluxes from this system should be quantified spatially and temporarily in this system in a long-term study.

## REFERENCES

Bastviken, David, Lars J. Tranvik, John A. Downing, Patrick M. Crill, et Alex Enrich-Prast. 2011. « Freshwater Methane Emissions Offset the Continental Carbon Sink ». *Science* 331 (6013): 50-50. https://doi.org/10.1126/science.1196808.

Beelen, Benjamin, et Wayne Parker. 2022. « A Probabilistic Approach to the Quantification of Methane Generation in Sewer Networks ». *Journal of Environmental Management* 320 (octobre): 115775. https://doi.org/10.1016/j.jenvman.2022.115775.

Benanti, Giuseppe, Matthew Saunders, Brian Tobin, et Bruce Osborne. 2014. « Contrasting Impacts of Afforestation on Nitrous Oxide and Methane Emissions ». *Agricultural and Forest Meteorology* 198-199 (novembre): 82-93. https://doi.org/10.1016/j.agrformet.2014.07.014.

Chamberlain, Samuel D., Anthony R. Ingraffea, et Jed P. Sparks. 2016. « Sourcing Methane and Carbon Dioxide Emissions from a Small City: Influence of Natural Gas Leakage and Combustion ». *Environmental Pollution* 218 (novembre): 102-10.

https://doi.org/10.1016/j.envpol.2016.08.036.

Cuna, Stela, Elise Pendall, John B. Miller, Pieter P. Tans, Ed Dlugokencky, et James W.C. White. 2008. « Separating Contributions from Natural and Anthropogenic Sources in Atmospheric Methane from the Black Sea Region, Romania ». *Applied Geochemistry* 23 (10): 2871-79. https://doi.org/10.1016/j.apgeochem.2008.04.019.

De Bernardi, María, María Eugenia Priano, María Elena Fernández, Javier Gyenge, et María Paula Juliarena. 2022. « Impact of Land Use Change on Soil Methane Fluxes and Diffusivity in Pampean Plains, Argentina ». *Agriculture, Ecosystems & Environment* 329 (mai): 107866. https://doi.org/10.1016/j.agee.2022.107866.

Donval, J.P., et V. Guyader. 2017. « Analysis of Hydrogen and Methane in Seawater by "Headspace" Method: Determination at Trace Level with an Automatic Headspace Sampler ». *Talanta* 162 (janvier): 408-14. https://doi.org/10.1016/j.talanta.2016.10.034.

Fernandez, J.M., H. Maazallahi, J.L. France, M. Menoud, M. Corbu, M. Ardelean, A. Calcan, et al. 2022. « Street-Level Methane Emissions of Bucharest, Romania and the Dominance of Urban Wastewater. » *Atmospheric Environment: X* 13 (janvier): 100153. https://doi.org/10.1016/j.aeaoa.2022.100153.

Guisasola, Albert, David de Haas, Jurg Keller, et Zhiguo Yuan. 2008. « Methane Formation in Sewer Systems ». *Water Research* 42 (6-7): 1421-30. https://doi.org/10.1016/j.watres.2007.10.014.

Harris, Eliza, Thomas Ladreiter-Knauss, Klaus Butterbach-Bahl, Benjamin Wolf, et Michael Bahn. 2018. « Land-Use and Abandonment Alters Methane and Nitrous Oxide Fluxes in Mountain Grasslands ». *Science of The Total Environment* 628-629 (juillet): 997-1008. https://doi.org/10.1016/j.scitotenv.2018.02.119.

Hu, Beibei, Dongqi Wang, Jun Zhou, Weiqing Meng, Chongwei Li, Zongbin Sun, Xin Guo, et Zhongliang Wang. 2018. « Greenhouse Gases Emission from the Sewage Draining Rivers ». *Science of The Total Environment* 612 (janvier): 1454-62. https://doi.org/10.1016/j.scitotenv.2017.08.055.

IPCC. 2013. « Carbon and Other Biogeochemical Cycles. In: Climate Change 2013: The Physical Science Basis. Contribution of Working Group I to the Fifth Assessment Report of the Intergovernmental Panel on Climate Change. Cambridge University Press, Cambridge, United Kingdom and New York, NY, USA. »

Isaksen, Ivar, Terje Berntsen, Stig Dalsøren, Kostas Eleftheratos, Yvan Orsolini, Bjørg Rognerud, Frode Stordal, Ole Søvde, Christos Zerefos, et Chris Holmes. 2014. « Atmospheric Ozone and Methane in a Changing Climate ». *Atmosphere* 5 (3): 518-35. https://doi.org/10.3390/atmos5030518.

Ito, A., et M. Inatomi. 2012. « Use of a Process-Based Model for Assessing the Methane Budgets of Global Terrestrial Ecosystems and Evaluation of Uncertainty ». *Biogeosciences* 9 (2): 759-73. https://doi.org/10.5194/bg-9-759-2012.

Kang, Mary, Shanna Christian, Michael A. Celia, Denise L. Mauzerall, Markus Bill, Alana R. Miller, Yuheng Chen, Mark E. Conrad, Thomas H. Darrah, et Robert B. Jackson. 2016. « Identification and Characterization of High Methane-Emitting Abandoned Oil and Gas Wells ». *Proceedings of the National Academy of Sciences* 113 (48): 13636-41. https://doi.org/10.1073/pnas.1605913113.

Kolb, Bruno, et Leslie S. Ettre. 2006. *Static Headspace-Gas Chromatography*. 2nd ed. Hoboken (N.J.): Wiley-Interscience.

Kyung, Daeseung, Dongwook Kim, Sora Yi, Wonyong Choi, et Woojin Lee. 2017. « Estimation of Greenhouse Gas Emissions from Sewer Pipeline System ». *The International Journal of Life Cycle Assessment* 22 (12): 1901-11. https://doi.org/10.1007/s11367-017-1288-9.

Lamb, Brian K., Maria O. L. Cambaliza, Kenneth J. Davis, Steven L. Edburg, Thomas W. Ferrara, Cody Floerchinger, Alexie M. F.

Heimburger, et al. 2016. « Direct and Indirect Measurements and Modeling of Methane Emissions in Indianapolis, Indiana ». *Environmental Science & Technology* 50 (16): 8910-17. https://doi.org/10.1021/acs.est.6b01198.

Magen, Cédric, Laura L. Lapham, John W. Pohlman, Kathleen Marshall, Samantha Bosman, Michael Casso, et Jeffrey P. Chanton. 2014. « A Simple Headspace Equilibration Method for Measuring Dissolved Methane ». *Limnology and Oceanography: Methods* 12 (9): 637-50. https://doi.org/10.4319/lom.2014.12.637.

McKain, Kathryn, Adrian Down, Steve M. Raciti, John Budney, Lucy R. Hutyra, Cody Floerchinger, Scott C. Herndon, et al. 2015. « Methane Emissions from Natural Gas Infrastructure and Use in the Urban Region of Boston, Massachusetts ». *Proceedings of the National Academy of Sciences* 112 (7): 1941-46. https://doi.org/10.1073/pnas.1416261112.

Phillips, Nathan G., Robert Ackley, Eric R. Crosson, Adrian Down, Lucy R. Hutyra, Max Brondfield, Jonathan D. Karr, Kaiguang Zhao, et Robert B. Jackson. 2013. « Mapping Urban Pipeline Leaks: Methane Leaks across Boston ». *Environmental Pollution* 173 (février): 1-4. https://doi.org/10.1016/j.envpol.2012.11.003.

Saunois, Marielle, Ann R. Stavert, Ben Poulter, Philippe Bousquet, Josep G. Canadell, Robert B. Jackson, Peter A. Raymond, et al. 2020. « The Global Methane Budget 2000–2017 ». *Earth System Science Data* 12 (3): 1561-1623. https://doi.org/10.5194/essd-12-1561-2020.

Snow, N.H., et G.P. Bullock. 2010. « Novel Techniques for Enhancing Sensitivity in Static Headspace Extraction-Gas Chromatography ». *Journal of Chromatography A* 1217 (16): 2726-35. https://doi.org/10.1016/j.chroma.2010.01.005.

Tate, Kevin R. 2015. « Soil Methane Oxidation and Land-Use Change – from Process to Mitigation ». *Soil Biology and Biochemistry* 80 (janvier): 260-72. https://doi.org/10.1016/j.soilbio.2014.10.010.

UNEP. 2021. « Emissions Gap Report 2011: The Heat Is On - A world of climate promises not yet delivered. Nairobi ».

Wang, Rui, Han Zhang, Wei Zhang, Xunhua Zheng, Klaus Butterbach-Bahl, Siqi Li, et Shenghui Han. 2020. « An Urban Polluted River as a Significant Hotspot for Water–Atmosphere Exchange of $CH_4$ and N2O ». *Environmental Pollution* 264 (septembre): 114770. https://doi.org/10.1016/j.envpol.2020.114770.

Wanninkhof, Rik. 1992. « Relationship between Wind Speed and Gas Exchange over the Ocean ». *Journal of Geophysical Research* 97 (C5): 7373. https://doi.org/10.1029/92JC00188.

Wanninkhof, Rik, William E. Asher, David T. Ho, Colm Sweeney, et Wade R. McGillis. 2009. « Advances in Quantifying Air-Sea Gas Exchange and Environmental Forcing ». *Annual Review of Marine Science* 1 (1): 213-44. https://doi.org/10.1146/annurev.marine.010908.163742.

Weiss, R.F. 1970. « The Solubility of Nitrogen, Oxygen and Argon in Water and Seawater ». *Deep Sea Research and Oceanographic Abstracts* 17 (4): 721-35. https://doi.org/10.1016/0011-7471(70)90037-9.

Wiesenburg, Denis A., et Norman L Guinasso. 1979. « Equilibrium Solubilities of Methane, Carbon Monoxide, and Hydrogen in Water and Sea Water ». *Journal of Chemical & Engineering Data* 24 (4): 356-60. https://doi.org/10.1021/je60083a006.

Yang, Shang-Shyng, I-Chu Chen, Liu Ching-Pao, Li-Yun Liu, et Cheng-Hsiung Chang. 2015. « Carbon Dioxide and Methane Emissions from Tanswei River in Northern Taiwan ». *Atmospheric Pollution Research* 6 (1): 52-61. https://doi.org/10.5094/APR.2015.007.

Zhao, Feng, Yongqiang Zhou, Hai Xu, Guangwei Zhu, Xu Zhan, Wei Zou, Mengyuan Zhu, Lijuan Kang, et Xingchen Zhao. 2022. « Oxic Urban Rivers as a Potential Source of Atmospheric Methane ».

*Environmental Pollution* 297 (mars): 118769. https://doi.org/10.1016/j.envpol.2021.118769.

ISSN 1582-1021
e-ISSN 2668-4764
Edited by "AUREL VLAICU" University
Arad, Romania

10.62591/Scien.Tech.Bull-Chem.FoodSci.Eng.2022.19.05

*Scien. Tech. Bull-Chem. Food Sci. Eng., Vol. 19(XX), 2022, 53-62*

## ARTICLE

# CHEMICAL AND ANTIOXIDANT CAPACITY EVALUATION OF *CENTAUREA JACEA* EXTRACTS FROM PLANTS HARVESTED IN ARAD COUNTY, ROMANIA

**Silvia Elena Lavinia MOT[1,2], Paul Andrei SALAJAN[1], Cristian MOISA[1], Lucian COPOLOVICI[1], Dana Maria COPOLOVICI[1*]**

*[1] "Aurel Vlaicu" University, Faculty of Food Engineering, Tourism and Environmental Protection; Institute for Research, Development, and Innovation in Technical, and Natural Sciences, Romania, 2 Elena Dragoi St., Arad, 310330, Romania*
*[2] Doctoral School of Biomedical Sciences, University of Oradea, 1 Universitatii St., 410087, Oradea, Romania*
**Corresponding author email: dana.copolovici@uav.ro*

***Abstract:*** *The phytochemical composition and biological activity of the plant extracts obtained in different solvents (water, 70% ethanol, methanol, and diethyl ether) of the brown knapweed (Centaurea jacea L.) harvested in Romania were obtained. The chemical composition of the extracts was determined by gas chromatography–mass spectrometry analysis, by total phenolic and flavonoid content. The antioxidative potential was determined using ferric-reducing antioxidant power (FRAP) and 2,2-dyphenyl-1-picrylhydrazyl (DPPH) scavenging methods. The methanolic extracts revealed the highest antioxidant activity by FRAP and DPPH assays. This study revealed, once again, the importance of the geographic and climate region of harvesting the plants used for biomedical applications.*

**Keywords**: *Centaurea jacea*, extracts, GC-MS, antioxidant capacity, total phenolic content; FRAP assay, DPPH assay.

## INTRODUCTION

*Centaurea jacea* L. (brown knapweed) is an Asteraceae family herbaceous plant. It is one of the most abundant plant families on the planet, with over 23,000 species (Wilson and Randall, 2005), but only herbaceous species are present in Romania. Numerous edible, ornamental, medicinal, industrial, and even invasive species belong to this family (Roche and Roche, 1991).

*Centaurea jacea* L. is a perennial plant native to Europe that reproduces solely via seeds. The leaves are lance-shaped and can reach a maximum length of 15 cm at the plant's base. The blossoms are typically pinkish-purple (Fig. 1) and occasionally white. The blooming period begins in July and continues through October. Each flower can produce up to twelve dark brown seeds that produce pollen and nectar, making this an attractive plant for beekeepers. The bracts encircling the flower range in color from light to dark brown and reflect a metallic golden hue when in bloom (Ayad and Akkal, 2019; Wilson and Randall, 2005). Several studies described the morphology, and phenotypes of Centaurea plants from diverse areas around the globe (Arnelas et al., 2018; DiTommaso et al., 2021; Dydak et al., 2009; Francini et al., 2008; Vanderhoeven et al., 2002; Villodre and Garcia-Jacas, 2000; von Cossel et al., 2021), including the cytogenetic analysis of several populations of *Centaurea jacea* (Dydak et al., 2009)

Traditional medicine employs the genus *Centaurea* L. extensively (Ayad and Akkal, 2019; Martkoplishvili and Kvavadze, 2015; Sharonova et al., 2021). In Russia, the blossoms of *Centaurea cyanus* L. (cornflower) are frequently employed as a diuretic. In Scottish medicine, *Centaurea cyanus* L. and *Centaurea scabiosa* L. (greater knapweed) are also employed as diuretics and tonics. Traditional Turkish medicine uses *Centaurea pulchella*, *Centaurea drabifolia*, and *Centaurea solstitialis* to treat abscesses, hemorrhoids, peptic ulcers, and colds. It is confirmed that *Centaurea* L.

species have biological potential with antimicrobial, antifungal, antiviral, antihelicobacterial, antioxidant, anti-inflammatory, and cytotoxic action (Albayrak et al., 2017; Ayad and Akkal, 2019; Bouafia et al., 2021; Ceyhan Güvensen et al., 2019; Martkoplishvili and Kvavadze, 2015; Milosevic et al., 2010; Özcan et al., 2019; Sharonova et al., 2021; Zater et al., 2016; Zavada et al., 2021). The research suggests that obtaining knapweed extracts for various applications, such as medical and food uses, mostly involves utilizing dried aboveground biomass, including leaves and flowers. At the same time, the biological activity of essential oils from various *Centaurea* L. species has been determined and includes antitumor, antidiabetic, anti-inflammatory, analgesic, antidepressant, antirheumatic, antioxidant, antimicrobial, and enzymatic properties.

The chemical composition of plants belonging to the genus *Centaurea* L. varies greatly based on species and geographic location. There is a scarcity of studies on plants belonging to the genus *Centaurea*, considered representatives of the flora in Central Russia (Sharonova et al., 2021). Several researchers investigated the indigenous Centaurea from Turkey, such as *Centaurea antiochia* var., *Centaurea hypoleuca (Özcan et al., 2019), Centaurea amaena Boiss. & Balansa (Albayrak et al., 2017), Centaurea aksoyi Hamzaoglu & Budak*, and *Centaurea babylonica* L. (Albayrak et al., 2017; Ceyhan Güvensen et al., 2019). Additionally, investigations have been conducted on *Centaurea pumilio* L. (Zater et al., 2016) and 26 other species from Africa (Ayad and Akkal, 2019). Flavonoids, lignans, alkaloids, phenolic compounds, steroids, and terpenes are the most distinct biologically active compounds. Despite this, pharmacological and chemical research on *Centaurea* L. plants is still limited. For many taxa, phytochemical composition data are insufficient or absent. A recent study, published in 2021 (Sharonova et al., 2021), sought to determine the phytochemical composition and biological activity of extracts derived from *Centaurea cyanus* L., *Centaurea jacea* L., and *Centaurea scabiosa* L. in order to assess their potential application in organic agriculture. The brown knapweed flowers extract included the fewest compounds, whereas the extract of bigger knapweed had the highest number of compounds. The content of extracts derived from the flowers of *Centaurea scabiosa* L. varied greatly depending on the solvents used. Extraction using non-polar solvents such as petroleum ether and MTBE revealed the highest number of components. During the initial evaluation phase, it was determined that the methanol extracts of recently collected knapweed biomass exhibited limited antimicrobial efficacy against phytopathogenic microorganisms. The minimum inhibitory concentrations ranged from 1250 to 10,000 µg/mL, while the minimum bactericidal and fungicidal concentrations were 2500 µg/mL or higher. The species *Centaurea scabiosa* L. exhibited the highest level of activity.

The antimicrobial activity of *Centaurea scabiosa* L. flower extracts, obtained using methyl tert-butyl ether (MTBE), exhibited the highest efficacy against the phytopathogens under investigation. The minimum inhibitory concentrations (MICs) ranged from 60 to 120 µg/mL, while the minimum fungicidal concentration (MFC) was determined to be 120 µg/mL. The minimum bactericidal concentration (MBC) was also found to be 250 µg/mL. The studied plants exhibited varying levels of antioxidant activity, with *Centaurea jacea* L. displaying the lowest activity. This finding was consistent with the levels of individual flavonoids and the overall flavonoid content present in the extracts. The application of knapweed extracts at a dosage of 0.1% did not exhibit any inhibitory effect on the germination of garden cress seeds. However, it did have an impact on the growth of the resulting seedlings. Notably, the most pronounced phytotoxic effect was observed when using extracts derived from larger knapweed.

The objective of this study was to add knowledge base on the current understanding of the phytochemical composition and biological activity of extracts derived from the bloomed plant of *Centaurea jacea* L. harvested in Romania. We aimed to accomplish the following objectives: (1) to examine the phytochemical composition of the plants extracts obtained in different solvents in order to identify and detect biologic active compounds by chromatographic and spectrophotometric methods and (2) to evaluate the antioxidant capabilities of the extracts using ferric ion reducing antioxidant power (FRAP) and the 2,2-diphenyl-1-picrylhydrazyl (DPPH) assays (Fig. 1).

## MATERIALS AND METHODS

### 2.1. Materials

All employed chemical reagents and solvents were of an appropriate analytical grade and were acquired from Sigma-Aldrich and Merck.

Plants of *Centaurea jacea* L. were collected from two different locations in Arad County, Romania, in 2022. The first batch of plants was collected from the resort of Moneasa, and the second batch was collected from Pecica. The plants were washed, dried at room temperature in the dark, and kept in a cool dry place.

Both flowers and leaves were detached from stems and grounded with an electric grinder. After grinding, each sample was divided into 4 parts. Plant extracts were made from dried biomass by a single maceration process. The maceration process used a ratio of plant material: solvent of 1: 10, and the following solvents: 1 – distilled $H_2O$; 2 - 70% ethanol; 3 – methanol; 4 - diethyl ether. The maceration was done for 3 hours at 19 ± 1 °C with continuous stirring, followed by filtration. PVDF-type filters were used for aqueous extracts and PTFE-type filters (45 µm) were used for the other three macerates. Thus 16 different types of extracts were obtained. These were stored at +4 °C until further analysis.

### GC-MS analysis

The chemical composition of three extracts (aqueous extract; 70% ethanolic extract; methanolic extract, as they showed the highest antioxidant capacity) was determined using a gas chromatograph (GC, Shimadzu 2010, Kyoto, Japan) and a mass spectrometer (MS, TQ 8040, Shimadzu, Kyoto, Japan). All chemical constituents were identified using the spectra libraries NIST 14 and Wiley 09 as described in (Popa et al., 2021).

### Determination of total polyphenolic content (Folin-Ciocalteu method)

To determine the total polyphenolic content of the extracts, 1 mL of 1:25 diluted sample was mixed with 0.5 mL Folin-Ciocalteu reagent, 2 mL $NaCO_3$ (20%), and 5 mL dist. $H_2O$. The reaction mixture was stirred and kept at room temperature in the dark for 90 min, and the absorbance was read at λ = 765 nm against the blank, which was prepared under the same conditions. Data was recorded using a UV-VIS double-beam spectrophotometer (Specord 200, Analytik Jena Inc., Jena, Germany). The results were expressed as mg gallic acid equivalents (GAE)/g dry weight (DW).

### Determination of flavonoid content

To determine the flavonoid content of the extracts, 0.250 mL of sample was mixed with 1.250 mL sodium acetate solution (100 g/L), 0.750 mL aluminium chloride solution (25 g/L), and 0.250 mL dist. $H_2O$. The reaction mixture was stirred and kept at room temperature in the dark for 15 minutes, and the absorbance was recorded at λ = 434 nm relative to the control sample, which was prepared under the same conditions. Data was recorded using a UV-VIS double-beam spectrophotometer (Specord 200, Analytik Jena Inc., Jena, Germany). The calibration curve was performed using rutin as standard in the concentration range 0.02-0.4 mM, and the results were expressed in mg rutin equivalent/g dry weight.

### Antioxidant capacity

**FRAP assay -** 200 µL sample and 1.5 mL FRAP reagent (freshly prepared by mixing 300 mM acetate buffer solution (pH 3.6), 20 mM $FeCl_3$, and 10 mM TPTZ (in 40 mM HCl)) were reacted in the dark for 20 minutes. Aqueous extracts were diluted 1:5. Absorbance was recorded at λ = 593 nm relative to $H_2O$ with a spectrophotometer (Specord 200, Analytik Jena Inc., Jena, Germany) and the calibration curve was performed with Trolox (concentration range 0-0.5 mM).

**DPPH assay -** The assessment of the radical scavenging activity of the extracts was conducted by employing the 1,1-diphenyl-2-picrylhidrazyl radical (DPPH) and afterwards measuring the absorbance at λ = 517 nm using a spectrophotometer. The reaction duration was set at 1 hour, and the experiment was carried out in a dark environment, following the methodology and calculation outlined in (Popa et al., 2021).

All analyses were performed in triplicates, and the results are reported as mean ± standard deviation.

## RESULTS AND DISCUSSIONS

In this study we obtained four extracts in different solvents (water, 70% ethanol, methanol, and diethyl ether) of leaves and flowers from plants of *Centaurea jacea* L. harvested in western part of Romania, in Moneasa and in Pecica, in Arad county.

The extracts of leaves and flowers of *Centaurea jacea* L., respectively, obtained in three solvents (aqueous extract; 70% ethanolic extract; and methanolic extract), as determined by GC-MS analyses, have a different chemical profile, conclusion that is supported in previously published reports (Albayrak et al., 2017; Bouafia et al., 2021; Sharonova et al., 2021; Zater et al., 2016). In the leaves' extracts (Table 1) 27 compounds with more than 0.5% concentration were totally identified in the analyzed samples, in diverse concentrations.

The major compounds were: glycidyl palmitate, 9,12,15-octadecatrienoic acid, ethyl ester; 1,E-11,Z-13-octadecatriene; 2,4-di-tert-butylphenol; glycidyl oleate; isomenthol*;* phytol; isopropyl octacosyl ether; decane and its derivatives; heptacosane; gitogenin acetate; benzeneacetic acid, 2-tetradecyl ester. In the flowers extracts 24 compounds were totally identified in the analysed samples, in diverse concentrations. The major compounds were: methyl (Z)-5,11,14,17-eicosatetraenoate; heptadecane, 2,6,10,14-tetramethyl; 1,8,11-heptadecatriene; 9,12-octadecadienoic acid; 2,4-tert-butylphenol; heptacosane; and minor compounds: fumaric acid, 2-isopropylphenyl pentadecyl ester; undecane and its derivatives, etc. The phytochemical compositions of the *Centaurea jacea* L. flowers' ethanolic extract presented 13 compounds in the samples obtained from Verkheuslonsky Municipality, Republic of Tatarstan, Russian Federation, in 2020. The main compounds from these sample, separated in a TraceGold TG-5 MS fused silica GC column, were 3',5,6-trihydroxy-3,4',7-trimethoxyflavone (60.42%), 2-hydroxy-5-methylbenzaldehyde (8.02%)' palmitic acid (6.49%), vitexicarpin (5.83%), catechol (5.65%) (Sharonova et al., 2021).

**Figure 1.** The presentation of the work plan followed in this study: material plant and the methods employed to obtain the extracts in four different solvents (water, 70% ethanol, methanol, and diethyl ether) and their analyses.

The chemical profile of the extracts obtained in this study reveals the presence of alkanes, esters, phenols, aldehydes, ketones, ethers and acids. The concentration of the compounds depends on the solvent used for extraction and on the geographical localisation of the grown plants.

**Table 1.** The chemical composition, as determined by GC-MS of the leaves' samples harvested in Moneasa and Pecica. The first letter is from the sample location: M is from Moneasa and P is from Pecica; L is for leaves, 1 - aqueous extract; 2 – 70% ethanolic extract; 3 – is a methanolic extract.

| **R.T. (min.)** | **Name** | **PL1** | **PL2** | **PL3** | **ML1** | **ML2** | **ML3** |
|---|---|---|---|---|---|---|---|
| 12.555 | Decane, 2,9-dimethyl- | 1.09 | 1.96 | 2.33 | n.d. | n.d. | n.d. |
| 12.905 | Decane | 0.57 | 1.73 | n.d. | n.d. | n.d. | n.d. |
| 15.118 | Octane, 2-methyl- | 0.95 | 1.31 | n.d. | n.d. | n.d. | n.d. |
| 19.611 | Decane, 2,6,6-trimethyl- | 0.97 | 2.18 | 3.95 | 3.95 | n.d. | n.d. |
| 20.113 | Decane, 2,6,7-trimethyl- | 1.35 | 4 | n.d. | n.d. | n.d. | n.d. |
| 20.396 | Heptane, 2,3,5-trimethyl- | 0.7 | 1.52 | n.d. | n.d. | n.d. | n.d. |
| 21.836 | Heptadecane, 2,6,10,14-tetramethyl- | 1.18 | 0.56 | 2.05 | 5.05 | 6.76 | n.d. |
| 22.24 | Isopropyl octacosyl ether | 2.41 | 1.5 | 2.71 | n.d. | 12.67 | n.d. |
| 22.56 | Oxalic acid, cyclobutyl tetradecyl ester | 1.06 | 4.09 | n.d. | n.d. | n.d. | n.d. |
| 23.759 | Undecane, 2,8-dimethyl- | 0.99 | 2.02 | n.d. | 3.94 | 4.95 | n.d. |
| 27.797 | Hexadecane, 8-hexyl-8-pentyl- | 1.25 | 9.91 | n.d. | n.d. | n.d. | n.d. |
| 28.362 | Tetracontane, 3,5,24-trimethyl- | 0.85 | 1.99 | n.d. | 3.55 | n.d. | 12.77 |
| 28.46 | Hexadecane | 2.99 | 2.74 | 5.36 | 10.68 | 11.56 | n.d. |
| 28.685 | Gitogenin acetate | 0.6 | 1.89 |  | 3.43 | 5.32 | n.d. |
| 29.055 | 2,4-Di-tert-butylphenol | 6.23 | 1.4 | 6.86 | 20.99 | 22.48 | 34.29 |
| 29.637 | Hexadecane | 0.98 | 1.51 | 3.04 | n.d. | n.d. | 4.28 |
| 33.509 | Eicosane | 0.61 | 18.79 | n.d. | 3.15 | 3.14 | 3.96 |
| 33.598 | Heptacosane | 1.55 | 3.13 | 5.81 | n.d. | 7.89 | 4.86 |
| 34.24 | Benzeneacetic acid, 2-tetradecyl ester | 0.92 | 1.56 | n.d. | 4.69 | n.d. | n.d. |
| 34.607 | Heptadecane, 2,6,10,15-tetramethyl- | 1.02 | 2.33 | n.d. | n.d. | n.d. | n.d. |
| 36.813 | Phytol | 1.1 | 0.56 | n.d. | 6.9 | 6.92 | n.d. |
| 41.465 | 1,8,11-Heptadecatriene, (Z,Z)- | 1.05 | 3.36 | n.d. | n.d. | n.d. | n.d. |
| 41.571 | 9,12,15-Octadecatrienoic acid, ethyl ester, (Z,Z,Z)- | 31.14 | 1.26 | 26.84 | n.d. | n.d. | n.d. |
| 41.882 | Glycidyl oleate | 3.91 | 1.9 | 8.63 | n.d. | n.d. | 3.62 |
| 42.74 | Glycidyl palmitate | 1.09 | 14.86 | 3.43 | 13 | 12.27 | 7.04 |
| 43.057 | Isomenthol | 2.07 | 1.69 | 4.13 | 9.3 | 6.04 | 6.67 |
| 43.371 | 1,E-11,Z-13-Octadecatriene | 31.37 | 8.48 | 21.4 | 2.07 | n.d. | 3.83 |

**Table 2.** The chemical composition, as determined by GC-MS of the flowers' samples harvested in Moneasa and Pecica. The first letter is from the sample location: M is from Moneasa and P is from Pecica; F is for flowers, 1 - aqueous extract; 2 – 70% ethanolic extract; 3 – is a methanolic extract.

| **R.T. (min.)** | **Name** | **MF1** | **MF2** | **MF3** | **PF1** | **PF2** | **PF3** |
|---|---|---|---|---|---|---|---|
| 12.897 | Undecane, 4,7-dimethyl- | 3.14 | 2.78 | n.d | 1.46 | 2.29 | 1.35 |
| 19.607 | Undecane, 3,7-dimethyl- | 1.97 | 2.02 | n.d | 2.92 | 2.71 | 0.77 |
| 20.409 | Decane, 2,9-dimethyl- | 2.09 | 4.03 | n.d | 2.54 | 5.52 | 1.55 |
| 21.833 | Isobutyl tetratriacontyl ether | 3.33 | 1.24 | 1.72 | 3.44 | 1.92 | 0.35 |
| 22.244 | Dodecane, 4,6-dimethyl- | 7.48 | 1.5 | 3.35 | 4.64 | 5.91 | 0.63 |
| 23.757 | Fumaric acid, 2-isopropylphenyl pentadecyl ester | 2.34 | 5.06 | 1.27 | 1.5 | 4.43 | 0.29 |
| 27.777 | Heptadecane, 2,6,10,14-tetramethyl- | 3.4 | 0.87 | 0.9 | 1.84 | 2.18 | 1.2 |
| 28.466 | Tridecane | 7.04 | 6.33 | 3.88 | 2.29 | 3.8 | 2.42 |
| 29.061 | 2,4-Di-tert-butylphenol | 2.02 | 1.24 | 5.18 | 8.56 | 3.49 | 0.76 |
| 29.531 | Undecane, 5,5-dimethyl- | 16.42 | 1.33 | 0.45 | 7.39 | 2.05 | 4.07 |
| 29.647 | Heptacosane | 1.4 | 0.9 | 1.18 | 1.09 | 2.02 | 5.96 |
| 32.747 | 2-(4a,8-Dimethyl-2,3,4,5,6,8a-hexahydro-1H-naphthalen-2-yl)propan-2-ol | 2.27 | 0.86 | 1.99 | 2.27 | 15.09 | 1.01 |
| 33.523 | Hexatriacontane | 1.38 | 1.66 | 1.31 | 0.75 | 3.31 | 1.79 |
| 33.596 | Heptacosane | 4.29 | 2.21 | 2.31 | 3.7 | 3.35 | 1.86 |
| 34.578 | Tridecane, 6-methyl- | 1.9 | 4.11 | 0.97 | 4.15 | 2.34 | 1.38 |
| 38.801 | Methyl (Z)-5,11,14,17-eicosatetraenoate | 0.66 | 22.1 | 0.4 | n.d. | 0.48 | n.d. |
| 38.938 | Heptadecane, 2,6,10,15-tetramethyl- | 5.17 | 1.08 | 1.45 | n.d. | 2.53 | 12.34 |
| 40.707 | Pentadecanoic acid | 2.75 | 1.46 | 4.79 | 23.3 | 1.59 | 4.63 |
| 41.568 | Methyl (Z)-5,11,14,17-eicosatetraenoate | 4.46 | 16.34 | 28.28 | 7.7 | 1.1 | 7.93 |
| 43.398 | 1,8,11-Heptadecatriene | 11.27 | 3.96 | 26.65 | 3.82 | 1.02 | 9.65 |
| 43.453 | 9,12-Octadecadienoic acid | 5.02 | 4.6 | 3.92 | 1.57 | 19.77 | 32.48 |
| 44.247 | Cholestan-3-one, cyclic 1,2-ethanediyl acetal, (5.alpha.)- | 6.05 | 1.4 | 1.36 | 3.83 | 7.26 | 1.6 |
| 45.794 | Glycidyl palmitate | 4.15 | 5.72 | 6.26 | 7.64 | 3.41 | 3.84 |
| 45.884 | Octacosane | n.d. | 2.73 | 2.38 | 3.6 | 2.43 | 2.14 |

As shown in Table 3, the highest amount of total polyphenols was recorded for methanolic extracts obtained from flowers (11.3243±0.1294 - 1.2089±0.0094 mg gallic acid equivalent/g of dry weight for flowers from Moneasa extracted in methanol and diethyl ether, respectively) and leaves (15.6468±0.3321 - 2.4314±0.2200 mg gallic acid equivalent/g of dry weight for leaves from Moneasa extracted in methanol and from Pecica extracted in diethyl ether, respectively), followed by aqueous extracts, ethanolic extracts, and diethyl ether extracts, respectively. A previously report determined for ethanolic flower extract 163.7 ± 2.25 mg GAE/L, while we determined a large concentration in the range 120.89±0.94 mg GAE/L (PF4, diethyl ether extracts from flowers harvested in Pecica) - 1132.43±12.94 mg GAE/L (MF3, methanolic extract from flowers harvested in Moneasa).

The chemical profile of the extracts is responsible for the biological activity of these extracts. There are many methods to determin the antioxidant properties of the biomolecules from plants.

The methanolic extracts revealed the highest antioxidant activity by DPPH and FRAP methods (maximum values of 1.6535±0.0040 and 1.4850±0.0122 mM TROLOX equivalent/g of dry weight for leaves extracted in methanol from Moneasa-ML3 and Pecica-PL3, respectively, and minimum value of 0.0320±0.0007 mM TROLOX equivalent/g of dry weight for flowers extracted in diethyl ether from Moneasa-MF4).

The most modest antioxidant activity was reported for the diethyl ether extracts for FRAP method and aqueous extracts for the DPPH method, respectively.

The chemiluminescent activity tests conducted on the ethanolic extracts derived from the flowers of the *Centaurea* plants in the study published by Sharonova et al. demonstrated limited antioxidant properties. The observed antioxidant effects were relatively weak, the effective concentration threshold for these effects was determined to be 0.01 mg/mL. Ethanol extracted *Centaurea jacea* flowers were most capable of binding free radicals in total reactive antioxidant potential (TRAP) method as compared with the extracts from *Centaurea cyanus* and *Centaurea scabiosa* (Sharonova et al., 2021). The authors concluded that this result was well corelated with the concentration of total flavonoid in the investigated samples. In the present study, could be also other biomolecules, beside polyphenols and flavonoids, that lead to the antioxidant capacity of the extracts.

## CONCLUSIONS

The chemical profile of *Centaurea jacea* L. extracts produced using four different solvents exhibits variation, as supported by previously published literature. The chemical composition of the extracts indicates the existence of alkanes, esters, phenols, aldehydes, ketones, and acids. According to the data, the methanolic extracts from flowers and leaves exhibited the highest concentration of total polyphenols. In descending order, this was followed by aqueous extracts, ethanolic extracts, and diethyl ether extracts. The flavonoid content analysis revealed a significant concentration of flavonoids in the flower and leaf samples when extracted using methanol, with ethanol extraction yielding slightly lower levels. The biological activity of the extracts was closely linked to their chemical composition. Methanolic extracts demonstrated superior antioxidant activity according to DPPH and FRAP assays, with leaves from Moneasa (ML3) and Pecica (PL3) showing the highest values, and flowers from Moneasa (MF4) displaying the lowest. The least potent antioxidant activity was observed in diethyl ether extracts using the FRAP method and in aqueous extracts using the DPPH method. The methanolic extracts of both flowers and leaves from *Centaurea jacea* will be further considered to be used in future applications due to their antioxidant activity.

## ACKNOWLEDGMENTS

This work was supported by a grant from the Ministry of Research, Innovation and Digitization, CNCS - UEFISCDI, project number PN-III-P4-PCE-2021-0639, within PNCDI III.

**Table 3.** The total polyphenols, flavonoids, and antioxidant capacity (by DPPH and FRAP assays) of the samples harvested in Moneasa and Pecica. The first letter is from the sample location: M is from Moneasa and P is from Pecica; L is for leaves, F is from flowers; 1 - aqueous extract; 2 – 70% ethanolic extract; 3 – is a methanolic extract; 4 – diethyl ether extract.

| **Sample** | **Total polyphenolic content** mg gallic acid equivalent / g of DW | **Total flavonoid content** mg rutin equivalent / g of DW | **Antioxidant capacity** | |
|---|---|---|---|---|
| | | | **FRAP assay** mM TROLOX equivalent / g of DW | **DPPH assay** Inhibition (%) |
| ML1 | 12.9936±0.7069 | 2.208±0.004 | 0.4167±0.0046 | 4.55±0.15 |
| MF1 | 11.1571±0.3416 | 1.211±0.007 | 0.3184±0.0087 | 10.17±0.21 |
| PL1 | 12.0160±0.6510 | 2.959±0.365 | 0.5077±0.0047 | 3.51±0.08 |
| PF1 | 8.5737±0.1406 | 0.730±0.083 | 0.3884±0.0056 | 4.86±0.02 |
| ML2 | 8.3647±0.1489 | 4.250±0.081 | 0.1325±0.0199 | 36.87±0.91 |
| MF2 | 6.2615±0.0783 | 2.083±0.004 | 0.6068±0.0296 | 32.47±0.79 |
| PL2 | 8.3301±0.3883 | 5.613±0.011 | 1.1007±0.0225 | 36.47±0.38 |
| PF2 | 8.6448±0.1812 | 3.711±0.007 | 0.6207±0.0350 | 38.55±0.93 |
| ML3 | 15.6468±0.3321 | 8.663±0.025 | 1.6535±0.0040 | 87.82±0.12 |
| MF3 | 11.3243±0.1294 | 3.887±0.027 | 1.2516±0.0086 | 92.02±0.1 |
| PL3 | 12.0256±0.2738 | 5.743±0.010 | 1.4850±0.0122 | 87.51±0.16 |
| PF3 | 10.2763±0.0508 | 3.814±0.004 | 0.8901±0.0088 | 87.34±0.96 |
| ML4 | 2.5712±0.1072 | 0.531±0.117 | 0.1091±0.0101 | 18.74±0.58 |
| MF4 | 1.2089±0.0094 | 0.178±0.067 | 0.0320±0.0007 | 3.70±0.06 |
| PL4 | 2.4314±0.2200 | 0.681±0.009 | 0.1658±0.0043 | 23.97±0.83 |
| PF4 | 2.6993±0.1700 | 1.088±0.0014 | 0.1176±0.0204 | 27.49±1.05 |

DW = dry weight. n. r. = not recorded. The values depicted are expressed in mean ±standard deviation. Triplicate measurements were performed.

## REFERENCES

Albayrak, S., Atasagun, B., Aksoy, A., 2017. Comparison of phenolic components and biological activities of two Centaurea sp. obtained by three extraction techniques. Asian Pacific Journal of Tropical Medicine 10, 599-606.

Arnelas, I., Perez-Collazos, E., Devesa, J.A., Lopez, E., Catalan, P., 2018. Phylogeny of highly hybridogenous Iberian Centaurea L. (Asteraceae) taxa and its taxonomic implications. Plant Biosystems 152, 1182-1190.

Ayad, R., Akkal, S., 2019. Chapter 12 - Phytochemistry and biological activities of algerian Centaurea and related genera, in: Atta ur, R. (Ed.), Studies in Natural Products Chemistry. Elsevier, pp 357-414.

Bouafia, M., Colak, N., Ayaz, F.A., Benarfa, A., Harrat, M., Gourine, N., Yousfi, M., 2021. The optimization of ultrasonic-assisted extraction of Centaurea sp. antioxidative phenolic compounds using response surface methodology. Journal of Applied Research on Medicinal and Aromatic Plants 25, 100330.

Ceyhan Güvensen, N., Keskin, D., Güneş, H., Kesik Oktay, M., Yıldırım, H., 2019. Antimicrobial property and antiproliferative activity of Centaurea babylonica (L.) L. on human carcinomas and cervical cancer cell lines. Ann Agric Environ Med. 26, 290-297.

DiTommaso, A., Milbrath, L.R., Marschner, C.A., Morris, S.H., Westbrook, A.S., 2021. Seed germination ecology of meadow knapweed (Centaurea x moncktonii) populations in New York State, USA. Weed Science 69, 111-118.

Dydak, M., Kolano, B., Nowak, T., Siwinska, D., Maluszynska, J., 2009. Cytogenetic studies of three European species of Centaurea L. (Asteraceae). Hereditas 146, 152-161.

Francini, A., Nali, C., Pellegrini, E., Lorenzini, G., 2008. Characterization and isolation of some genes of the shikimate pathway in sensitive and resistant Centaurea jacea plants after ozone exposure. Environmental Pollution 151, 272-279.

Martkoplishvili, I., Kvavadze, E., 2015. Some popular medicinal plants and diseases of the Upper Palaeolithic in Western Georgia. Journal of Ethnopharmacology 166, 42-52.

Milosevic, T., Argyropoulou, C., Solujic, S., Murat-Spahic, D., Skaltsa, H., 2010. Chemical Composition and Antimicrobial Activity of Essential Oils from Centaurea pannonica and C. jacea. Natural Product Communications 5, 1663-1668.

Özcan, K., Acet, T., Çorbacı, C., 2019. Centaurea hypoleuca DC: Phenolic content, antimicrobial, antioxidant and enzyme inhibitory activities. South African Journal of Botany 127, 313-318.

Popa, C.L., Lupitu, A., Mot, M.D., Copolovici, L., Moisa, C., Copolovici, D.M., 2021. Chemical and Biochemical Characterization of Essential Oils and Their Corresponding Hydrolats from Six Species of the Lamiaceae Family. Plants 10, 2489.

Roche, C.T., Roche, B.F., 1991. Meadow Knapweed Invasion in the Pacific-Northwest, United-States-America, and British-Columbia, Canada. Northwest Science 65, 53-61.

Sharonova, N., Nikitin, E., Terenzhev, D., Lyubina, A., Amerhanova, S., Bushmeleva, K., Rakhmaeva, A., Fitsev, I., Sinyashin, K., 2021. Comparative Assessment of the Phytochemical Composition and Biological Activity of Extracts of Flowering Plants of Centaurea cyanus L., Centaurea jacea L. and Centaurea scabiosa L. Plants-Basel 10.

Vanderhoeven, S., Hardy, O., Vekemans, X., Lefebvre, C., de Loose, M., Lambinon, J., Meerts, P., 2002. A morphometric study of populations of the Centaurea jacea complex (Asteraceae) in Belgium. Plant Biology 4, 403-412.

Villodre, J.M., Garcia-Jacas, N., 2000. Pollen studies in subtribe Centaureinae (Asteraceae): the Jacea group analysed with electron microscopy. Botanical Journal of the Linnean Society 133, 473-484.

von Cossel, M., Pereira, L.A., Lewandowski, I., 2021. Deciphering Substrate-Specific Methane Yields of Perennial Herbaceous Wild Plant Species. Agronomy-Basel 11.

Wilson, L.M., Randall, C.B., 2005. Biology and Biological Control of Knapweed, in: U.S. Department of Agriculture, F.H.T.E.T. (Ed.), http://www.fs.fed.us/foresthealth/technology/.

Zater, H., Huet, J., Fontaine, V., Benayache, S., Stévigny, C., Duez, P., Benayache, F., 2016. Chemical constituents, cytotoxic, antifungal and antimicrobial properties of Centaurea diluta Ait. subsp. algeriensis (Coss. & Dur.) Maire. Asian Pacific Journal of Tropical Medicine 9, 554-561.

Zavada, T., Omand, K.A., Malik, R.J., Tsirelson, D., Kesseli, R.V., 2021. Testing for hybridization between Centaurea stoebe and Centaurea jacea (Asteraceae) in the isolated island setting of Nantucket, Massachusetts, USA. Rhodora 123, 1-10.

ISSN 1582-1021
e-ISSN 2668-4764
Edited by “AUREL VLAICU” University
Arad, Romania

10.62591/Scien.Tech.Bull-Chem.FoodSci.Eng.2022.19.06

**Edited by "AUREL VLAICU"**
**University Arad, Romania, 2022**